FREE

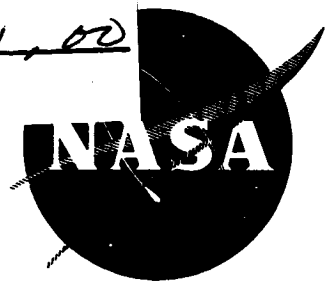

NASA CR-54722
TEI - TP 259

INVESTIGATION OF FIBER SYSTEMS OF ABLATIVE MATERIALS

by

Gordon H. Miller and George C. Robinson, Jr.

prepared for

NATIONAL AERONAUTICS AND SPACE ADMINISTRATION

CONTRACT NAS3-4196

TEXACO EXPERIMENT INCORPORATED
Richmond, Virginia 23234

NOTICE

This report was prepared as an account of Government sponsored work. Neither the United States, nor the National Aeronautics and Space Administration (NASA), nor any person acting on behalf of NASA:

A. Makes any warranty or representation, expressed or implied, with respect to the accuracy, completeness, or usefulness of the information contained in this report, or that the use of any information, apparatus, method, or process disclosed in this report may not infringe privately owned rights; or

B. Assumes any liabilities with respect to the use of, or for damages resulting from the use of any information, apparatus, method or process disclosed in this report.

As used above, "person acting on behalf of NASA" includes any employee or contractor of NASA, or employee of such contractor, to the extent that such employee or contractor of NASA, or employee of such contractor prepares, disseminates, or provides access to, any information pursuant to his employment or contract with NASA, or his employment with such contractor.

Requests for copies of this report should be referred to

National Aeronautics and Space Administration
Office of Scientific and Technical Information
Attention: AFSS-A
Washington, D. C. 20546

NASA CR-54722
TEI - TP 259

FINAL REPORT

INVESTIGATION OF FIBER SYSTEMS OF ABLATIVE MATERIALS

by

Gordon H. Miller and George C. Robinson, Jr.

prepared for

NATIONAL AERONAUTICS AND SPACE ADMINISTRATION

September 30, 1965

CONTRACT NAS3-4196

Project Management
NASA Lewis Research Center
Cleveland, Ohio 44135
Chemical and Nuclear Rocket Systems
Technology Procurement Section
Steven M. Cohen

TEXACO EXPERIMENT INCORPORATED
P. O. Box 3407
Richmond, Virginia 23234

INVESTIGATION OF FIBER SYSTEMS OF ABLATIVE MATERIALS

by

G. H. Miller and G. C. Robinson, Jr.

ABSTRACT

12273

The desired properties for advanced fibers to be used as reinforcing agents for ablative composites were defined after consideration of the ablation process and the anticipated environmental conditions in advanced thrust chambers of liquid-fuel rocket engines. Based on their physical properties and their calculated and experimentally determined resistance to the combustion products from H_2/F_2 or B_2H_6/OF_2 fuel-oxidizer combustions, graphite, tungsten-coated boron, TiC, TiB_2, ZrB_2, B_4C, ZrO_2, and carbon-coated boron were recommended. The feasibility of preparing fibers of graphite, tungsten-coated boron, TiB_2, TiC, and ZrB_2 by chemical vapor plating was investigated. The TiB_2 fibers had the highest strengths (up to 378 kpsi) and highest moduli (up to 84 million psi) of all the fiber materials investigated. Fibers of these materials were tested in an argon arc plasma to determine their chemical resistance to oxidizing media consisting of separately injected H_2O and BF_3.

Author

CONTENTS

CONTENTS (cont'd)

FIGURES

FIGURES (cont'd)

FIGURES (cont'd)

FIGURES (cont'd)

TABLES

TABLES (cont'd)

INVESTIGATION OF FIBER SYSTEMS OF ABLATIVE MATERIALS

by G. H. Miller and G. C. Robinson, Jr.

TEXACO EXPERIMENT INCORPORATED

SUMMARY

The objective of this investigation was to develop reinforcing fibers that would lead to more-effective ablative composites for use in liquid-fuel rocket-engine thrust chambers. The investigation was divided into three tasks:

I. Definition of properties and selection of fibers;

II. Fabrication and property determination of fibers; and

III. Recommendation of fibers for further development.

The desired properties for reinforcing fibers for advanced ablative materials were defined after consideration of the ablation process and the anticipated environmental conditions in advanced thrust chambers. Choice of fiber materials was predicated on their physical properties and on calculated or experimentally determined resistance to the combustion products from H_2/F_2 or B_2H_6/OF_2 fuel-oxidizer combustions. Pyrolytic graphite, tungsten coated boron, titanium carbide, titanium diboride, zirconium diboride, boron carbide, zirconium dioxide, and carbon coated boron are recommended for liquid-fuel rocket-engine thrust chambers.

The feasibility of preparing fibers of graphite, tungsten-coated boron, titanium carbide, titanium diboride, and zirconium diboride by chemical vapor plating was investigated on a batch basis. Pyrolytic graphite fibers with tensile strengths up to 73 kpsi were prepared by the pyrolysis of acetylene at reduced pressure. The addition of BCl_3 to the plating gas increased the deposition rate and density but had no effect on tensile strength. Tungsten coated boron fibers with tensile strengths up to 89 kpsi were prepared by depositing 0.2-mil tungsten on boron fibers by the hydrogen reduction of WF_6 at reduced pressure. Titanium diboride fibers were prepared by codeposition from BCl_3 and $TiCl_4$ at atmospheric pressure. An average tensile strength of 256 kpsi and a

maximum strength of 378 kpsi were obtained in fibers produced in a pilot run. The elastic modulus of these fibers varied, but values ran as high as 84 million psi. The preparation of titanium carbide and zirconium diboride fibers was less successful. Several good quality TiC fibers were prepared by codeposition of Ti and C from $TiCl_4$ and a volatile carbon precursor, but poor experiment repeatability was a major deterrent to their successful development. The strongest fiber prepared had a tensile strength of 63 kpsi. This fiber was made at atmospheric pressure using ethyl bromide as the carbon precursor. When CCl_4 was used as the carbon precursor, graphite deposition occurred in distinct layers under somewhat unpredictable manner. Neopentane and n-butane are promising carbon precursors for low-temperature TiC preparation. Fibers of zirconium diboride were produced by three approaches: (1) reduction of BCl_3 by a zirconium substrate; (2) codeposition from $ZrCl_4$ and BCl_3; and (3) deposition of boron from diborane on the surface of a zirconium substrate, followed by a diffusion heat treatment. The reduction of BCl_3 by a zirconium substrate, produced tubular ZrB_2 fibers that were porous and fragile. The codeposition experiments were only partially successful because deposits containing only 15 to 30 percent by volume (balance boron) were obtained. Major difficulty was experienced with the $ZrCl_4$ sublimer which produced a $ZrCl_4$ flow of only a fraction of that desired. Zirconium diboride was prepared by deposition of boron on zirconium from diborane, but the deposits so produced had poor adherence and were quite fragile.

Fibers of pyrolytic graphite, titanium carbide, titanium diboride, zirconium diboride, and tungsten-coated boron were tested in a plasma arc to determine their chemical resistance to oxidizing media containing H_2O and BF_3 separately. The behavior of the TiB_2 fibers was erratic. One TiB_2 specimen failed structurally in the tests, probably due to grain boundary weakening resulting from excess titanium in the deposits. Another had high erosion while one other had good resistance to the test media. The tungsten coated boron specimens failed by melting and, consequently, their chemical resistance was not obtained. TiC displayed good resistance to the BF_3 medium, while pyrolytic graphite offered the best resistance. In the H_2O medium, graphite, TiB_2, and ZrB_2 completely eroded away.

It is recommended that scale-up from batch to a continuous process be carried out for the preparation of titanium diboride and that investigations be undertaken to determine the feasibility of scale-up for titanium carbide. Pyrolytic graphite fibers should be made by a continuous process to ascertain their potential strength and modulus, but if these do not fall at least in the range of 300 to 500 kpsi tensile and 20 to 30 million psi modulus, further development should be stopped.

Investigations should be continued to show the feasibility of preparing fibers of zirconium diboride and, when feasibility is established, scale-up should be pursued. Scale-up for tungsten coated boron is feasible, but should be given a lower priority than the other fibers because of its relatively low melting temperature. It is also recommended that an investigation be conducted of the high-temperature structural and chemical behavior of the recommended fibers. The effect of temperature and composition of these fibers on their metallurgical stability, mechanical properties, and chemical resistance should be investigated.

I. INTRODUCTION

Ablative liner materials, used to cool the thrust chambers of liquid-propellant rocket engines, permit simplification of design and operation by eliminating the requirement for pumping liquids to provide regenerative or transpiration cooling. Current liner materials appear to be marginal with propellants such as N_2O_4/50 percent N_2H_4/50 percent UDMH or LO_2/LH_2. The more-energetic propellant systems, such as F_2/H_2 or OF_2/B_2H_6, demand more-effective ablative composites in order to function satisfactorily. This is because of their higher flame temperatures, more-corrosive combustion products and, in some cases, increased erosion due to the presence of solid particles.

Ablative resins currently used, or improved resins now being developed, are capable of absorbing the heat from the motor, but they require reinforcing fibers with properties such that the resulting composites will have adequate strength to endure the physical demands. This means that the majority of liner improvements must come from new and improved fibers. Accordingly, this program is concerned with the development of reinforcing fibers that will lead to more-effective ablation composites for use in advanced liquid-fuel rocket-engine thrust chambers.

The investigation is divided into three tasks: (1) definition of properties and selection of fiber materials, (2) investigation of the feasibility of preparing these materials in fiber form by chemical vapor plating, and the subsequent testing of the fibers produced, and (3) recommendations of fibers for further development.

The results of this program serve as a basis for evaluating the probability of success of developing reinforcing fibers for advanced liquid-fuel rocket-engine thrust chambers and also provide the foundation upon which scale-up to continuous fiber preparation may be pursued in future work.

The authors wish to acknowledge the major contributions of: J. A. Haefling, Jr. who conducted the study of TiC fibers, the pyrolytic graphite fibers prepared from carbon precursors other than acetylene and the TEI arc plasma studies; of Barbara G. Fox who conducted the fiber evaluations including metallographic examinations; of L. J. Parcell for the material selection portion of the program; and of H. P. Woods who carried out the pyrolytic graphite studies using acetylene and the preliminary studies of tungsten on boron and zirconium diboride. The various chemical vapor plating units were effectively operated by J. P. Brown, Jr. and L. R. Taylor, who conducted the fiber preparation experiments.

II. DEFINITION OF PROPERTIES AND SELECTION OF FIBERS

The definition of properties and the selection of fibers have been based on several factors. The properties desired are indicated by a consideration of the ablation process. A number of candidate materials were selected as favorably meeting these properties. As a screening process, chemical reactivity with the propellant combustion products was considered, using published technical information as a guide, and with calculations under equilibrium conditions being conducted. Experimental arc plasma evaluations of a number of materials, under conditions simulating OF_2/B_2H_6 propellants were carried out. And finally, based on these factors and the feasibility of producing the fibers, recommendation for preparation of certain fibers was made. The details are presented in the following sections.

1. Process of Ablation

A qualitative picture of the ablation of a fiber-reinforced phenolic resin, which is one of the more effective liners, may help in indicating the types of materials problems involved. In the combustion zone, heat is transferred from the flame to the liner by convection, conduction, and radiation. The liner temperature begins to rise at a rate influenced by the rate of heat inflow from the flame and the heat conducted into the base of the liner. The temperature of the surface continues to rise until some phase or chemical change takes place on the liner surface. This may be represented by melting, vaporization, sublimation, or cracking of chemical bonds. In the case of the phenolic resin, this initially takes the form of charring in which the endothermic cracking liberates gaseous hydrogen and various fragmented C-H molecules. This phase change absorbs substantial amounts of energy. Furthermore, the evolved gases form a "blocking" action by increasing the gas film interference to heat flow from the flame which is often as much as 50 percent. The mass of evolved gas also increases the diffusional barrier which controls the chemical reaction rate between the products of propellant combustion and the liner materials.

The char of carbon conducts heat into the liner to the interface with virgin resin, where new charring is taking place. This region between charring and virgin resin regresses deeper into the liner with the generated gases absorbing heat as they emerge through the porous char and continue the blocking at the surface. As the char depth increases, the cooling effect at the surface is lessened and the surface temperature rises until the carbon char now begins to sublime. Thereafter, in the absence of physical or chemical erosion, the surface regression and the char-resin interface regression proceed at a relatively steady state for

the duration of the firing time. In the virgin resin, the temperatures are relatively low and the conductivity is such that the resin serves to insulate the outer wall of the rocket case.

Up to this point, the role of the fiber reinforcement has not been considered. The principal reason for the fiber is to provide strength to the liner and to prevent loss of the ablating material by spalling, by shearing action of the combustion gases, by thermal stresses, or by pressure rupture from the buildup of ablation gases inside the layer. It may also provide a heat sink by reacting with the matrix. Glass fibers are thought to react with the char type resins in a highly endothermic manner (1).

Initially the fibrous material will be protected from very high temperatures by the resin, but, as the latter begins to ablate at the surface, more of the fiber becomes exposed and its temperature will rise as that of the surface. Part of the heat will travel along the fiber, depending upon its thermal conductivity. As the temperature of the outer surface of the fiber increases, a phase change finally takes place. For most materials, melting occurs, but in some instances sublimation or chemical dissociation (analogous to charring or cracking of the resin) may occur. Thus, another possible advantage of fibers is that as the matrix recedes, radially disposed fiber stubs would provide a large surface area for endothermic phase changes, thus cooling the gas at the surface.

These phase changes absorb heat and help to hold down the temperature rise of the fiber. If the substance melts, it is preferable to have a high liquid viscosity and low surface tension to minimize removal by the combustion gases. The liquid remaining provides some protection to the ablation surface and absorbs appreciably more heat as it is vaporized. As an example, SiO_2, which has a higher liquid viscosity than Al_2O_3, is a preferred fiber even though it melts at a lower temperature than Al_2O_3.

The portion of the fiber below the surface is conducting heat into the resin mass. If the thermal conductivity is too high, internal charring of the resin may take place and, unless the gases produced can be adequately vented to the surface, the fibers may loosen or blow out of the matrix. This is why granular materials cannot be used as reinforcements and why fibers parallel to the flow of gases at the surface tend to peel off and allow chunks of liner to break loose. For this reason, fibers are usually embedded in the resin normal to the surface or else "shingled" at an angle in the direction of combustion gas flow. An alternate scheme makes use of randomly oriented, short fibers. Flake material would also be permissible provided the large face is normal to the surface.

In the absence of chemical or physical erosion, the thermal erosion or ablation of fiber and resin should reach a steady state and the total surface recede slowly and smoothly. In the combustion zone, in the absence of undesirable and correct-

able flame impingement, gas velocities at the wall are low, physical erosion is minor, and chemical attack from the combustion products is usually low. This results in part from the diffusion barrier or blocking offered by the emerging ablation gases.

At the nozzle throat and in the entrance and exit cones, the above conditions are no longer true. The sonic velocity of the combustion gas in the throat can cause physical erosion, especially if condensed solids are present. Also, the surface film which serves as a reaction barrier is largely swept away and chemical erosion increases. At the very place where conditions for all types of erosive loss are greatest, it is desirable to have a minimum of dimensional change. The throat should be kept as nearly constant as possible to maintain rocket efficiency. For very large diameter throats this is not as critical since the ablative dimensional change causes only a small percentage change in thrust.

It is at this location where end-grain pyrolytic graphite or tungsten inserts have been used with fair success. These, however, have problems and become more difficult to use as the diameter increases. Therefore, developments of a superior fiber composite with minimum dimensional changes is highly desirable.

2. Physical and Chemical Properties Desired of Ablative Fibers

The combustion environment has a great influence on fiber effectiveness. Pressure, fuel-oxidizer ratio, flame temperature, chemical reactivity with the fiber, velocity, and shear effects are all important and each fiber reacts differently. Strength, modulus, density, and melting point are initially important. If the fibers are inherently too weak, melt at temperatures which are too low, and have excessive density, they can be immediately discarded. Choice then rests on other factors. Table I lists a number of key properties and indicates the direction they should take.

Some of the property values should be as high as possible. This includes strength and stiffness to provide maximum integrity to the composite. The heats of phase change and the heat capacity should be as high as possible in order to more effectively absorb the heat from the thrust chamber. If the fibers sublime, as do carbon fibers, or dissociate as do some nitrides, then maximum heat is taken up. If the fibers melt there is chance for loss of liquid. However, if the melt is viscous enough to stay until it is evaporated, then more heat is advantageously absorbed. The net result of any of the above processes might be called the heat of ablation and a high figure is, or course, desired. The heat capacity of the solid is small in comparison to the heats of phase change but high heat capacity is wanted.

Table I

IMPORTANT PROPERTIES OF REINFORCING FIBERS

Values to be as High as Possible	Values to be Generally High	Values to be as Low as Possible
Strength and Stiffness	Temperature of Phase Change	Density
Heat of Phase Change	Melting	Thermal Conductivity
Melting	Sublimation	
Vaporization	Dissociation	Coefficient of Thermal Expansion
Sublimation	Ablation	
Dissociation		
Ablation	Viscosity	Radiation Absorptivity
Heat Capacity	Isotropy	Difference between Melting and Boiling Point
Resistance to:		
Chemcial Reaction		Surface Tension
Physical Erosion		
Thermal Shock		

High resistance to thermal shock and chemical and physical erosion are obviously important. They will be discussed later in connection with some specific candidate materials.

Property values, which should be generally high, include temperature of phase change, isotropy, and liquid viscosity which has already been mentioned. Isotropic materials, with properties relatively uniform in the a, b, and c directions of the lattice, are generally less prone to problems at high temperature. For example, pyrolytic graphite and pyrolytic boron nitride, which have large differences in thermal conductivity, thermal expansion (a 15-fold difference for pyrolytic graphite), and strength in the c direction are possibly subject to thermal and physical shock damage and delamination.

The temperature at which phase changes take place for each material can affect its use in various circumstances. Rocket-propellant flame temperatures depend on chemical composition and the pressure. For fluorine-containing oxidizers these are apt to be high. The following tabulation shows theoretical flame temperatures for two combinations.

THEORETICAL FLAME TEMPERATURE FOR VACUUM EXHAUST AT MAXIMUM SPECIFIC IMPULSE (36)

Propellant	Chamber Pressure Psi	Temperature °C	Temperature °F
OF_2/B_2H_6	1000	4307	7785
	300	4047	7317
F_2/H_2	1000	3827	6921
	300	3627	6561

Flame temperatures for the F_2/H_2 system of 6500°F may give ablation surface wall temperatures up to 4040°F (2) or up to 5300°F for graphite heat-sink type nozzle liners (3). They will be somewhat higher for the OF_2/B_2H_6 system.

As far as phase change is concerned, it would be well if the melting point were above the wall temperature, but sublimation or dissociation temperatures may be somewhat lower and by their very endothermic act reduce the wall temperature below what it would otherwise be.

Table I also shows those properties whose values should be as low as possible. Low density means desirable low weight for the finished composite or means

that a thicker ablation liner may be used for better protection at equivalent weight. The need for low thermal conductivity has already been indicated. Low thermal expansion decreases the possibility of thermal shock and delamination. If dissimilar materials are bonded or composited, similar expansion properties are desired.

Radiation reflectivity can be an important factor in the rate of heat absorption from the high-temperature flames. Since the composite and fiber can not re-radiate to a colder temperature as can an atmospheric re-entry ablator, high emmissivity is not needed, but a high reflectivity is desired. With less radiant heat from the flame, the convective and conductive heat transfer can be more easily handled by the ablative composite.

Finally, for fibers which melt, they will be more readily retained on the surface of the liner if the surface tension of the liquid is low and the wall is wetted. Also, chances of loss are reduced if the material boils at only a small temperature difference above the melting point. The vaporization then can contribute to heat absorption.

3. Candidate Fiber Materials

In view of the above discussion of properties, some candidate materials shown in Table II were subject to further analysis. These included boron, borides, carbides, nitrides, oxides, mixed oxides and silicates. All the materials, with the exception of SiO_2 which is shown for comparison, and Si_3N_4 which sublimes, have melting points above 2000°C (3600°F) and densities below 8 gm/cm^3. Some refractory fibers with higher densities are not shown but should be considered subsequently if outstanding properties can override their undesirable weight. Strength properties of the various substances are not shown because their fiber strengths are not generally established and bulk strengths are apt to be misleading.

As a group, the melting points of the carbides are highest, followed in decreasing order by borides, nitrides, and oxides. Thermal conductivities, with a few exceptions, are of the same order of magnitude at room temperatures and they tend to decrease at high temperature. Coefficients of expansion show some differences but in themselves can not eliminate any candidates. Initial choice of the more favored candidates was based in part on possible chemical erosion. A description of characteristics of several fiber groups follows:

a. Carbides

The carbides are among the highest melting point materials known. They are

Table II

SOME PROPERTIES OF CANDIDATE FIBER MATERIALS

Fiber	Boil Pt. °C	Melt Pt. °C	Melt Pt. °F	Density	Thermal Conductivity cal/cm sec°C	Thermal Conductivity Temp. Range, °C	Coefficient of Thermal Expansion 10^{-6}/°C	Coefficient of Thermal Expansion Temp. Range, °C	References
Boron		2040	3704	2.35	0.003	20-80	8.3	RT	4, 5
Borides									
ZrB_2		3040	5504	6.17	0.058	23	6.63	RT-1200	6
					0.060	200			
NbB_2		3000	5432	7.21	0.040	23	7.9-8.3	RT-1200	
					0.062	200			
TiB_2		2980	5396	4.50	0.058	20	5.5-9.7	RT-1800	
					0.10	1000-1400			
90% ZrB_2-10% $MoSi_2$		2350	4262	6.1			8.22	RT-1350	
WB		2920							
Carbides									
ZrC		3375	6107	6.7	0.049	20	6.7	RT-1500	6
NbC		3500	6332	7.8	0.034	20	6.5	RT-1200	
TiC		3147	5697	4.93	0.066	20	7.7	RT-1500	
					0.012	3250			
SiC		2540	4604	3.21	0.10	20-425	3.9	RT-1000	
B_4C		2470	4478	2.5	0.065	20	4.5	RT-1000	
Nitrides									
ZrN		2980	5396	6.9	0.033	200	-		4
					0.013	890	9.35		
TiN		2950	5342	5.21	0.07	100			
					0.014	950	*		
BN		3000 (subl)	5432	2.34	0.0035**	o			
					0.007	800			
AlN		2230	4046						
NbN		2300 (decomp)	4172	8.4					
Si_3N_4		1900 (subl)	3452	3.44					
Oxides									
MgO	2825	2800	5072	3.58	0.086	100	14.0	RT-1400	4
					0.016	1600			
ZrO_2	4300	2677	4851	6.1	0.0047	100	5.5	RT-1200	
					0.0058	1400			
Al_2O_3	2980	2015	3659	3.97	0.072	100	8.0	RT-1580	
					0.015	1600			
SiO_2	2950	1728	3142	2.32	0.016		5.2	RT-1250	
					0.030				
Silicates									
$ZrO_2 \cdot SiO_2$		2420	4388	4.6	0.014	200	5.5	RT-1200	4
					0.0092	1400			
Others									
$SrO \cdot ZrO_2$		> 2700	4892	5.48					4

* Expansion larger than pyrolytic graphite in "c" direction, less than "a" direction.
** "a" direction 0.15 from 0-800°C

stable and compatible with other materials and are excellent under reducing conditions. They are more resistant to oxidation than graphite. They are subject to oxidation above 1832°F except for SiC which does not oxidize rapidly until near 3000°F (6). This is thought to be due to the intermediate formation of SiO_2 which tends to protect against further oxidation. Extreme brittleness has been a drawback but high purity fibers have been lacking on these compounds and results may show useful materials for ablation fibers.

Titanium carbide has the best tensile properties of the carbides at low temperatures and B_4C has the best strength-to-weight ratio of the carbides. Silicon carbide has been studied more than any other carbide and, because of its better oxidation resistance, is a good contender among this group.

b. Borides

Property data on borides are still rather limited but some general trends have been established (7). Borides have high melting points which are comparable to nitrides and oxides but are somewhat lower than carbides. They have extreme hardness and high thermal and electrical conductivity. Their corrosion resistance is similar to carbides and silicides but oxidation resistance at high temperature is only fair. They are stable in the presence of carbon. Zirconium diboride resists oxidation to about 1400°C (2552°F) and TiB_2 up to 1500°C (2732°F). The strength-to-weight ratio of TiB_2 is not exceeded by any bulk material in the range of 1600 to 2000°C.

c. Nitrides

Nitrides have extreme brittleness in bulk and pressed form, but fiber qualities have not been established. Although melting points are very high, the nitrides have a tendency to dissociate. In fact, Si_3N_4, AlN, and BN are reported to sublime which may mean only that they decompose below their melting point. This factor is of interest in ablation since most other fiber materials melt. Boron nitride is very anisotropic but has good oxidation resistance at 3000°F and, even at 4000°F, is superior to pyrolytic graphite. Titanium nitride can resist thermal shock but begins to show slight oxidation at bright-red heat (4).

d. Oxides

Refractory oxides are outstanding for resistance to oxidation but, unfortunately, do not retain strength at high temperatures as well as some other materials. However, they have merited study both because strength characteristics for

pure filaments may be better than heretofore recognized and because it may be advantageous to deposit them over stronger substrates which are not so highly oxidation resistant. Magnesium oxide has the highest melting point and lowest density but does go through an undesirable crystal phase change. Zirconium dioxide also undergoes a phase change at 1000°C but has good oxidation resistance and, like SiO_2, may have a favorable high viscosity when melted.

e. Boron

Boron, with a low density and great stiffness, has one of the best strength- and modulus-to-weight ratios of the fiber materials. Although it may be subject to considerable oxidation, it should make an excellent substrate to which could be applied coatings of more refractory materials which would themselves be too heavy. For example, tungsten nozzle inserts appear to work quite well but are very heavy. Use in large nozzles, therefore, becomes questionable. However, a thin tungsten coating on a strong boron fiber could make a major reduction in weight.

It is also of interest that nylon and similar organic fibers make excellent ablating fibers with phenolic composites. They are good to quite high temperatures but, because of fiber weakness, are not effective when erosion occurs. Use of light weight boron for stiffness and strength and coated with the charring nylon may make an excellent fiber.

Several programs have been carried out under Air Force sponsorship to analytically assess the extent of reactions between possible liner materials and propulsion products (2, 8, 9, and 10). For fluorine-containing oxidizers the principal corrosive product is HF. The only outstanding materials known to resist HF are carbon and tungsten. In fact, with these substances the HF corrosion is not so severe a problem as generally believed (2). However, ZrO_2, SiO_2, ZrC, SiC, TiC, and BN were found in an increasing order to be reacted with HF under equilibrium conditions at high temperature.

With propellants producing CO_2 and H_2O, these were found to be strong oxidizing agents (2). They react quantitatively with all the carbides and strongly with BN. No reaction is indicated for SiO_2 or ZrO_2 but some attack of carbon is shown.

On the basis of the above discussions, the following candidate materials appeared to merit further consideration in choosing new fibers. They are:

a. Carbon
b. Boron
c. TiB_2
d. ZrB_2
e. B_4C
f. SiC
g. TiC
h. BN
i. Si_3N_4
j. TiN
k. MgO
l. ZrO_2
m. ZrO_2-SiO_2
n. Boron coated with nylon
o. Boron coated with carbon
p. Boron coated with W
q. Carbon coated with W

4. Chemical Reactivity

The chemical reactivity of fibers with the gases of combustion and with the matrix are an important factor in their usefulness. Chemical-equilibrium calculations reported in the literature, as well as those conducted under this program, serve to indicate the relative resistance of candidate fibers. These calculations, however, do not reflect the kinetics involved and are indicative only of a possible order of merit. Experimental screening, to be subsequently discussed, is also necessary.

a. Equilibrium Calculations Reported in the Literature

The reactivity of the candidate materials with various gaseous systems at equilibrium have been reported and these data are summarized in Table III. The results differ from system to system as would be expected and differ somewhat between investigators, depending upon various assumptions and conditions used. For the OF_2/B_2H_6 system investigated by Rindal and coworkers (Ref. 11 and 12), ZrO_2 shows the least reactivity, considering only chemical equilibrium. This is followed by the other materials shown in Table III, with low reactivity, in general, being shown by BeO, W, C, and B_4C. Somewhat higher reactivity, but still acceptable, is indicated for HfO_2, HfB_2, TiB_2, and TiC. However, when surface temperatures, melting points of the solid phase, and other factors are considered, the resulting calculated linear recession rate of the surface produces a somewhat different order. Titanium diboride, HfB_2, C, B_4C, W, and TiC appear attractive, with the oxides generally having higher rates.

In the study by Batchelor and coworkers (2), using H_2 or CO, they found carbon, ZrO_2, and several carbides to be satisfactory. In fluoride systems, the carbon exhibited the lowest reactivity, ZrO_2 was somewhat more reactive, and

Table III

REPORTED REACTIVITY OF CANDIDATE MATERIALS AT EQUILIBRIUM

Gaseous System	Conditions	Increasing Order of Equilibrium Reactivity		Increasing Order of Linear Recession Rate	Reference
OF_2/B_2H_6	5.8 oxidizer-to-fuel ratio 50 psia	ZrO_2 BeO B_4C W C HfO_2 HfB_2 TiB_2		HfB_2 C TiB_2 B_4C W BeO HfO_2 ZrO_2	11
OF_2/B_2H_6	3.0 oxidizer-to-fuel ratio 100 psia	ZrO_2 W BeO C B_4C HfO_2 TiB_2 TiC		TiB_2 B_4C C W TiC BeO HfO_2 ZrO_2	12
		Reactivity of Solid Substances			
		Slightly	Moderately	Highly	
H_2, CO Individually	1 atm	C ZrO_2 SiC ZrC TiC TaC BN			2
HF, BF_3 Individually	1 atm	C	ZrO_2 SiO_2	SiC ZrC TiC TaC BN	2
CO_2, H_2O HBO_2, BOF Individually			ZrO_2 SiO_2	C SiC ZrC TiC TaC BN	

the carbides showed rather high rates. With oxygen containing systems, carbon and the carbides did not show up well, but the oxides were only slightly affected.

b. Equilibrium Calculations Conducted for this Program

To extend the information available from the literature, a series of equilibrium calculations was made as shown in Table IV. The calculations were performed by the Service Bureau Corporation*. Four temperatures from 2000 to 3000°C were chosen to bracket the anticipated wall temperature of a thrust chamber. All calculations were made at a pressure of 300 psia but several were repeated at 100 psia to determine the effect of lower pressure. Because of the indicated low recession rate in the literature for HfB_2 and TiB_2 and the low reactivity of ZrO_2, it was believed that ZrB_2 would show promise. Accordingly, this was compared to ZrO_2, HfB_2, and HfO_2. Zirconium carbide and ZrN were included to observe the effect of other functional groups on the Zr compounds. Carbon (graphite) was included to determine the effect of the char on the equilibrium composition.

The results of the equilibrium calculations are shown in Figs. 1 through 12, and a typical computer print-out is shown in Table V. The basic data for the program were taken from the JANAF Tables (13) but data for the hafnium compounds were taken from Oliver and Baier (14). Figures 1 through 4 show the ratio of the mass of solid consumed at equilibrium to the mass of reaction gas at equilibrium at various temperatures. It is seen that ZrO_2 and HfO_2 are the least reactive of the compounds in either system, and that they are somewhat more reactive in the F_2-H_2 system than in the OF_2-B_2H_6 system. The materials ZrB_2 and HfB_2 alone look quite promising, but in the F_2-H_2 system, the presence of carbon causes increased reaction.

Figures 1 and 2 also show the effect of reducing pressure from 300 to 100 psia at 2700°C. The degree of chemical erosion was substantially the same at both pressures and it is believed that no change in relative ratings of the materials occurs at the lower pressure.

Figures 5 through 12 indicate what happens to the initial material as it disappears in the equilibrium reactions. Generally, the material is converted to another condensed phase, depending on temperature, and is seldom lost entirely as a reaction gas. In the presence of oxygen and fluorine, the oxide or fluoride condensed phases are formed. In the presence of carbon, represented by the char,

* The Service Bureau Corporation, 2450 Watson Court, Palo Alto, California

Table IV

CHEMICAL EQUILIBRIUM CALCULATIONS MADE FOR F_2/H_2 (MOLE RATIO 1.0) AND OF_2/B_2H_6 (MOLE RATIO 3.0) OXIDIZER/FUEL SYSTEMS

Temperature, °C	2000	2300	2700		3000
Pressure, psi	300	300	300	100	300
Candidate Material					
ZrB_2	X	X	X	X	X
ZrB_2 + C	X	X	X	X	X
HfB_2	X	X	X		X
HfB_2 + C	X	X	X		X
ZrC	X	X	X	*	X
ZrN	X	X	X	X	X
ZrO_2	X	X	X	X	X
HfO_2	X	X	X		X

* ZrC calculation made at 100 psi for OF_2/B_2H_6 but not F_2/H_2.

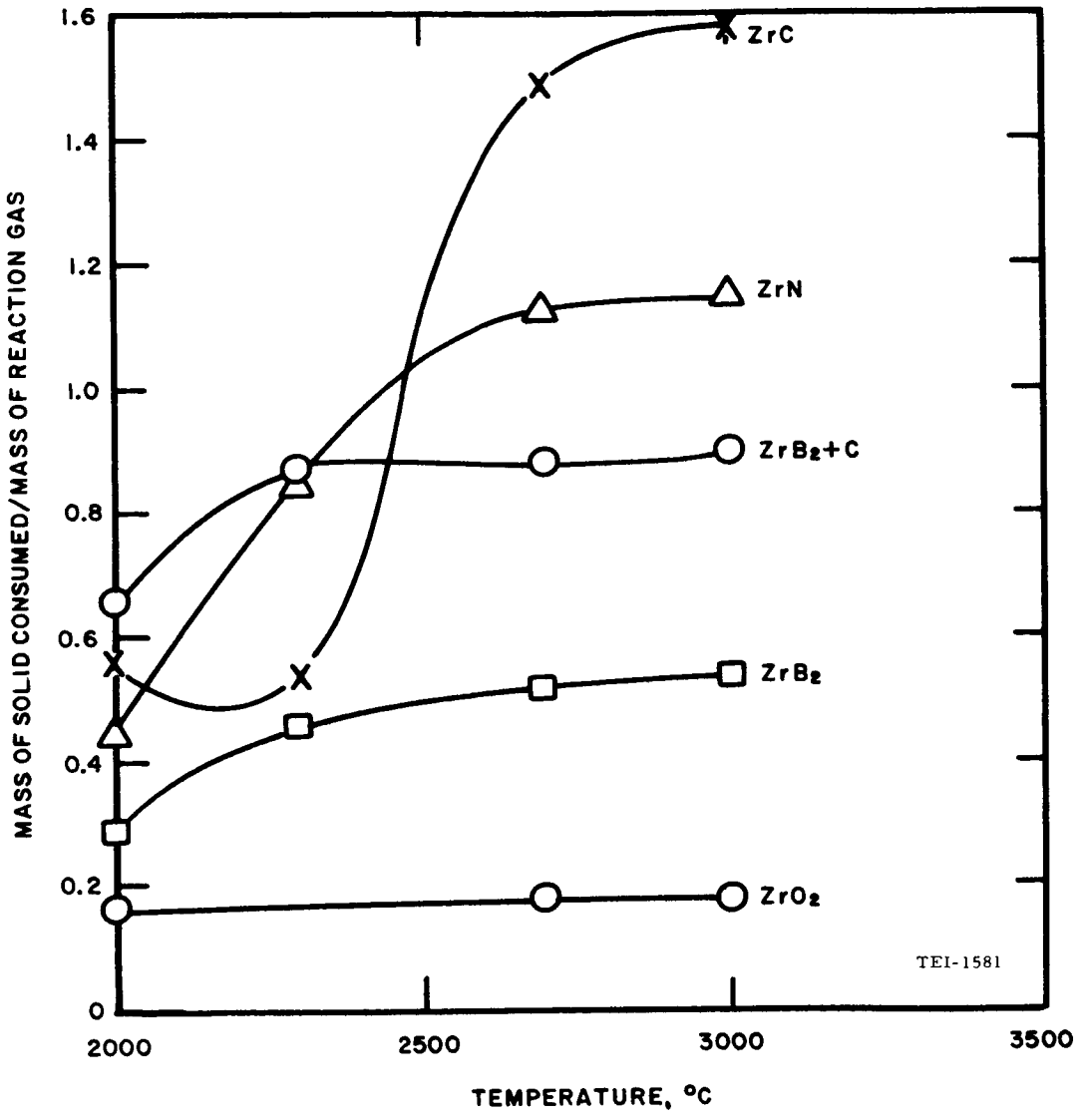

Fig. 1 Degree of Chemical Erosion of Zirconium Compounds in F_2/H_2 (Mole Ratio 1.0) at Equilibrium

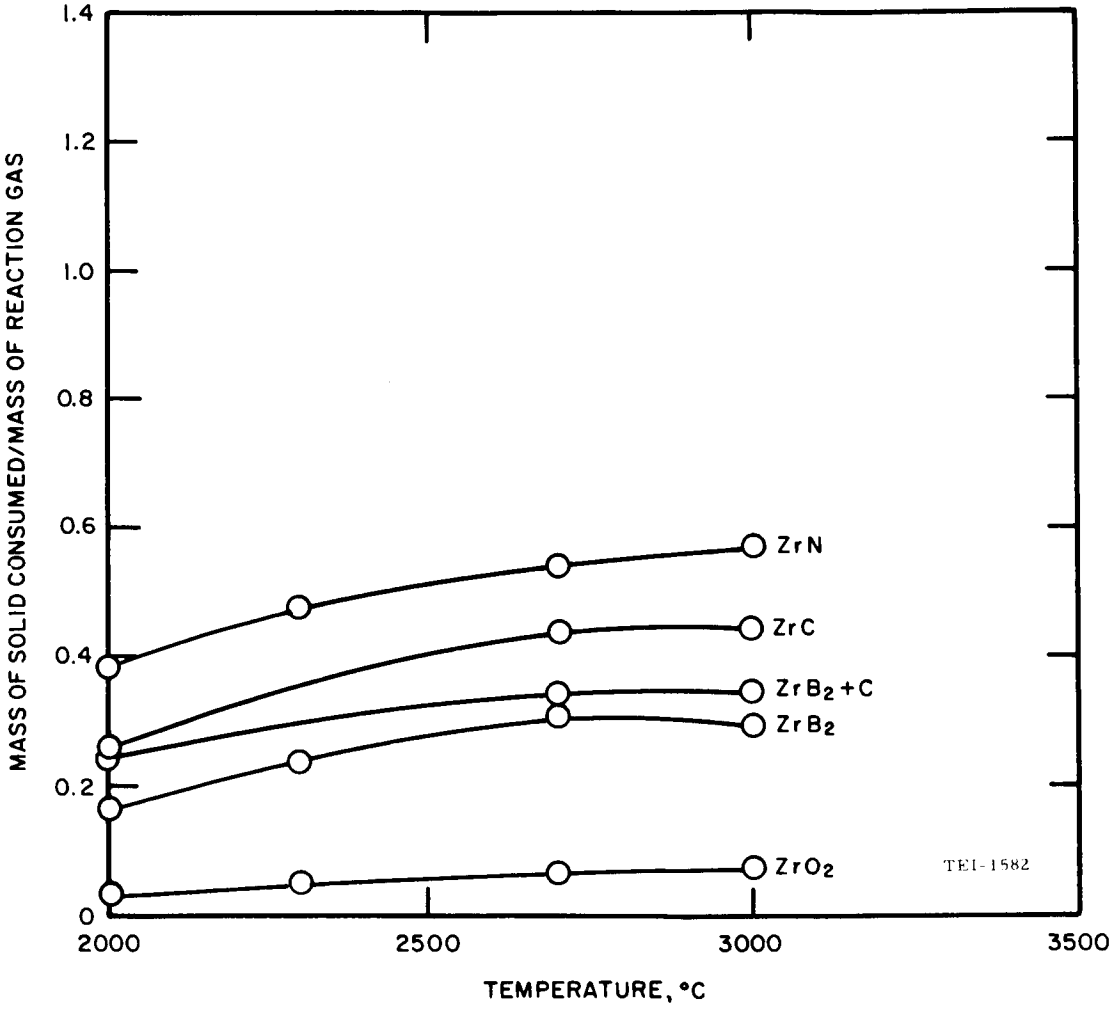

Fig. 2 Degree of Chemical Erosion of Zirconium Compounds in OF_2/B_2H_6 (Mole Ratio 3.0) at Equilibrium

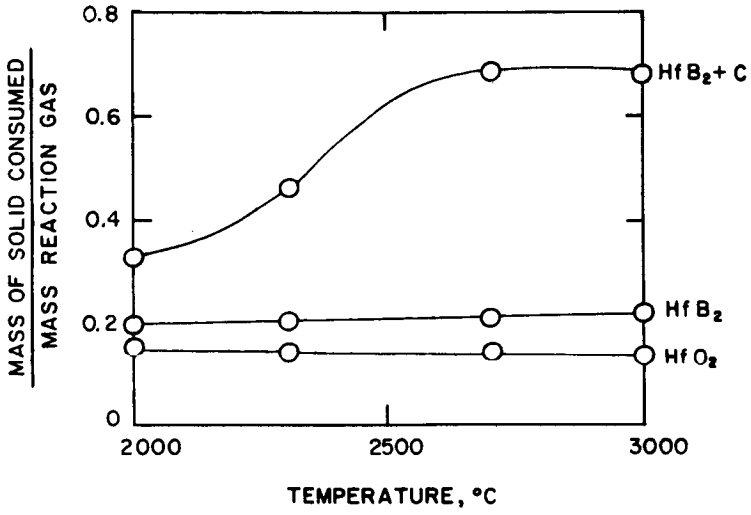

Fig. 3 Degree of Chemical Erosion of Hafnium Compounds in F_2/H_2 (Mole Ratio 1.0) at Equilibrium

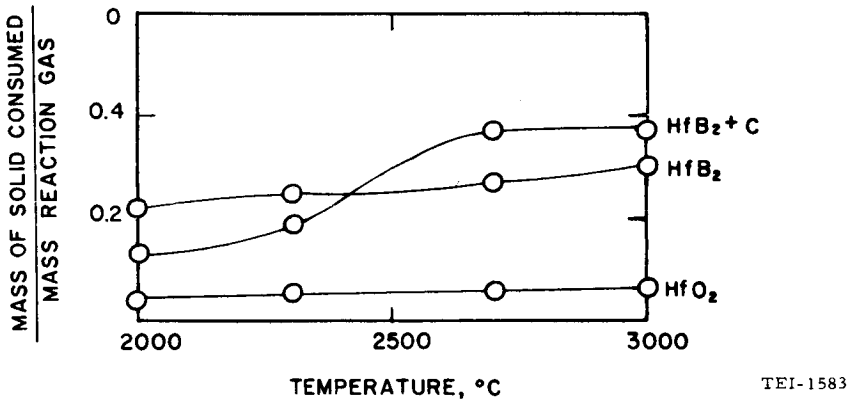

Fig. 4 Degree of Chemical Erosion of Hafnium Compounds in OF_2/B_2H_6 (Mole Ratio 3.0) at Equilibrium

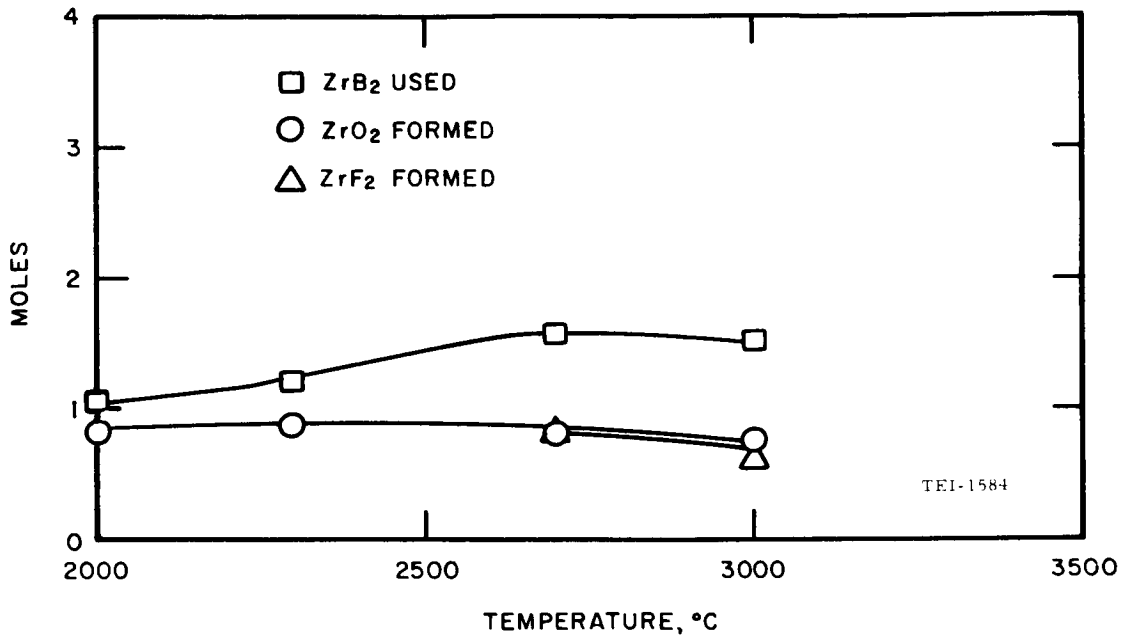

Fig. 5 Disappearance of ZrB_2 and Appearance of Condensed Phase in OF_2/B_2H_6 (Mole Ratio 3.0)

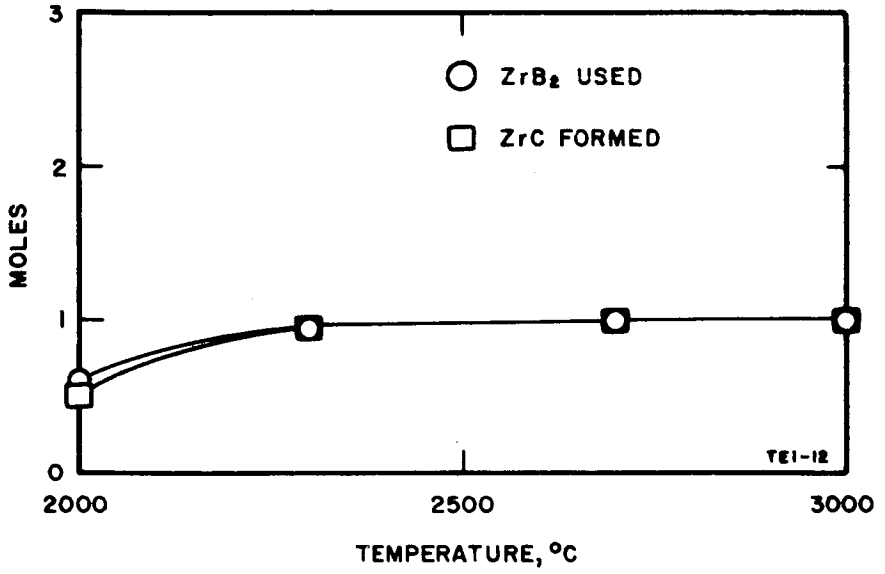

Fig. 6 Disappearance of ZrB_2 in C and Appearance of Condensed Phase in F_2/H_2 (Mole Ratio 1.0)

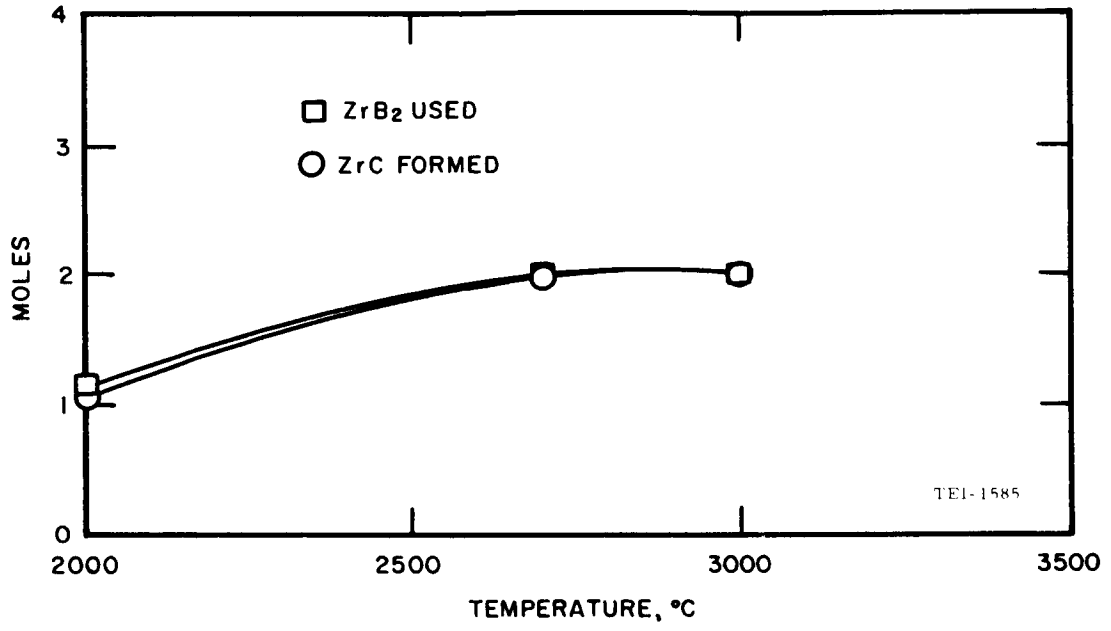

Fig. 7 Disappearance of ZrB_2 in C and Appearance of Condensed Phase in OF_2/B_2H_6 (Mole Ratio 3.0)

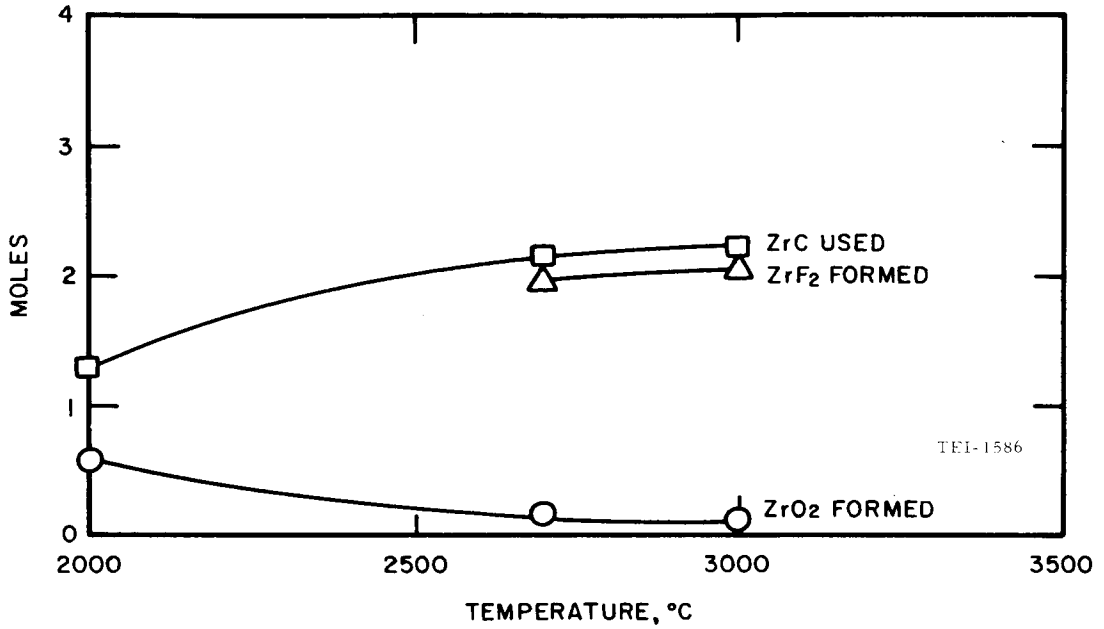

Fig. 8 Disappearance of ZrC and Appearance of Condensed Phase in OF_2/B_2H_6 (Mole Ratio 3.0)

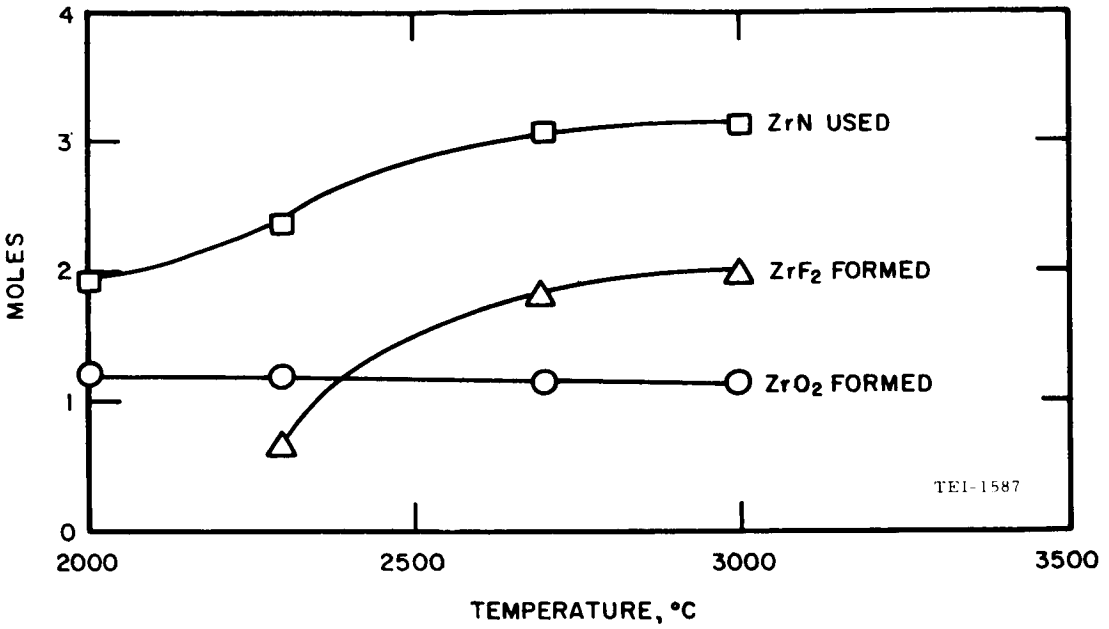

Fig. 9 Disappearance of ZrN and Appearance of Condensed Phase in OF_2/B_2H_6 (Mole Ratio 3.0)

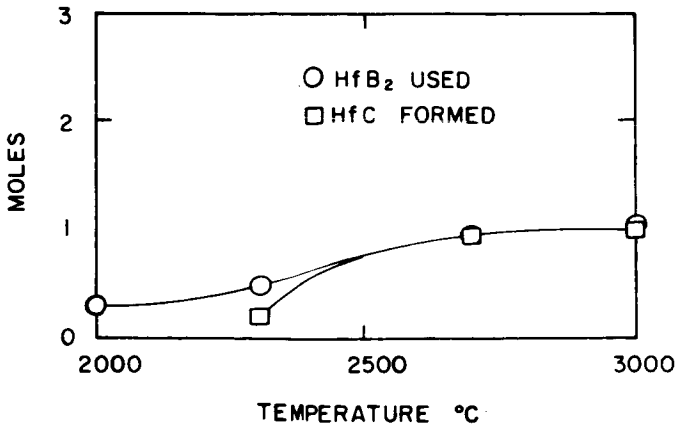

Fig. 10 Disappearance of HfB_2 in C and Appearance of HfC in F_2/H_2 (Mole Ratio 1.0)

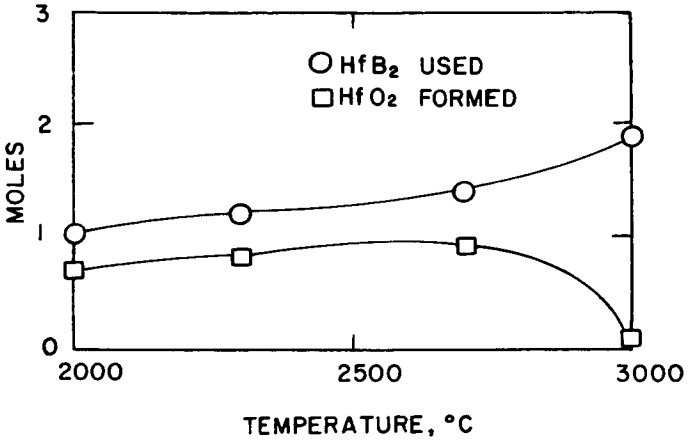

Fig. 11 Disappearance of HfB_2 and Appearance of HfO_2 in OF_2/B_2H_6 (Mole Ratio 3.0)

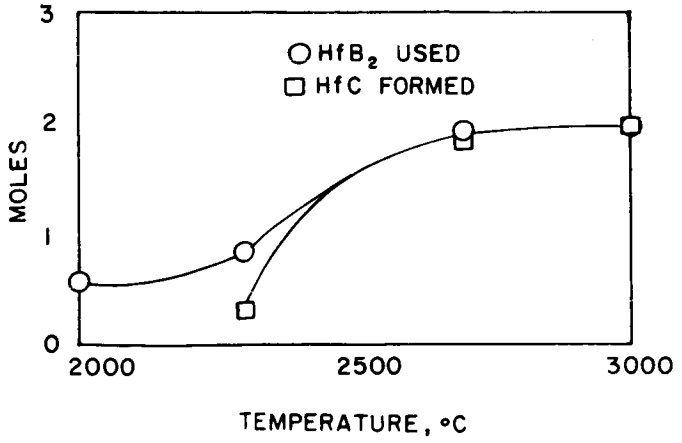

Fig. 12 Disappearance of HfB_2 in C and Appearance of HfC in OF_2/B_2H_6 (Mole Ratio 3.0)

Table V

TYPICAL COMPUTOR PRINT-OUT OF AN EQUILIBRIUM CALCULATION

CHEMICAL EQUILIBRIUM ANALYSIS

CASE 1

ELEMENTS IN REACTANTS, ATOMS		FUEL	OXIDIZER
H	2.0000	2.00	0.
F	2.0000	0.	2.00
B	2.0000	2.00	0.
Zr	1.0000	1.00	0.
RATIO O/F	1.0000		

	CHAMBER
PRESSURE, ATM	20.4137
TEMPERATURE, DEG K	2273.1498
HEAT CAPACITY, CAL/DEG K	37.8064
ENTHALPY, KCAL	-155.3077
ENTROPY, CAL/DEG K	147.8730
MOLS OF GAS	1.8576
MOLECULAR WEIGHT	59.1813
DENSITY, GM/CC	0.009006210

PRODUCTS OF COMBUSTION, MOLS		
H		2.4808602E-03
F		2.0493416E-07
B		5.3162334E-08
Zr		6.9659327E-12
BF		3.9981699E-01
BF_2		4.6456487E-03
BF_3		1.4435567E-01
BH		1.3186120E-07
BH_2		1.3858955E-05
BH_3		6.9868537E-05
B_2		8.1636266E-14
B_2H_6		2.2182924E-12
B_5H_9		4.4642293E-25
$B_{10}H_{14}$		0.
HF		6.6309067E-02
ZrF		1.7661513E-06
F_2		6.1783597E-16
ZrF_2		4.1331841E-05
ZrF_3		6.2005956E-03
ZrF_4		2.6820855E-01
H_2		9.6548630E-01
ZrH		2.3062649E-11
ZrB_2	S	7.2554893E-01
ZrB_2	L	0.

SBC COMPUTING SCIENCES DIVISION, PALO ALTO, CALIF.

only the carbide is formed. For example, in Fig. 5, the ZrB_2 used is converted to ZrO_2, the most stable Zr compound. The ZrB_2 is known to form a dense adherent coating of ZrO_2 upon oxidation with oxygen (Ref 4). The ZrO_2 may act as a temporary protective coating to lessen further corrosion of the original compound. The same may also be true of the ZrF_2 liquid (which appears between 2300 and 2700°C) if it behaves as does molten SiO_2, (in silica-fiber ablation composites) and is not physically removed from the surface. Figures 8, 9, and 11 show the same general trends for ZrC, ZrN, and HfB_2 in the OF_2/B_2H_6 system where they disappear to form the corresponding oxide or fluoride.

Figures 6, 7, 10, and 12 show that, in the presence of carbon, the boride compounds are converted only to the carbide condensed phase when exposed to F_2/H_2 and OF_2/B_2H_6. This carbide formation may or may not be beneficial, depending on its final properties. The calculations in which carbon was used show that it is more reactive on a molar basis than the borides in the OF_2-B_2H_6 system. It has been found elsewhere (2) that carbon is quite reactive in any atmosphere containing such oxidizers as H_2O, CO_2, HBO_2, and BOF, but is quite stable in HF. It appears from these calculations and the literature results previously discussed that ZrO_2 and HfO_2 are the most stable materials for OF_2-B_2H_6 systems. The fiber strength of ZrO_2 is not well established, and may be adversely affected by a phase change which occurs about 1000°C, unless stabilized by a suitable additive such as MgO or Al_2O_3. The best choice of the zirconium compounds may be ZrB_2 since an adhering coating of ZrO_2 may be formed in the OF_2-B_2H_6 system. Because it is expensive and also dense, HfO_2 may not be desirable for fibers. Carbon is very unreactive in F_2H_2 systems, but is somewhat reactive in OF_2-B_2H_6 systems. Tungsten appears attractive in both systems but, because of its high density, is at a disadvantage, especially for large rocket motors. Therefore, consideration should be given to vapor plating it on a light, strong substrate such as boron to take advantage of tungsten's chemical resistance but at a lower effective density. The other materials of interest are B_4C, TiB_2, and TiC.

The above materials appear promising on the basis of equilibrium calculations, but this evaluation approach does not take into account the kinetics of reaction and the possibly large divergence from the equilibrium state in an actual ablation reaction. Therefore, the list of good candidates may be enlarged by the results of experimental evaluations which are discussed in the following section.

5. Kinetic Resistance to Chemical Erosion--Experimental Determination by the Use of a Plasma Jet

To obtain an experimental evaluation of the chemical resistance to various candidate materials, a series of samples was obtained for exposure to high temperature and corrosive gases. This evaluation was conducted for us by the Vidya Division of Itek Corporation, Palo Alto, California, using their arc-plasma generator. The materials sent to Vidya were representative of various refractory borides, carbides, nitrides, oxides, and certain other materials of interest. The samples were a nominal 1/4-in. diameter by 4-in. long and were, for the most part, prepared by powder compaction and sintering. A list of the samples together with the supplier, the density, the percent of the best literature values of density, and the rod diameter is given in Table VI. Fifteen materials were to be evaluated but zirconium silicate was sent as an extra in case one of the other samples could not be used.

The test program utilized the Vidya 300-kw arc-plasma generator. Appropriate gases were injected into the unit so that an exhaust stream was produced characteristic of the combustion products of the OF_2/B_2H_6 system with an oxidizer-to-fuel weight ratio of 5.85 (mole ratio of 3.0). Full details of the test are given in Ref. 15.

Initially it was planned that the arc-heated combination of boron trifluoride and steam would be used to satisfy the following idealized reaction.

$$1.581\ OF_2 + 0.527\ B_2H_6 \rightarrow 1.054\ BF_3 + 1.581\ H_2O$$

Attempts were made by Vidya to operate the arc-plasma generator using BF_3 as the arc-heated gas and introducing steam into a mixing plenum downstream from the arc. Mass fractions of 0.715 BF_3 and 0.285 H_2O were used.

Difficulty occurred, however, when portions of the injected steam condensed in the plenum and caused severe corrosion. After due consideration it was agreed that the steam should be replaced by an appropriate fraction of elemental oxygen. The resulting composition contained a mass fraction of 0.740 BF_3 and 0.260 O_2. The calculated composition for this mixture at 3227°C (3500°K) very closely duplicated the BOF content estimated for OF_2/B_2H_6 combustion. However, due to the absence of hydrogen, the new combination produced F atoms in place of HF and increased the O and O_2 content somewhat. It was believed that the new combination gave more severe corrosion to the specimens but that it gave a reasonable, comparative evaluation of the candidate materials.

It was desired to subject the specimen to a surface temperature of 2800°K on a 1/4 in. diameter rod. Graphite was chosen as a standard for comparison and

Table VI

SAMPLES EVALUATED IN THE PLASMA ARC

Material	Supplier	Measured Density	Percent of Best Literature Value	Rod Diameter, In.
1. Hafnium diboride	Cerac, Inc.	10.05	95.8	1/4
2. Titanium diboride	Cerac, Inc.	4.59	100.0	1/4
3. Zirconium diboride	Cerac, Inc.	5.26	95.7	1/4
4. Boron carbide	Cerac, Inc.	2.14	85.0	1/4
5. Silicon carbide	Carborundum Metals	3.44	100.0	1/4
6. Titanium carbide	Cerac, Inc.	4.85	97.8	1/4
7. Boron nitride	Carborundum Metals	2.27	98.9	1/4
8. Silicon nitride	Cerac, Inc.	3.08	96.3	3/8
9. Titanium nitride	Cerac, Inc.	5.01	92.8	1/4
10. Zirconium nitride	Cerac, Inc.	6.77	95.5	3/8
11. Aluminum oxide	Norton Co.	3.89	98.1	1/4
12. Magnesium oxide	Cerac, Inc.	3.45	96.4	1/4
13. Zirconium oxide	Norton Co.	5.67	98.3	1/4
14. Zirconium silicate	Cerac, Inc.	4.50	97.9	1/4
15. Boron	TEI	2.35	93.4	1/8 to 1/4
16. Pyrolytic carbon	High Temp. Materials, Inc.	2.08	93.7	1/4

preliminary tests revealed that a gas stream total temperature of about 3400°K was required. It was also found that the specimen models should be shortened from 4 to 2 in. to reduce their thermal capacity and radiated energy so that the desired surface temperatures could be attained. The 2 in. lengths were wrapped around the lower portion with an insulating material, Fiberfrax. This material was below the jet impingement region and served to wedge the specimens in the mechanical rod-holder.

The tests were conducted with an axisymmetric 0.5-in. throat diameter convergent nozzle with the test specimens positioned in cylinder cross flow, 0.3-in. from the nozzle exit plane. A total gas-flow rate of 0.0132 lb/sec. was used for all tests. The total flow was comprised of 0.00975 lbs/sec of BF_3 and 0.00345 lb/sec of O_2. The chamber pressure was 1.55 atmospheres.

The procedure involved adjusting the plasma arc to standard flow rates and electrical input, and then, by means of a mechanical arm, rotating the 1/4 by 2 in. long specimen into the flame. After a 30-sec exposure time, during which surface temperatures (radiation pyrometer) were about 2300-2400°C, the sample was removed and quenched by a stream of nitrogen, and a second sample was rotated into the flame. Still and motion pictures of the ablating specimen and a temperature history of the sample were obtained. Weight losses and diameters were measured.

During the runs a number of materials stood up remarkably well and although they "ablated" away during the high temperature exposure, the rate of loss and the temperature history could be measured. Some of the other substances broke during the runs, probably from thermal shock. This may or may not be indicative of their action if they had been in the form of high strength fibers rather than the available lower strength compressed and sintered form. Therefore, specimen fracture should not automatically cause a material to be rated as a failure. Several specimens, although breaking off, left a substantial portion in the flame and the rate of diameter change could still be measured reliably.

The results of the tests are shown in Table VII. The diameters of HfB_2, ZrO_2, BN, and ZrB_2 rods were taken from the motion pictures. In the calculation of the rate of erosion (mils/sec), the length of time at which the samples were above 2000°C (2273°K) was used instead of the total test time because of the different heating rates. The order of samples in resistance to erosion was: C, HfB_2, ZrB_2, TiB_2, TiC, BN, and SiC. Samples which showed good resistance before breaking were Al_2O_3, B_4C, and ZrO_2. The Si_3N_4 specimen, because of its 3/8 in. diameter, did not go above 1950°K and, therefore, showed a relatively small loss after 40 seconds of testing. Had the temperature exceeded 2200°K, sublimation is expected to have been serious. The TiN sample ablated rapidly and, at the same time, large fragments broke away.

Table VII

PLASMA ARC TEST RESULTS

Substance	Max Temp, °K	Diameter (in.) Initial	Final	Time Above 2273°K, sec	Erosion Rate mils/sec	Remarks
C	2670	0.251	0.186	22.5	2.9	
Al_2O_3	2500	0.244	-	2.0	-	Sample broke before ablation occurred
B_4C	2570	0.256	-	1.5	-	Sample broke before ablation occurred
TiB_2	2550	0.252	0.156	21.5	4.5	
TiC	2550	0.253	0.119	21.0	6.4	
HfB_2	2470	0.244	0.17	23.0	3.2	Top portion broke off but main portion remained in flame
Si_3N_4	1950	0.375	0.314	-	-	Sample ablated little because of its larger size and lower temperature
ZrO_2	1600	0.247	0.247	-	-	Sample broke after 5 sec. No ablation observed.
ZrN	-	0.376	-	-	-	Sample broke immediately
MgO	-	0.252	-	-	-	Sample broke immediately
BN	2450	0.274	0.216	6.0	9.7	
SiC	2500	0.288	0.040	23.0	10.8	
TiN	-	0.296	-	-	-	Sample ablated rapidly and broke
ZrB_2	2800	0.248	0.198	10.2	4.9	Plasma failed after 15 sec
ZrB_2	3000	0.254	0.200	21.5	2.5	Tip broke off before conclusion of run
B	-	0.125	-	-	-	Sample broke immediately

6. Recommendation of Materials for Fiber Preparation

Based on the experimental arc-plasma results, equilibrium calculations, literature estimates of corrosion, melting points, and other attributes of candidate materials, several fibers were recommended for preparation. A summary of pertinent information used in making the recommendation is given in Table VIII and the final choices are presented in Table IX.

Table VIII shows the calculated chemical resistance of 11 candidates and the relative experimental rating of 7 of the materials run on the arc plasma. Advantages, disadvantages, and the probability of successful preparation are also shown.

Graphite has indicated excellent theoretical resistance to F_2/H_2 and, although somewhat subject to oxygen reaction, was among the better materials for the OF_2/B_2H_6 system. In the experimental test it was ranked No. 1. Graphite has the advantage of being compatible with an organic ablation matrix and is relatively simple to prepare although its low plating rate is a disadvantage.

Hafnium diboride and zirconium diboride appear to have good resistance to chemical attack both by equilibrium calculation and by arc plasma test. The two materials would be quite similar in their properties and method of preparation. Because of the high density and relatively higher cost of the hafnium material, ZrB_2 is preferred and should be studied. Successful preparation was rated only probable in recognition of the fact that the plating compounds of Zr have low volatility and require high temperature vaporizers or sublimers and high temperature plating chamber walls to prevent condensation of the plating materials or the reaction products.

Titanium diboride has chemical resistance rated fair by equilibrium calculations and rated quite highly on estimated linear recession rate (see Table III). The arc plasma results looked quite promising and the probability of successful preparation was judged good. As will be discussed later, TiB_2 has a high Young's modulus and, therefore, a potentially excellent strength; it was considered one of the better candidates.

Titanium carbide chemical resistance is only fair by equilibrium calculations but experimentally it rated relatively well. It is compatible with the matrix and should have a good probability of preparation.

Boron nitride and silicon carbide do not show up well in the OF_2/B_2H_6 systems by calculation and were the most chemically attacked of the samples which could be rated by the arc plasma apparatus. They have some promise but do

Table VIII

MATERIAL EVALUATION SUMMARY

Fiber	Chemical Resistance: Calculated	Chemical Resistance: Experimental Rating *	Advantage	Disadvantage	Probability of Successful Preparation
C	Good	1	Compatible with matrix, simple to prepare	Low Plating Rate	Good
HfB_2	Good	2, Broke		High Density	Similar to ZrB_2
ZrB_2	Good	3			Probable
TiB_2	Fair	4	Potential very high strength and modulus		Good
TiC	Fair	5	Compatible with matrix		Good
BN	Poor	6, Broke		Reacts with water	Good
SiC	Poor	7		Forms low melting SiO_2	Good
ZrO_2	Best	Broke		Phase Change at 1000°C	Difficult
B_4C	Fair	Broke	Low density, compatible with matrix		Good
W on B	Good	-	Low density compared to W		Good
C on B	Good	-	Improved strength over C		Good

*Tests performed by Vidya Division of Itek Corporation.
Numbers refer to the relative rank of materials

Table IX

RECOMMENDED FIBERS FOR OF_2-B_2H_6 SYSTEM

1. Carbon
2. Tungsten Coated Boron
3. Titanium Carbide
4. Titanium Diboride
5. Zirconium Diboride
6. Zirconium Dioxide
7. Boron Carbide
8. Carbon Coated Boron

not appear as attractive as other materials being considered.

Zirconium dioxide has indicated the lowest calculated chemical attack and, therefore, merits attention. Unfortunately, the sample broke during the arc plasma run and was not effectively evaluated. Zirconium dioxide has a disadvantage in that it undergoes a phase change at 1000°C. This causes large dimensional changes and may result in structural failure unless the ZrO_2 is stabilized. This is accomplished in bulk form by incorporating several percent of oxides such as Al_2O_3, MgO, CaO, ThO_2, or others. The necessity of stabilizing the ZrO_2 fiber, possibly by coplating the stabilizing oxide, makes this a more difficult task for preparation by chemical vapor plating. Other methods such as electrophoretic fiber forming may be effective. Boron carbide has fair resistance as indicated by calculation but, unfortunately, it also broke during the arc plasma run. This material has the advantage of being compatible with the matrix and of having low density and probable high strength. No work was initially planned with B_4C under this contract since exploratory work was to be carried out for another agency. Preliminary results were encouraging but the program objectives were altered and no further work was planned on this compound. Boron carbide, therefore, does merit future attention.

Tungsten and graphite both have given good promise of chemical resistance to the fluorine-containing systems. Tungsten has, of course, been effectively used in rocket nozzles, but because of its high density is at a disadvantage, especially in large nozzles. Tungsten supported on a light, strong substrate would be desirable. Graphite, with excellent resistance, might be advantageously improved in strength by depositing it on a light, strong substrate. In both instances, boron appears attractive as a basic fiber to be coated by W or C. Boron with tensile strengths of several hundred thousand psi and a modulus of about 55×10^6 psi has a density of about 2.3 gm/cm^3. Its oxidation rate in fluorine-containing oxidizers alone would be high, but protected by W or C, should offer good resistance. The melting point of boron of 2040°C is somewhat lower than might be desired but it is over 1000°C above the softening point of glass and is 300°C above the melting point of SiO_2, the two most widely used ablation reinforcing fibers at the present time.

The final recommended list of fibers to be prepared is shown in Table IX. At a project review meeting with NASA personnel on April 21, 1965, it was agreed that in addition to work already carried out on pyrolytic graphite and tungsten coated boron, the effort during the remaining contract period would be concentrated on fibers of TiC, TiB_2, and ZrB_2. Other fibers would be prepared only if early success was achieved with the above and if time permitted.

III. PREPARATION AND TESTING OF FIBERS

1. Chemical Vapor Plating Equipment

A block diagram showing the essential elements of the batch-type chemical vapor plating (CVP) units used in this work is presented in Fig. 13. The heart of the unit is the deposition chamber, where deposition of the desired fiber material on a heated wire substrate was accomplished. Four distinctly different deposition chambers were used in this work; each is described in detail later.

The balance of the system is made up of gas-handling equipment, a power supply, and an optical pyrometer. The flows of the plating gases were measured by rotameters before the gases entered the deposition chamber. Most of the rotameters were calibrated by the procedure outlined in Appendix A, but, in some cases, flows were estimated using approximate relationships as described in the appendix in order to expedite the experiments.

A Welch R-1402 mechanical vacuum pump was used to obtain the desired pressures in reduced-pressure plating experiments and for pump-down/purging prior to the experiments. Pressures were measured with Helicoid gauges and absolute differential manometers. When the pump was used during the plating experiments, the exhaust gases from the deposition chamber were passed through cold traps to remove unreacted plating gases or reaction products which would otherwise be harmful to the pump. Dry ice/alcohol and dry ice/acetone mixtures were used to trap the higher-boiling-point materials such as BCl_3, $TiCl_4$, CCl_4, and CH_3CH_2Br. In most cases, to avoid plugging of the traps, the composition of the dry ice/alcohol mixtures was selected on the basis of providing temperatures which would liquefy but not solidify these materials. Liquid nitrogen was used in the second trap to remove HCl from the exhaust gases. In atmospheric pressure experiments, however, the exhaust gases were usually vented to the atmosphere through a stack.

The fibers were heated resistively with a variable-voltage, DC power supply through variable resistors in series with the fiber. The resistors reduced the effect of voltage fluctuations and also reduced the sensitivity of the Variac, thereby making possible smoother control of the current. DC power was used because it was learned in the initial experiments that AC power causes the substrate to vibrate violently. Manual power control was used in all experiments.

Fiber temperatures were measured with a Pyro Model 95 micro-optical pyrometer mounted on a tripod adjacent to the deposition chamber. The observed temperatures were used for control purposes only and no attempt was made to obtain

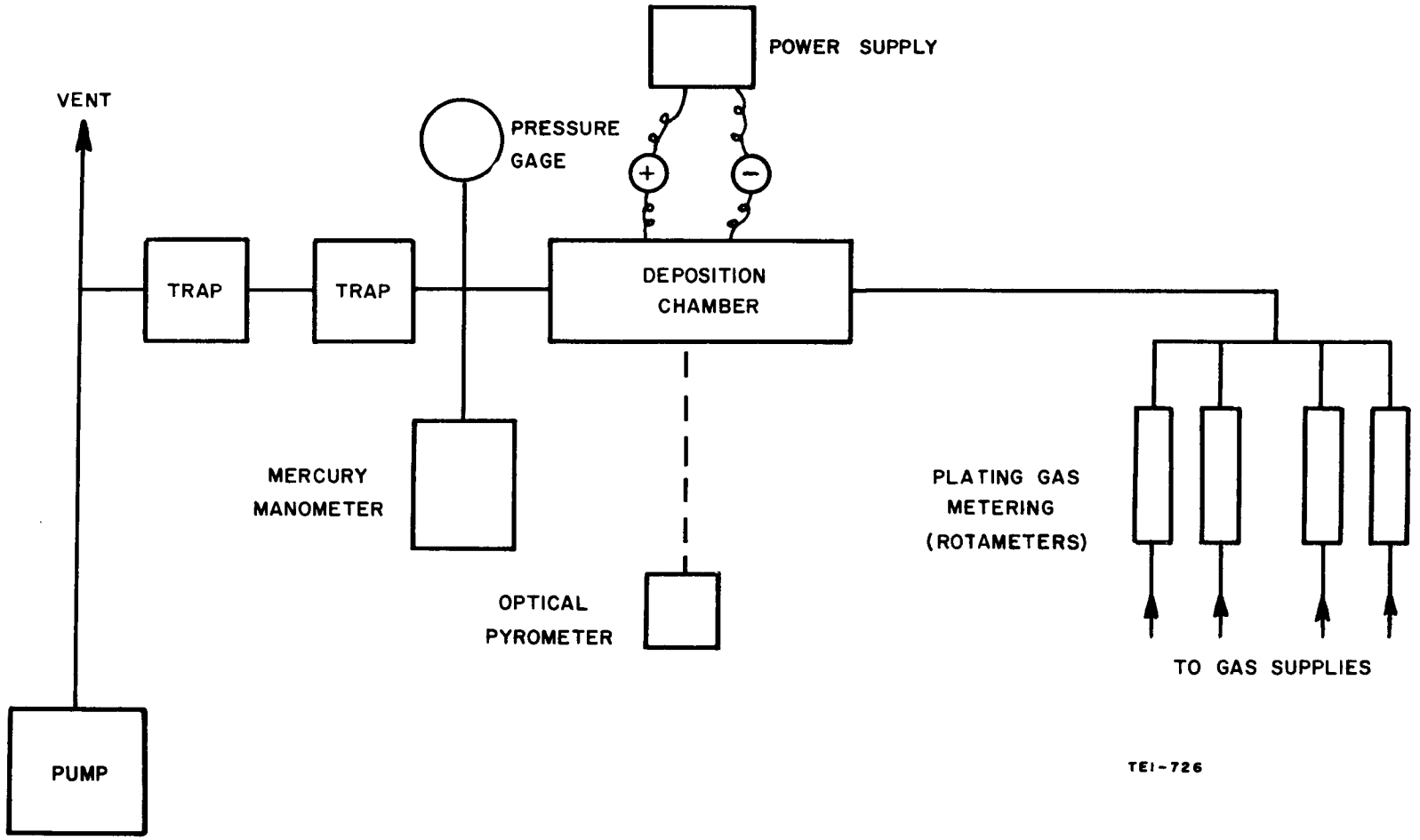

Fig. 13 Block Diagram of Chemical Vapor Plating Units

the true temperatures. No corrections were made for the emissivity of the fiber or for absorption of radiant energy by vapors in the deposition chamber or by condensed material on the chamber wall. As a general rule, temperatures were not read when vision was obscured by vapors or condensed materials on the chamber. The reproducibility of the observed temperatures was within about ± 50°C in the temperature range of 1000 to 1700°C. In some instances, we estimate that the true temperatures could have been 50 to 150°C higher than the observed temperatures.

The four deposition chambers used in this work are shown schematically in Fig. 14a, 14b, 15, and 16. They differ primarily in the way the substrate wire was mounted and the position of the substrate relative to the direction of flow of the gases. Other differences are apparent from examination of the illustrations.

Figure 14a shows Chamber A which is a parallel-flow chamber (i.e., gas flow is parallel or nearly parallel to the substrate). The tungsten electrodes are permanently fixed in a teflon plug, which permits installation and removal of the electrodes and substrate as an integral assembly through a 1-in. diameter port in the end plate. The substrate is tied to rhenium metal tabs at the ends of the electrodes. A small weight is attached to the substrate to maintain constant tension on the wire.

Chamber B, shown in Fig. 14b, is similar to Chamber A, except that the substrate is mounted differently, a vaporizer is provided for volatilizing liquid reactants, and a jet is provided for spraying a small area of the inside surface of the chamber with argon to minimize condensation of low-volatility reactants and reaction products. One end of the substrate is attached to the lower electrode tab and at the other end to a rhenium strip which is loosely coiled around the upper electrode to form a low-friction sliding contact. Tension is applied to the substrate by a dead weight acting over a teflon pulley and attached to the rhenium sliding contact by a 10-mil diameter wire. This arrangement eliminates the weight required at the center of the substrate in Chamber A and increases the length of straight fiber that can be produced. The argon jet tube maintains a narrow band of the deposition chamber parallel to the substrate relatively free of condensed vapors so that the effect of condensed vapors on the observed temperatures is minimized. The vaporizer consists of a reservoir of the liquid to be vaporized and a constant-temperature water bath which maintains the liquid at the desired temperature. A carrier gas is bubbled through the liquid with the intent of saturating the carrier with the vapor. Saturation is enhanced by injecting the carrier gas through a hypodermic needle so that small bubbles of the carrier gas pass through the liquid. The line carrying the vapor to the deposition chamber is heated by heater cords. Rough determinations of the vapor flow from the vaporizer were made by observing

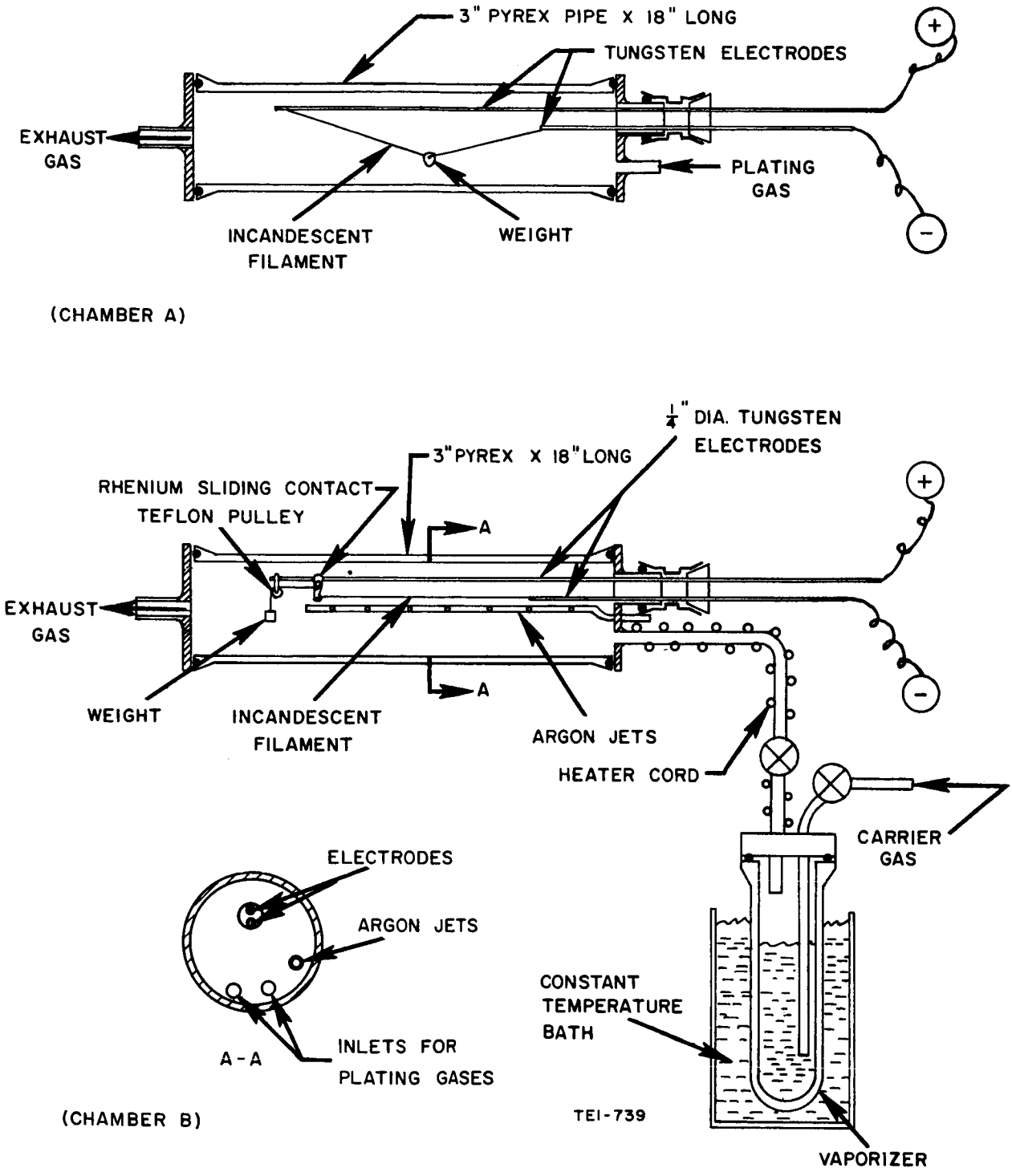

Fig. 14 Horizontal Deposition Chambers

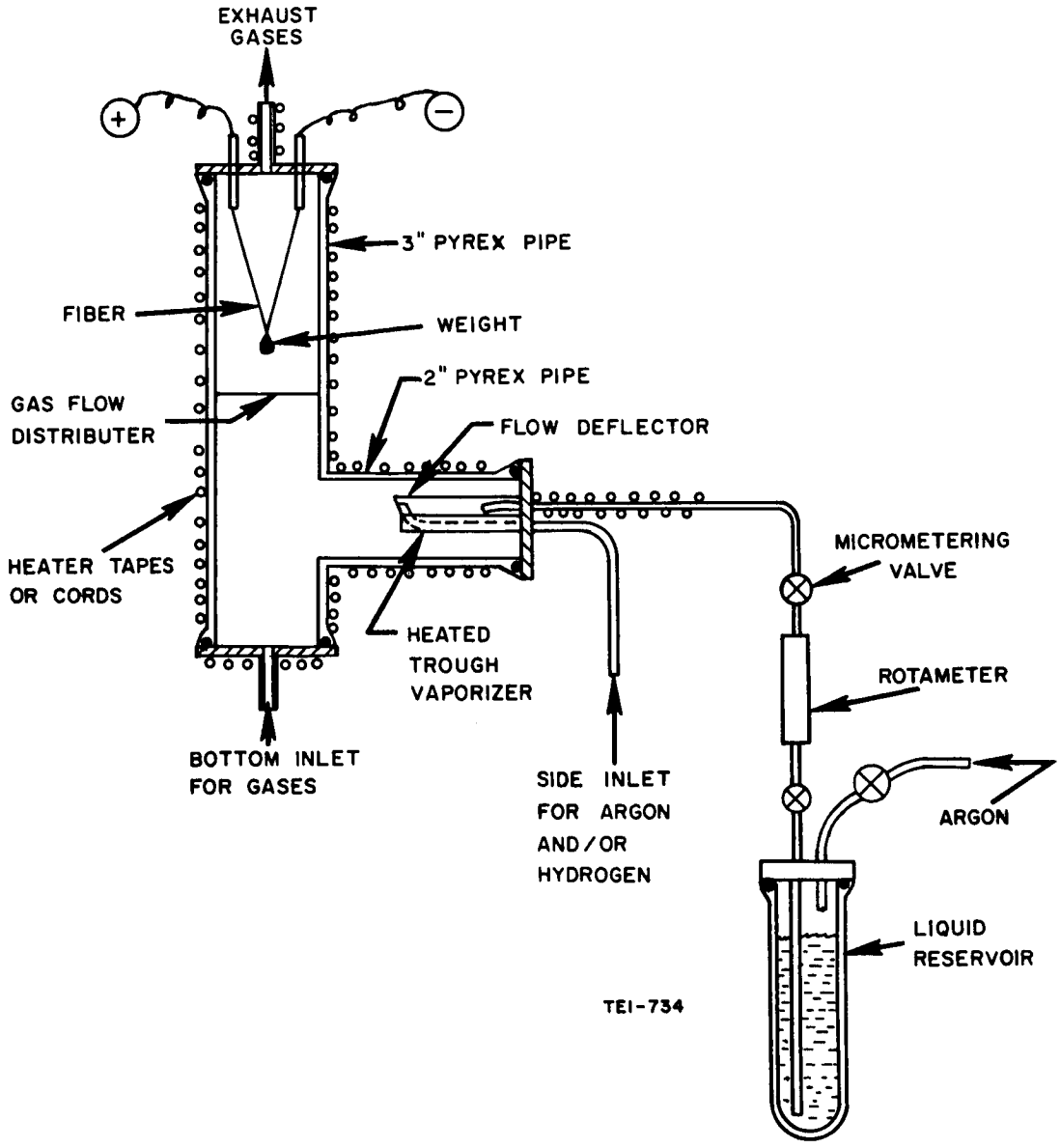

Fig. 15 Vertical Deposition Chamber C

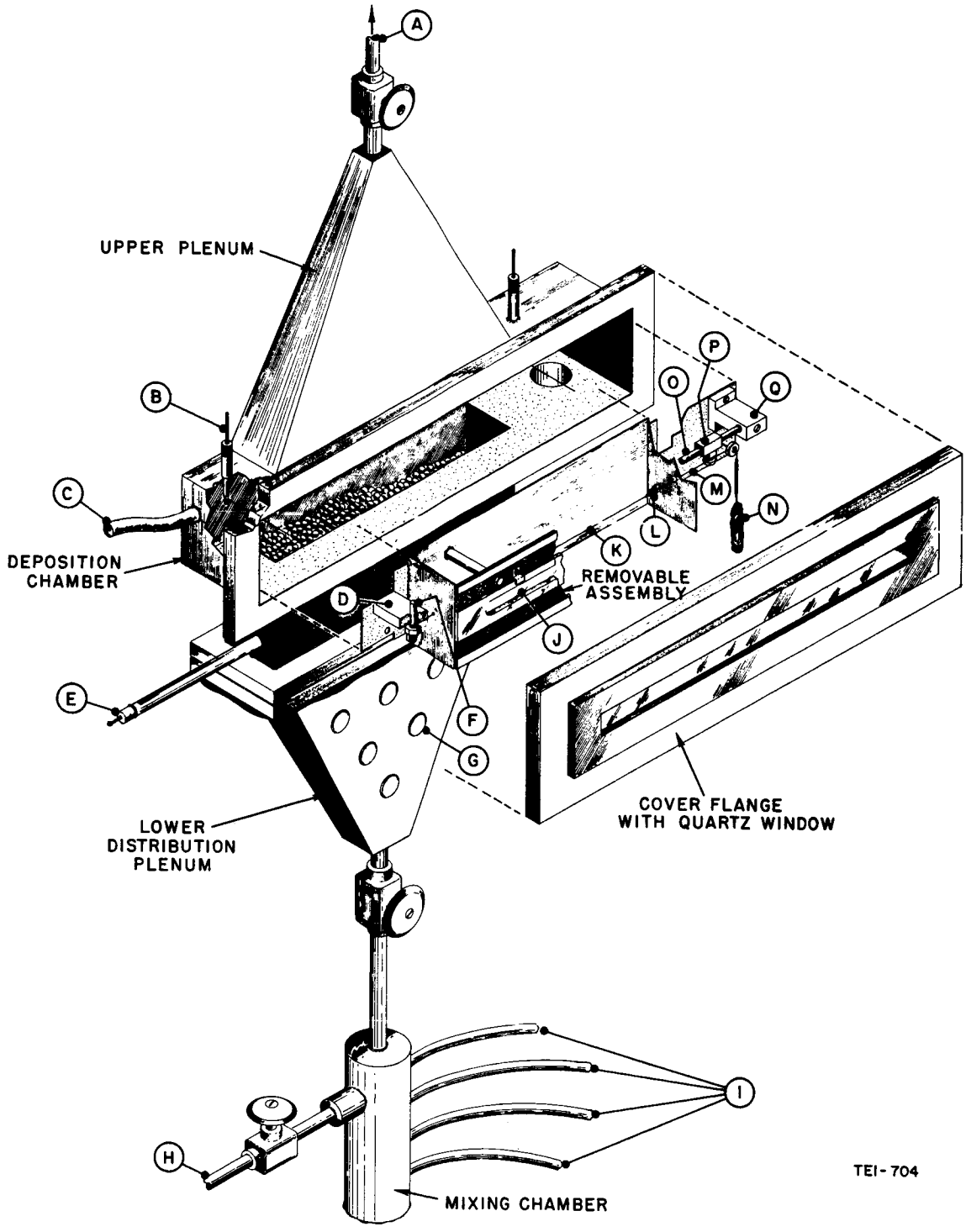

A. Exhaust Gases
B. Electrode Connections
C. Argon Purge - Both Ends
D. Teflon Mount
E. Heater
F. Electrode Connection
G. Plug Type Heater
H. Vent
I. Gas Inlet Lines
J. Quartz Window
K. Substrate
L. Rhenium Tab-Both Ends
M. 20 mil Tungsten-Rhenium Wire - Both Ends
N. Weight
O. Electrode Connection
P. Sliding Contact
Q. Teflon Mount

Fig. 16 Cross Flow Deposition Chamber D

the drop in liquid level over a time interval, usually a time period slightly longer than the duration of the experiment.

Deposition chamber C is shown in Fig. 15. The fiber is suspended from two tungsten electrodes mounted in the top flange of a vertical pyrex pipe. A small weight is used to keep the fiber taut. The plating gases enter from the bottom of the vertical chamber and/or from a 2-in. diameter pyrex-pipe side arm and pass up through a screen which serves as a flow distributor. The walls of the chamber are heated with heater tapes to keep materials from condensing on them. The exhaust gases leave the chamber through a port in the top flange. Liquid reactants such as $TiCl_4$ and CCl_4 are vaporized in the 2-in. diameter side-arm. The liquid reactant is placed in a reservoir which is equipped with a dip-pipe and a tube for pressurizing the liquid with argon. The liquid, under pressure, is forced through a rotameter and then a micrometering valve which controls the flow. As the liquid enters the side arm, it drips into a heated trough where it is flash vaporized. Argon and/or hydrogen are introduced into the trough to help carry the vapor into the vertical chamber. The rotameter was calibrated for the liquid flow using the procedures outlined in Appendix A. When two of the reactants are liquids and are mutually soluble, they are mixed in the proper ratio and then vaporized, using the above system. Mixtures of $TiCl_4/CCl_4$ and $TiCl_4/CH_3CH_2Br$ were vaporized in this manner.

Deposition chamber D is a cross-flow unit (i.e., gas flow is perpendicular to the fiber) and is illustrated in Fig. 16. This chamber was constructed primarily for fiber preparations which, because of low volatility of reactants or reaction products, require the chamber to be heated to temperatures in the range of 350 to 450°C. It is constructed principally of Inconel to make it more rugged than the pyrex units and to offer suitable resistance to corrosion by the reactants and reaction products at the high temperatures. The unit consists of four principal parts: (1) a mixing chamber for the gaseous reactants, (2) a lower distribution plenum for distributing the reactants uniformly along the length of the fiber, (3) a deposition chamber, and (4) an upper plenum for carrying the gases away from the fiber. The mixing chamber consisted of a 1-in. diameter tube heated with heater cord. All reactants entered the chamber through 1/4-in. diameter tubing with the least volatile reactant entering at the top. The lower distribution plenum was filled with glass beads to distribute and further mix the gases. Heat was furnished by plug-type heaters mounted in the side of the plenum. The lower plenum was connected to the deposition chamber by a flanged joint employing a Viton O-ring. The upper plenum was integral with the deposition chamber and was heated by heater cords wrapped around the outside surface. The deposition chamber was equipped with a removable assembly containing the suspended substrate. The design of the assembly was such that, when it was in place, a plenum was created on both ends where the electrodes were located and on the front side between the cover plate on the assembly and the cover

flange of the deposition chamber. During the experiments, this plenum was purged with argon so that the plating gases could not reach the electrodes and the quartz window in the cover flange of the deposition chamber. The quartz window in the cover plate of the removable assembly was kept clear of condensed vapors by leakage of argon behind the window.

Zirconium tetrachloride vapor was supplied to deposition Chamber D by volatilizing the $ZrCl_4$ in the sublimer shown in Fig. 17 and piping the vapor to the gas mixing chamber in a heated line. The $ZrCl_4$ powder was heated to the desired temperature which was indicated by the thermocouple in the well. Argon was passed through the $ZrCl_4$ powder in an attempt to saturate it with $ZrCl_4$ vapor. The plug heater in the cover plate provided sufficient heat to prevent condensation of the $ZrCl_4$ vapor in the upper regions of the sublimer. The $ZrCl_4$ flow was determined from tests made at a particular argon flow and sublimer temperature. In these tests, the quantity of $ZrCl_4$ collected in a cold trap over a given flow period was determined.

2. Experimental Procedures

A. Deposition Experiments

In the preparation of each of the fiber materials of interest, the experimental procedures were varied somewhat because it was suspected, in some instances, that the procedure could influence fiber properties. As examples of this, the sequence of introducing the plating gases and heating the substrate, the sequence of terminating gas flow and reducing temperature, and the pre-conditioning of the substrate were varied in attempts to improve nucleation conditions, improve fiber surface conditions or reduce cracking of the deposits and improve adherence. Thus, because of the wide variety of procedures used, only a general description of procedures will be outlined here. Specific changes to the procedures will be covered later in the report.

The general experimental procedure for our chemical-vapor-plating experiments is outlined below. A length of the desired substrate material was suspended from the tungsten electrodes. Connections were made simply by wrapping, threading, and tying the substrate around the pointed rhenum metal tabs. Care was taken to ensure that the final contact between the substrate and the tabs was at or near the point. This prevented heating of the portion of the substrate that was wrapped around the tabs. After suspending the substrate, it was cleaned with acetone or methanol, and then the electrode assembly with the suspended substrate was installed in the deposition chamber. At this point, the system was pumped down and a pressure recovery rate was obtained if the run was to be made at reduced pressure. Arbitrarily, a recovery rate of less than 10

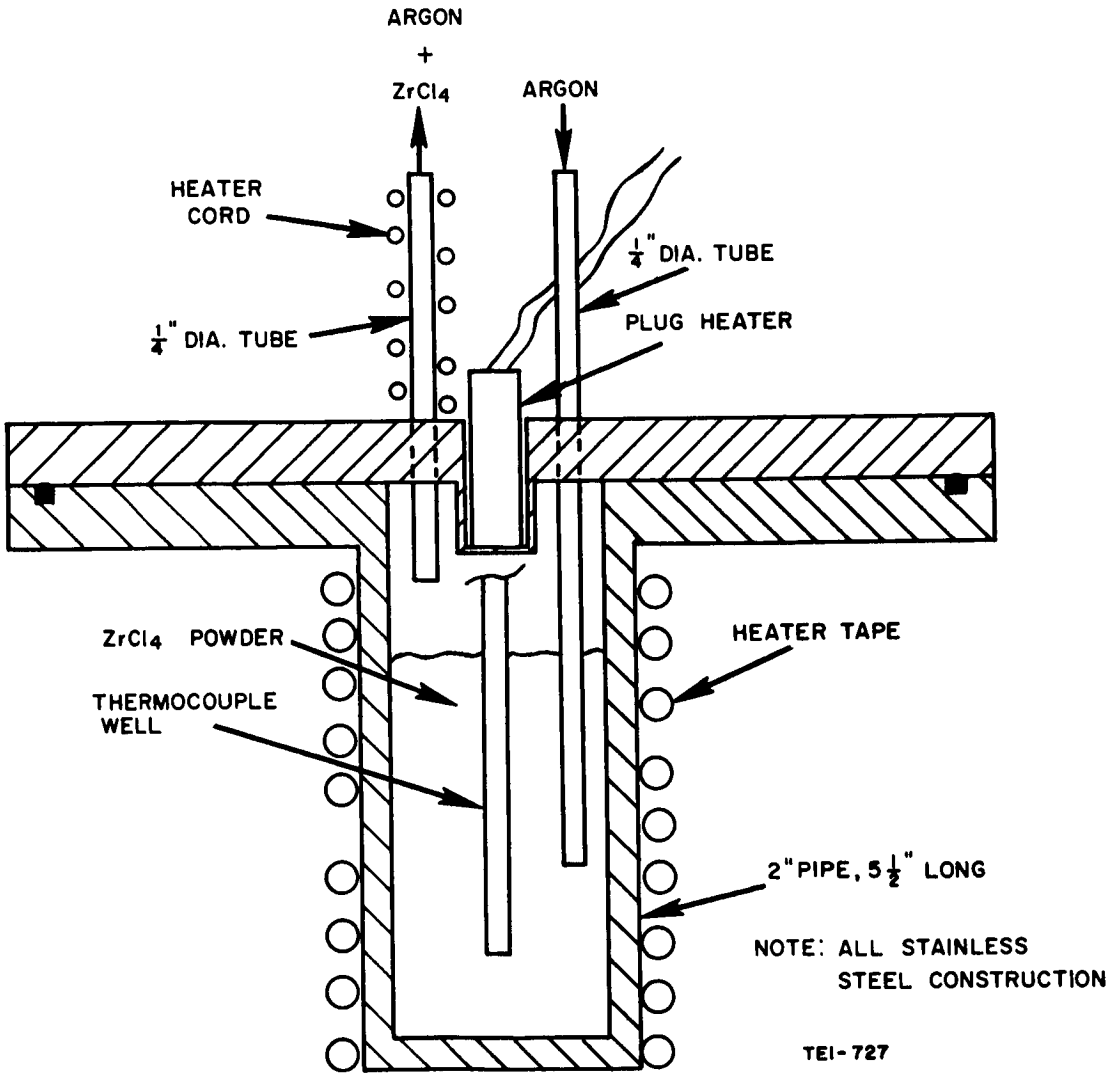

Fig. 17 $ZrCl_4$ Sublimer

microns per minute was considered acceptable. It should be noted that pressure recovery was affected by actual leaks in the system and, probably more importantly, by the high vapor pressure of materials condensed on the walls of the system. If the run was to be performed at atmospheric pressure, the system was usually purged for several minutes with argon before introducing the other plating gases, although in some instances, such as the first run following a general system overhaul, the system would be pumped down to check the pressure recovery rate.

The particular experiment was then conducted. In some experiments the tungsten substrate was preconditioned by heating it in hydrogen for a few minutes at temperatures in the range of 1100 to 1500°C. This had the effect of reducing hot spots during the subsequent deposition and causing more-uniform nucleation of the deposits. After adjusting the gas flows, pressure, and substrate temperature, deposition was carried out for a predetermined time. During deposition, the gas flows and temperature were monitored and recorded at frequent intervals. Adjustments were made to the power supply to compensate for changes in temperature as the deposit increased in diameter. In many of the experiments, the power characteristics (voltage and amperes) were recorded at frequent intervals. Changes in the current were conveniently used to note whether or not deposition was proceeding. At the conclusion of deposition, the power was turned off slowly, the gas flows were terminated, and the system was then purged with argon. The electrode assembly was removed from the deposition chamber to permit retrieval of the fiber, but sometimes the fiber would break upon cooling, and it would have to be retrieved from the bottom of the chamber. The fibers were then evaluated as described in the next section.

B. Fiber Evaluation

Since one of the primary goals of this work was to develop high-strength fibers, the primary criterion for success was the tensile strength of the fibers produced. Thus, a conventional tensile test was made on most of the fibers, using the procedure described in Appendix B. However, many of the fibers produced were so fragile that the tensile tests could not be performed. For example, the slight compression resulting from a micrometer was sufficient to break or sometimes fragment some of the fibers.

The density of pyrolytic graphite fibers was determined by the density-gradient method, described in Appendix C. Since all of the other fibers produced in this program had densities greater than 3 g/cc, the maximum density determinable by the density-gradient method, another method had to be used to obtain their density. After studying several possibilities, we decided to compute the density of these heavier fibers from the measured mass and volume calculated from the

measured length and diameter of the sample. When the fiber surface is smooth, the probable error in the density determined by this method is about ± 2 percent. The procedures used for the density determinations are presented in Appendix C.

Debye-Scherrer x-ray diffraction and chemical analysis were used to identify the crystallographic species and chemical species, respectively, that were present in the fiber. Appendices D and E, respectively, describe the procedures used in these analyses. In the x-ray analyses, samples of the as-produced fiber and powdered samples were employed. Crystallite texturing was noted qualitatively from the absence of reflections from certain crystallographic planes. Metallography was employed to show the microstructural features of the deposits, including the distribution of porosity and phases.

The elastic modulus of some of the fibers was determined by a method based on the critical buckling load of a slender column (the fiber). The procedure for the method is outlined in Appendix F.

C. Materials

The materials used in this program were all commercially available, although some were purchased as "experimental chemicals". Since the quantities that were required were generally small, and in order to minimize the possible effects of impurities on fiber deposits, we used premium grade materials whenever they were available. It is quite probable that lower grade materials could be used without ill effects, but no attempt was made in this program to study material purity as a variable. The materials used are identified below. Table X presents handbook values for some of the physical constants of the compounds used in the program.

Argon	-	High purity grade (99.995% min argon)
Hydrogen	-	Ultra pure grade for ZrB_2, TiB_2 and tungsten coated boron fiber preparations. High purity grade for TiC preparations.
Acetylene	-	Purified grade (99.6% min acetylene)
Butane	-	Instrument Grade
WF_6	-	High purity grade (99.8% min WF_6) - Allied Chemical Corp., General Chemical Division

$TiCl_4$	-	Purity about 99.96% $TiCl_4$ National Lead Company, Titanium Division
$ZrCl_4$	-	High-Purity Grade, Low hafnium, -20 mesh power. National Lead Company, Research Department, No. 1802 Lot 1
Ethyl bromide	-	Reagent Grade
Carbon Tetra-chloride	-	Analytical Reagent Grade
BCl_3	-	C. P. Grade (99.5% min BCl_3)
WCl_6	-	Identified as "Experimental Chemical", Climax Molybdenum Co.
$W(CO)_6$	-	Identified as "Experimental Chemical", Climax Molybdenum Co.
Toluene	-	Reagent Grade
Tungsten wire	-	General Electric Company; 0.5 and 1.5-mil diameter wire was C.S. Grade; 0.75 mil diameter wire was E.E.S. Grade.
Tantalum wire	-	2 mil diameter wire was unannealed Lot No. MG 96, purchased from Fansteel Metallurgical Corp. 3 mil diameter wire, purity unspecified, purchased from A. D. MacKay, Inc.
Zirconium wire	-	10 mil diameter, purity unspecified, purchased from H. Cross Co.
Titanium wire	-	5 mil diameter, purity unspecified, purchased from A. D. MacKay, Inc.

Table X

PHYSICAL CONSTANTS OF COMPOUNDS

Compound	Specific Gravity	Melting Point, °C	Boiling Point, °C	Sublimation Temp., °C
BCl_3	1.434	-107	12.5	--
$TiCl_4$	1.726	-30	136.4	--
$TiCl_3$	2.64	(2)	660 (3)	--
CCl_4	1.595	-23	76.8	--
WF_6	3.44	2.5	19.5	--
$W(CO)_6$	2.65	--	175	--
WCl_6	3.52	275	346.7	--
$ZrCl_4$	2.80	437 (1)	--	331
CH_3CH_2Br	1.43	-119	38	--
HCl	--	-112	-83.7	--

(1) At 25 atmospheres

(2) Decomposes at 440°C

(3) At 108 mm Hg pressure

With the exception of the wire, all of the materials were used in their purchased form. No additional purification was made except in the case of the zirconium diboride experiments where the argon was passed over hot titanium metal chips to remove oxygen and moisture. The wire substrate materials were given specific surface treatments in some experiments in order to ascertain effects on the nucleation and character of the deposits. Reference is made to these treatments in the Results section of this report.

3. Results and Discussion

A. Titanium Diboride Fibers

Two approaches to the preparation of titanium diboride fibers were investigated. Initially, fibers were prepared by the reduction of BCl_3 on a hot 5-mil diameter titanium substrate. It was conjectured that the boron produced on the surface of the titanium wire would diffuse into the wire and form the compound TiB_2. This approach is inherently simple from an operability standpoint because only one plating gas is involved. However, the fibers produced by this approach were of very poor quality. The second approach, which proved to be quite successful, involved the codeposition of titanium and boron in the stoichiometric ratio by the hydrogen reduction of $TiCl_4$, and BCl_3. This approach requires the control of three plating gases, one of which ($TiCl_4$) is a liquid at ambient conditions (Table X) and must be produced by a suitable scheme of vaporization. In addition, $TiCl_4$ is reduced to $TiCl_3$ by hydrogen so that provisions must be made to keep the low volatility $TiCl_3$ from condensing on the chamber walls. In spite of these factors which complicate system operability, a satisfactory system was developed for TiB_2 fiber preparation by this approach.

(1) Preparation by reduction of BCl_3 on titanium substrate

Very little effort was put on this approach because the results of the initial experiments were not encouraging. The fibers were prepared in deposition chamber A. In order to ascertain the heating characteristics of the 5-mil titanium substrate, a piece of the substrate was suspended in the deposition chamber and its temperature was increased incrementally from 950 to 1500°C in an argon flow of 300 cc/min at 760-mm Hg. Over this temperature range the voltage was increased from 43 to 68 V, while the current increased from 0.88 to 1.33 amps. At 1500°C, the substrate broke. In a follow-up test, a piece of the substrate was lightly etched in a solution of HNO_3 and HF, installed in the deposition chamber, and heated 40 minutes at 1200°C without incident in an argon flow of 300 cc/min. Based on these tests, 1200°C was selected as the temperature for preparation of the TiB_2 fiber.

In the deposition experiments, the titanium wire substrate was etched in the HNO_3-HF solution to remove about 0.5 mil off the diameter and then heated to 1200°C in 900 cc/min of argon. Boron trichloride was then admitted (100 cc/min) for the prescribed deposition time. Soon after the BCl_3 was admitted, a fog of condensed vapor developed, but after about four minutes the fog ceased, leaving a deposit on the chamber.

The fibers produced by this procedure were quite fragile and could not be tensile tested. The deposits would crumble quite easily. Metallography of a transverse cross section was not totally successful because of the fragility of the deposit. However, a rough-polished cross section of a fiber which was reacted for 15 minutes revealed a core of titanium metal about 2.5 mils in diameter, surrounded by a fragile deposit of material (diameter about 5 mils) which was grossly porous. Although no x-ray analysis was made, the porous deposit was probably TiB_2. The chemical equation representing the reaction suggests that the fog which was observed during the boron deposition was most likely one or more of the chlorides of titanium. Since the overall diameter of the fiber did not change significantly, the porosity was probably caused by volatilization of titanium as a chloride.

In view of these results, no further TiB_2 preparations were attempted using this approach.

(2) Preparation by Co-deposition

Our next attempt to produce TiB_2 fibers involved the co-deposition of titanium and boron on a tantalum substrate by hydrogen reduction of titanium tetrachloride and BCl_3. The experimental procedure was as follows. A piece of 3-mil tantalum wire, precleaned in methanol, was attached to the electrodes in deposition chamber A. Boron trichloride was admitted directly to the deposition chamber, whereas the $TiCl_4$ was introduced by bubbling hydrogen through the $TiCl_4$ which was maintained at the desired vaporization temperature. The entire hydrogen flow was passed through the $TiCl_4$. The desired BCl_3 and hydrogen flows were adjusted, after which the substrate was heated to the desired deposition temperature. After deposition, the temperature was gradually decreased while the flow of BCl_3 and hydrogen was stopped. Argon was introduced at this point to purge the system. If the deposition was to be carried out at reduced pressure, the system was pumped down to the desired dynamic vacuum after gas flows were set but before the substrate was heated. Using this procedure, four experiments were run at about 5-mm Hg pressure and one experiment was run at atmospheric pressure. The deposition conditions are presented in Table XI.

Table XI

CODEPOSITION EXPERIMENTS[1] - DEPOSITION CHAMBER 'A'

Titanium Diboride Fibers

Fiber No.	Temp. °C	H_2 Flow cc/min	BCl_3 Flow cc/min	$TiCl_4$ Vaporizer Temp., °C	Pressure mm Hg	Deposition Time, min	Fiber Dia. Mils	Relative Flexibility	Relative Adherence	X-Ray[2]
193-126	1300-L[3] 1200-R	650	135	70	760	4	~ 14	none	poor	no test
193-129	1700-L[3] 1500-R	900	35	41	7	3	~ 5.5	good	good	TiB_2
193-130	1400	900	25-35	44	5	10	9.0-L[3] 7.7-R	poor	good	no test
193-131	1400	900	35	44	5	13	9.0-L[3] 7.2-R	good	fair	TiB_2
193-132	1500-L[3] 1400-R	900	35	40	5	6	7.9-L[3] 7.5-R	fair	good	TiB_2

Notes:

(1) Deposition on 3 mil tantalum substrate. Total H_2 flow was passed through the vaporizer.

(2) X-ray diffraction analysis of fiber as produced. No powdered samples were run.

(3) L and R denote that portion of the fiber lying on the left and right side of the weight respectively.

The quality of the results obtained in these experiments was impaired by the following factors:

(1) Titanium trichloride, resulting from hydrogen reduction of $TiCl_4$ in the vapor phase, condensed on the chamber and reduced the optical pyrometer reading by an unknown amount. Thus, the reported temperatures are those that were obtained early in the experiment before view was obscured.

(2) Numerous hot spots developed on the substrate and temperatures were usually higher on the left side than on the right side (closest to the gas inlet ports) of the weight. Thus test samples were not precisely correlatable with temperature.

(3) The actual $TiCl_4$ flow was not determined.

Although these shortcomings make it impossible to make a detailed analysis of these fibers, there are two general observations that can be made. First, the quality of the fiber produced at atmospheric pressure (193-126) was by far the poorest. It was composed of grey crystalline spires oriented perpendicular to the substrate on the right end and a rather sparse population of thin platelets on the left side. In comparison, the right sides of the fibers made at the reduced pressures were smooth and crystalline in appearance. The appearance of the left sides of these fibers was varied, but they generally had a very poor surface appearance. The other observation is that x-ray diffraction analysis of the as-produced fibers, both right and left sides, revealed the presence of TiB_2 only. This finding was somewhat surprising because it is quite possible that the deposition temperatures and the $TiCl_4/BCl_3$ mole ratio were significantly different in this series of experiments. Subsequent work reported herein also suggests that the $TiCl_4/BCl_3$ mole ratio is not critical over a rather wide range.

Metallographic examination of transverse cross sections revealed that each fiber (both right and left sides) has a tightly adherent deposit of metallic-like material adjacent to the tantalum substrate. A narrow band of interaction between the tantalum substrate and the deposit is evident. Figure 18, a rough-polished cross section of the right side of Fiber No. 193-132-1, is typical of the deposit adjacent to the substrate.

The left side of each fiber has a band of porous, fragile deposit which appears to lie well outside the diameter of the main portion of the fiber. Fiber No. 193-130-1 has two layers. Occasionally, lesser amounts of the same type of material were deposited on the right side. The porous bands of material are probably due to vapor-phase reaction. The tensile strengths of the right sides of these fibers were below 25 kpsi. Two of the fibers were too brittle to test.

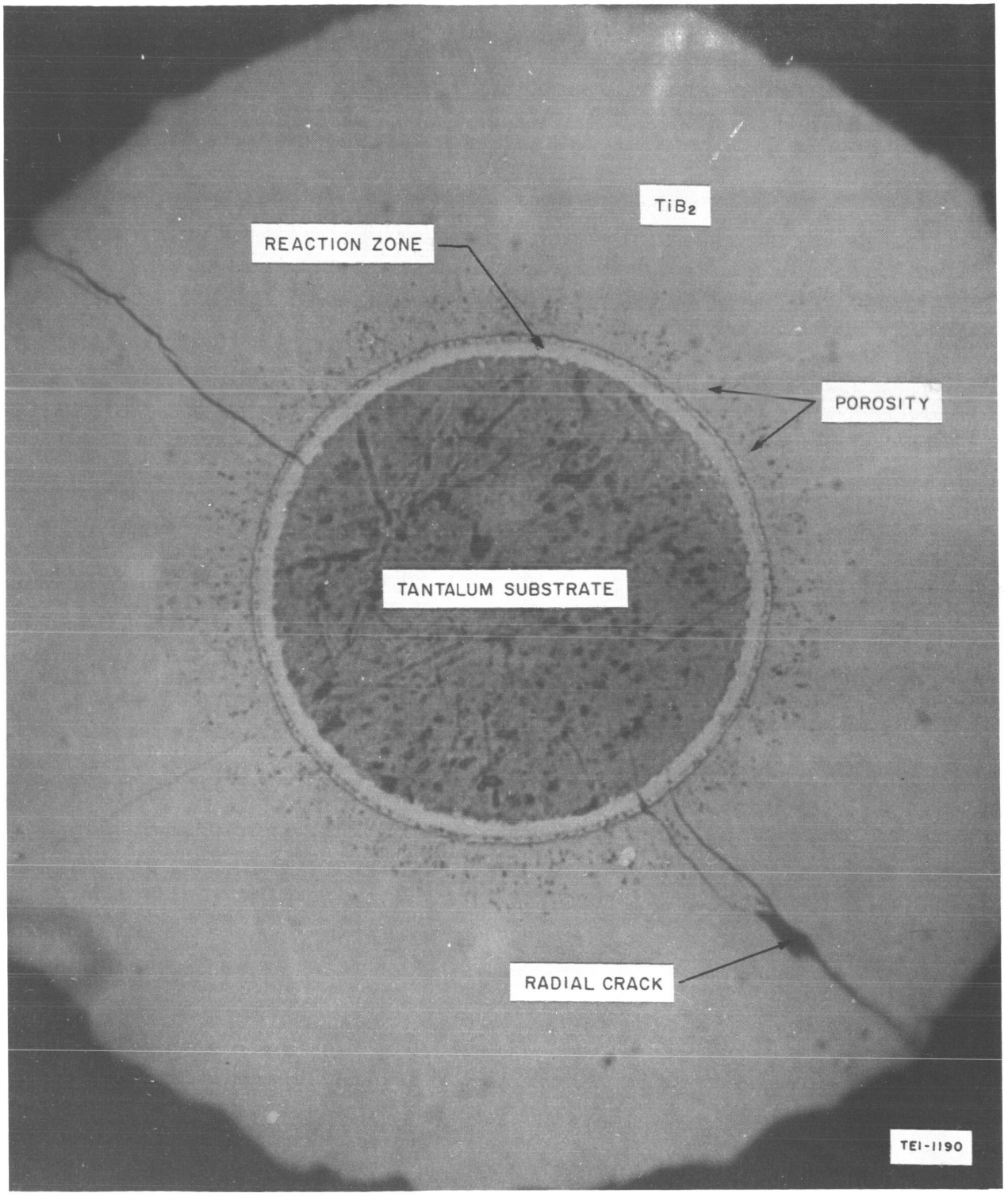

Fig. 18 TiB_2 Fiber No. 193-132-1. Polished Cross Section (Right Side, Magnified 400 X, enlarged 2-1/4 X)

These initial codeposition experiments demonstrated the need for an improved deposition chamber, one that would permit unobscured vision of the fiber during the experiment and one that would eliminate the differences in fiber quality between right and left sides. In addition, some means of measuring the $TiCl_4$ flow was badly needed. These shortcomings were overcome in deposition chamber 'B' (Fig. 14b), which was simply chamber 'A' with two modifications. Referring to Fig. 14b, a 1/4-in. diameter stainless tube, containing several small holes on one side along the length, was placed inside the chamber so that jets of argon could be directed onto the chamber wall to keep $TiCl_3$ from condensing in the area of the jets. This kept the wall clear and permitted vision of the fiber throughout the experiment. In addition, the method of suspending the substrate was changed as shown to eliminate the weight at the center of the fiber and to get the fiber parallel to the "windows" made by the argon jets. In chamber 'B', estimates of $TiCl_4$ flow were made by noting the rate of depletion of the $TiCl_4$ reservoir during the experiment.

In subsequent experiments, these modifications proved to be highly successful. The addition of the argon jets vastly improved the reliability of the deposition temperature. Hot spots on the substrate were all but eliminated and the temperature of the substrate was usually uniform from end to end. We are not certain, but it is likely that the uniform temperature distribution was brought about by better gas mixing and higher gas velocities in the deposition chamber as a result of the argon jets.

Our next codeposition experiments consisted of ten fiber preparations in which all conditions except temperature were held constant. Temperature was varied in 100°C increments over the range of 1100 to 1400°C. Based upon work of others (16) a $TiCl_4/BCl_3$ mole ratio of 1.6 was selected as the most promising ratio to begin with. Since reduced pressure runs are more difficult to accomplish, we decided to run the initial experiments at atmospheric pressure, and, if encouraging trends did not develop, then to extend the series of experiments to reduced pressures.

The significant difference between these experiments and the previous ones was that the total gas flow are more than doubled by using argon as a diluent for the reactants. The flow of argon was based on the quantity of diluent required to make the density of the reactants equilvalent to their density at 20-mm Hg pressure. The combined flow of reactants (BCl_3, $TiCl_4$, and hydrogen) was set at 500 cc/min and the proportion of each was determined on the basis of a $TiCl_4/BCl_3$ mole ratio of 1.6 and sufficient hydrogen to reduce all of the $TiCl_4$ and BCl_3. A portion of the argon flow (450 cc/min) was diverted through the $TiCl_4$ vaporizer to carry the $TiCl_4$ vapor into the deposition chamber. The quantity of argon required through the vaporizer was computed from the $TiCl_4$ vapor pressure data and the desired $TiCl_4$ flow.

Experiments were conducted at temperatures of 1100, 1300, and 1400°C using either 3-mil annealed (unetched) or as-drawn (unannealed) and etched tantalum substrate. Etching was performed in a solution composed of 5 percent HF (48 percent), 45 percent HNO_3 and 50 percent water. Based on flow measurements made in subsequent experiments, it is estimated that the $TiCl_4$ flow was less than that required for a $TiCl_4/BCl_3$ mole ratio of 1.6. We estimate that the average mole ratio was about 1.4.

The experimental procedure employed in these fiber preparations is presented below. The substrate was installed in Chamber 'B' with just enough dead weight to keep it taut. The system was purged with argon for at least 2 minutes, after which the gas flows were adjusted. After waiting a minimum of one minute to achieve uniform gas mixing, the substrate was heated to the deposition temperature. When deposition was completed, the flow of plating gases was stopped and the fiber was slowly cooled in argon to room temperature.

The deposition conditions and certain characteristics of the fibers produced are presented in Table XII. In all runs, high deposition rates were experienced. The lowest deposition rate occurred at 1100°C; at 1400°C, the rate was 2 to 3 times higher. In general, the quality of the fibers decreased as the deposition temperature increased, but in all cases, these fibers were substantially better than any of the TiB_2 fibers produced previously at reduced pressures and low argon flow. Also, as the temperature increased, the surfaces became rougher and more crystalline in appearance, and flexibility and strength decreased. Densities appear to increase as the deposition temperature is increased but the validity of this trend was not verified. If this is a valid trend, however, the chemical analyses suggest that the trend is not due to a shift in composition. There is a tendency for the densities to be lower than theoretical.

Wet chemical analysis indicates that the composition of the deposits is close to stoichiometric TiB_2 (68 w/o Ti). In addition, x-ray diffraction analysis identified only TiB_2 in all of the deposits regardless of deposition temperature or whether the diffraction analysis was performed on the as-produced fiber or on a powdered sample.

The x-ray diffraction patterns for the as-produced fibers reveal that the TiB_2 deposits have varying degrees of preferred orientation. The fibers produced at 1300 and 1400°C exhibited some preferred orientation but only at the low reflection angles. However, the fibers produced at 1100 and 1200°C appear to be more strongly oriented with the (100) planes aligned parallel to the substrate. Using the Scherrer equation, the average crystallite size of the TiB_2 deposits was estimated from x-ray line broadening to be in the range of 50 to 300 angstroms.

Table XII

DEPOSITION CONDITIONS AND FIBER CHARACTERISTICS FOR TiB_2 EXPERIMENTS (1)

Fiber No.	Substrate Dia (mils)	Deposition Temp, °C	Deposition Time, min	Fiber Dia, mils	Density (4)	Analysis by X-Ray Diffraction (3)	% Ti in Deposit (5)	Tensile Strength kpsi
219-1	2.0 Ta	1050/1100	9	9.8	4.14	TiB_2	67.8	150
219-2	2.0 Ta	1050/1130	9	9.1	4.33	TiB_2	66.5	225
219-9	0.5 W	1050/1100	6	6.7	-	TiB_2	-	184
219-3	2.0 Ta	1160/1200	9	13.5	4.48	TiB_2	63.6	45.7
219-4	2.0 Ta	1150/1190	9	14.2	3.20	-	-	-
193-149	2.0 Ta	1250/1300	9	15.5	-	-	-	20.1
193-150	2.1 Ta	1280/1300	9	15.9	-	TiB_2	-	53.7
193-148	3.0 Ta	1350/1400	9	20.2	-	TiB_2	-	3.32
193-147	3.0 Ta	1380/1420	9	27.2	-	-	-	2.12
193-146	3.0 Ta	1350/1400	9	17.5	4.52	-	~ 68	11.9
193-145	3.0 Ta	1300/1400	12	14.4	-	TiB_2 (2)	~ 68	Broke while being mounted

Notes:

(1) Gas Flows, cc/min
BCl_3 - 67
$TiCl_4$ - ~ 94
H_2 - 325
Ar - 1850
Total - ~ 2350
760 mm Hg

(2) Powdered sample

(3) X-ray made on fiber as-produced uless noted otherwise

(4) Density of deposit. Theoretical density of TiB_2 is 4.48

(5) Wet chemical analysis, probable error in result is $\pm$ 3.0% absolute

The highest quality fibers were produced at the 1100°C deposition temperature. They had very smooth surfaces and were very flexible. Fibers 219-1 and -2 were made on 2-mil tantalum substrate and their tensile strengths were 150 and 225 kpsi, respectively. An additional fiber (219-9) was produced at 1100°C by the same procedure using a 0.5-mil tungsten substrate: its tensile strength was 184 kpsi.

The elastic modulus on two of the 1100°C fibers was determined to be 75 to 84 million psi.

Metallographic preparation of the fibers produced at 1100°C was quite difficult due to their extreme hardness. Slight variation in hardness between concentric layers of the deposit was noted during polishing and the as-polished surface texture of the layers seems to vary. Our best explanation for the layering is that the interface between the layers corresponds to an adjustment in temperature. In comparison, the fibers produced at higher temperatures were somewhat softer, and surface pitting due to the metallographic preparation was more apparent. Figure 19 is a polished and etched cross section of Fiber No. 219-9 showing the layering.

Having produced several TiB_2 fibers of quite respectable properties, we decided to produce a sufficient number of fibers by the same procedure to permit a detailed evaluation of their quality and to provide samples for testing in the plasma flame. Before the pilot run was attempted, the system was cleaned and certain repairs were made, including replacement of two of the rotameters. Following these repairs, we were unable to produce good quality fibers by the previously successful procedure. Deposition rates were quite low (i.e., a 4-mil fiber was produced on a 2-mil tantalum substrate in 15 minutes deposition time) and the surfaces of the fibers produced were generally crystalline in appearance. However, x-ray diffraction analysis revealed that the deposits were TiB_2.

A number of things were tried to rectify the problem, but none was completely successful. In general, we tried to explore the possible effects which the several known changes to the system may have had on the deposition conditions. Good deposits were finally obtained when we increased the BCl_3 flow to about 185 cc/min ($TiCl_4/BCl_3$ mole ratio of about 0.5). After this a pilot run was made in which ten TiB_2 fibers were prepared. The deposition conditions are presented below:

Substrate	0.5 mil tungsten
Temperature	1100°C

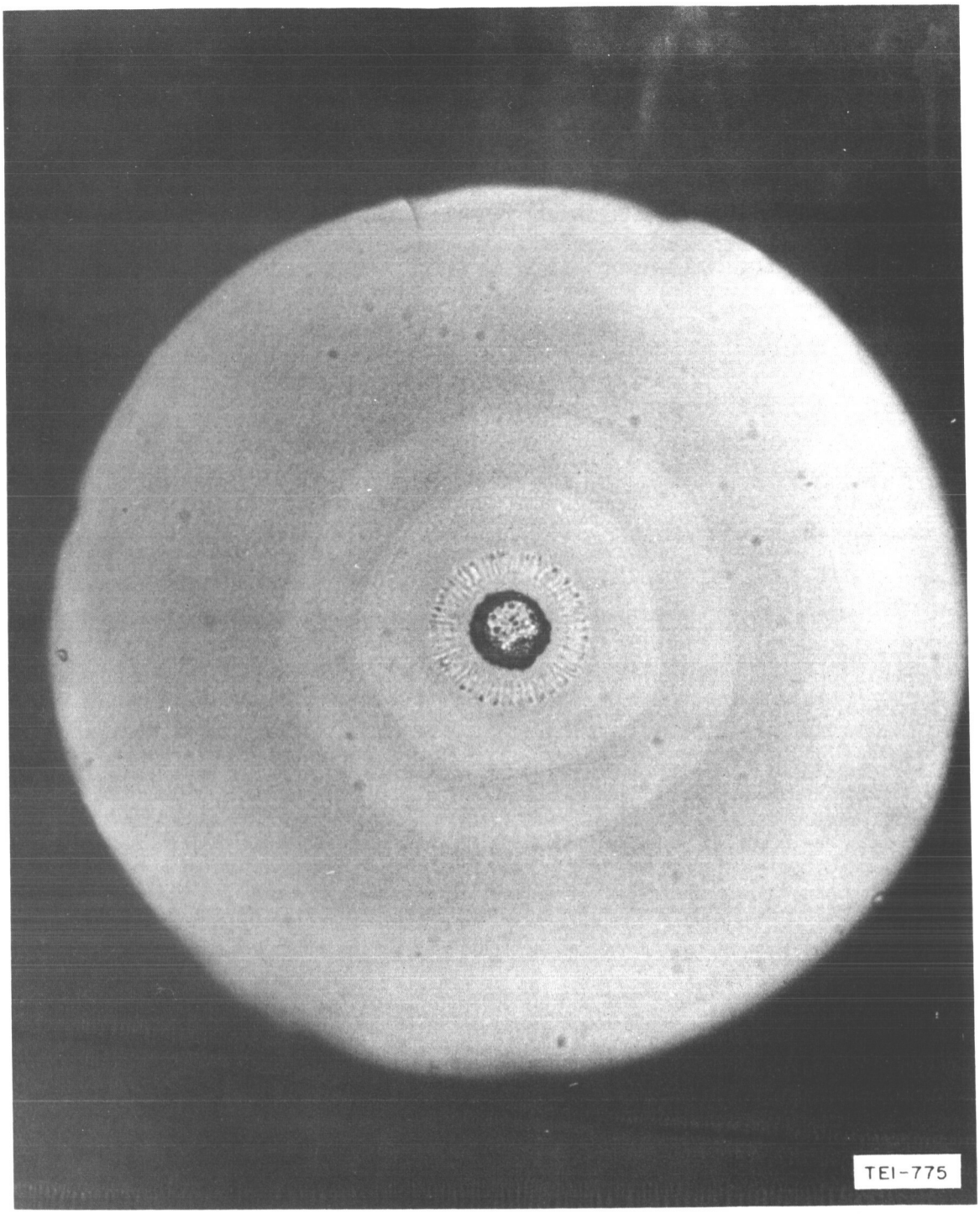

Fig. 19 TiB_2 Fiber No. 219-9. Polished Cross Section, etched, (Magnified 400 X, enlarged 2-1/4 X)

Pressure	760 mm Hg
Deposition Time	15 minutes
BCl_3 Flow, cc/min	185
$TiCl_4$ Flow, cc/min	94 (σ = 22)
$TiCl_4$ Temp., °C	83
Argon Flow, cc/min	1850
Hydrogen Flow, cc/min	325

The argon flow was split as follows: 450 cc/min through the $TiCl_4$ vaporizer, 700 cc/min through the jet, and 700 cc/min directly into the chamber. The $TiCl_4$ flow was determined from the depletion of $TiCl_4$ in the vaporizer and the flow time period for each experiment. The experimental procedure used for the pilot run was the same as that used to produce the fibers tabulated in Table XII.

In order to see if a lower deposition temperature would improve fiber quality, particularly the tensile strength, four fibers were produced at a temperature of 1000°C using the same procedure and conditions employed in the pilot run.

Considerable difficulty was experienced with the control of the $TiCl_4$ flow. As the level of $TiCl_4$ in the reservoir decreased, the $TiCl_4$ flow decreased. This variation caused a variation in the $TiCl_4/BCl_3$ mole ratio for individual fibers from about 0.27 to 0.68. In spite of this variation, x-ray diffraction analysis of powdered samples as well as the as-produced fibers identified only TiB_2 in the deposits. Exposures were long enough to permit identification of any boron present. Chemical analysis shows that eleven of the fibers (including the four produced at 1000°C) had titanium contents of 70 to 75 w/o, whereas the other three fibers contained only 48.5 to 63.5 w/o titanium. The analysis of these latter three fibers is in some doubt, since only TiB_2 was found in the deposits. The stoichiometric compound TiB_2 contains 68.9 w/o titanium, but the phase diagram of the titanium-boron system indicates that the TiB_2 phase covers a broad composition range (perhaps 60 to 70 w/o titanium). Attempts were made to correlate the $TiCl_4/BCl_3$ mole ratio with the composition of the deposits, density, and tensile strenght, but no correlation was found. In addition, no correlation was found between chemical composition, density, and tensile strength.

The properties of the fourteen titanium diboride fibers are summarized in Table XIII.

Table XIII

PROPERTIES OF TITANIUM DIBORIDE FIBERS

Deposition Temperature, °C	Number of Fibers Produced	Property	Values of Property			
			High	Low	Average	Variance
1000	4	Diameter, mils	5.40	4.15	4.94	-
		Density, g/cc[1] (of deposit)	4.42	4.19	4.31	-
		Tensile Strength				
		Unetched, kpsi	266	185	234	-
		Etched, kpsi	378	167	256	-
1100	10	Diameter, mils	8.85	7.05	7.78	5.3%
		Density, g/cc (of deposit)	4.83	3.92	4.43	7.2%
		Tensile Strength				
		Unetched, kpsi	312	40	150	53.7%
		Etched, kpsi	290	47	188	43.7%

(1) The density of only two of the fibers was determined.

The density of the deposits was determined from the mass and calculated volume of selected samples after making an allowance for the mass and volume of the substrates. The accuracy of the density determinations is no better than about ± 7 percent as indicated by the high values which exceeded the theoretical density by this amount.

It appears that etching with a solution composed of one part HNO_3, one part HF and three parts lactic acid improved the average strength and reduced the variance of these fibers. Even so, the variance was still quite large. All but one of the fractures of the as-produced fibers originated at the surface. Etching significantly reduced the number of fractures which originated at the surface.

The elastic modulus of three of the fibers produced at 1100°C was determined to be in the range of 29.8 to 58.2 x 10^6 psi. The modulus of one of the fibers produced at 1000°C was determined to be 81.5 x 10^6 psi. In comparison, the modulus of TiB_2 fibers produced previously in this program (Table XII) were in the range of 75 to 84 x 10^6 psi.

Figure 20 is a photomicrograph of a polished and etched transverse cross section of Fiber 219-41 and shows the layering and cone growth of the deposit.

In summary, the titanium diboride fibers produced at both 1000 and 1100°C are substantially TiB_2. The tensile strength of the fibers produced at 1100°C is about 150 kpsi (unetched). The deposits made at 1000°C appear to be significantly stronger, but it is quite possible that the difference in strength is due to the difference in diameter of the two groups of fibers. The elastic modulus of the fibers produced at 1100°C is substantially lower than the modulus of TiB_2 fibers produced previously in this program. The average elastic modulus of all the fibers produced at 1100°C was 65.1 x 10^6 psi. Finally, control of the $TiCl_4$ flow in these experiments was quite poor, but apparently adequate. Future programs should pursue an improved system for admitting $TiCl_4$ into the deposition chamber.

B. Titanium Carbide Fibers

Titanium carbide fibers were prepared by the codeposition of titanium and carbon. In all experiments, $TiCl_4$ was used as the titanium precursor, but five carbon precursors were employed: acetylene, carbon tetrachloride, ethyl bromide, butane, and neopentane. Deposition with acetylene, carbon tetrachloride, ethyl bromide, and some of the butane runs were carried out in chamber 'C' shown in Fig. 15. When carbon tetrachloride or ethyl bromide was used, they were mixed with the titanium tetrachloride in the desired proportions and fed

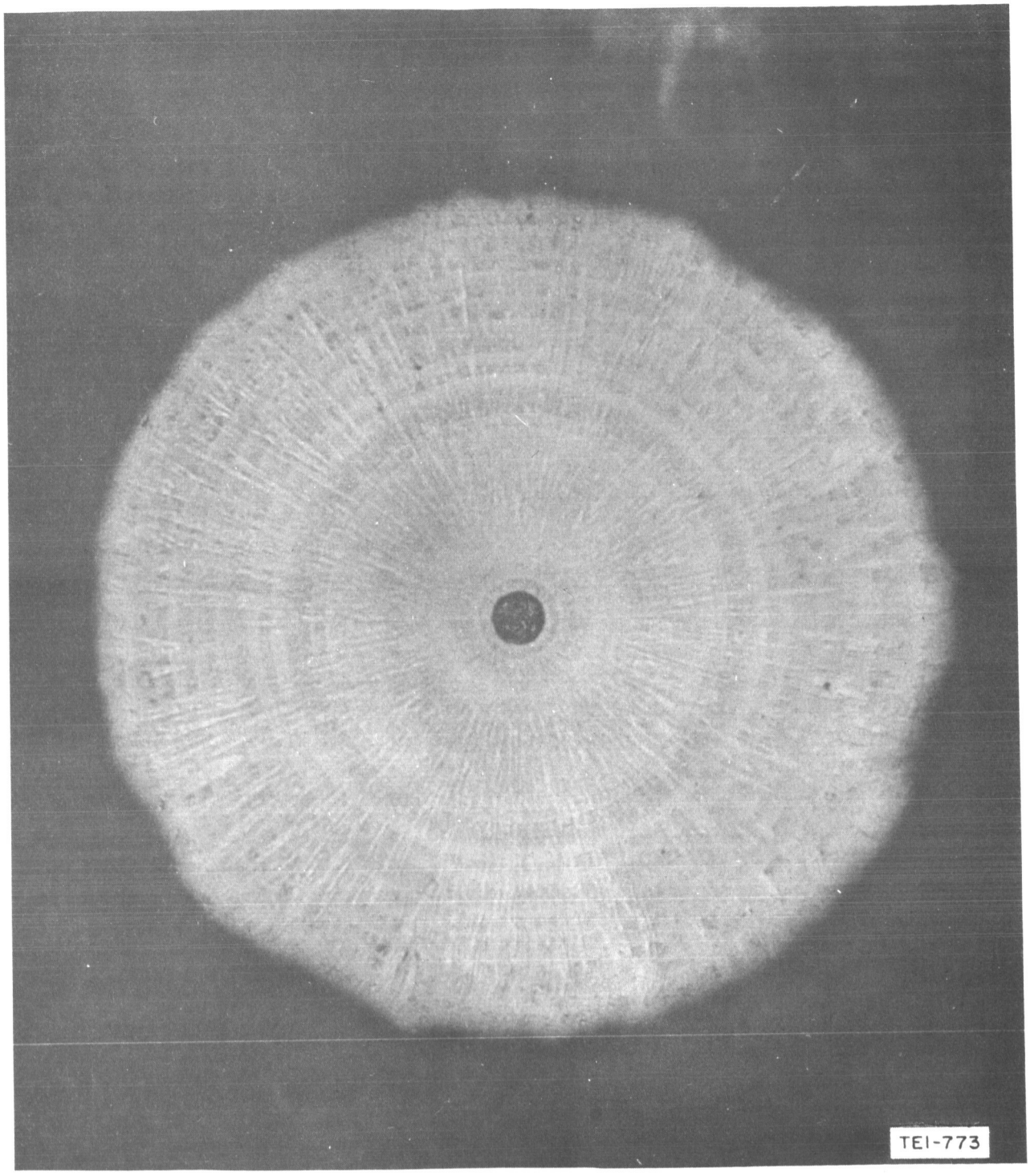

Fig. 20 TiB_2 Fiber No. 219-41. Polished Cross Section, etched, (Magnified 250 X, enlarged 2-1/4 X)

into the deposition chamber as a solution, where they were then flash vaporized in the heated trough. When acetylene or butane was used as the carbon precursor, the $TiCl_4$ was loaded into the liquid reservoir and fed into the deposition chamber and flash vaporized. Argon and hydrogen for reducing the $TiCl_4$ were admitted to the chamber through the side inlet. When large amounts of argon were used, some of the argon was admitted to the bottom of the vertical chamber. When acetylene was used as the carbon precursor, it was admitted at the side inlet.

The experiments involving neopentane and a few of the butane experiments were conducted in chamber 'B' (Fig. 14b), which was modified slightly to permit the introduction of $TiCl_4$ as a liquid by the scheme used in chamber 'C'. The $TiCl_4$ was metered into a heated gas-mixing chamber where the $TiCl_4$ was flash vaporized and mixed with all of the other gases before entering the deposition chamber.

(1) Deposition from CCl_4-$TiCl_4$ Mixtures

Most of the experiments were performed using carbon tetrachloride as the carbon precursor. In these experiments, pressure, temperature, and gas composition were varied in an attempt to find deposition conditions that would produce satisfactory titanium carbide fibers. Deposition time, for the most part, was very difficult to control because freeze-up of the traps, hot spots on the fibers, and other difficulties caused premature termination of some of the experiments.

Tantalum substrates were used in all but two experiments because the tantalum heated much more evenly than the tungsten wire. Since the 2-mil tantalum was badly discolored, it was etched in a solution composed of 5v/o HF (48%), 45v/o HNO_3 and 50 v/o water. The 3-mil tantalum and tungsten substrates were simply cleaned in methanol prior to their use.

The deposition conditions and characteristics of the fibers produced from $TiCl_4$-CCl_4 mixtures are tabulated in Table XIV. Titanium carbide was produced in almost all of the deposits, but in some fibers, graphite was deposited as a distinct layer over the initial titanium carbide deposit. Figure 21, a transverse cross section of fiber No. 197-87-2 is typical of these fibers. Porosity is evident in the TiC layer; note the delamination and cone growth in the graphite. In the reduced pressure experiments, with the exception of 197-106, graphite layers were produced in only those experiments in which the pressure increased momentarily to atmospheric pressure due to freeze-up of the cold traps. In those experiments in which the traps froze at the end of the run, no graphite was formed except in the case of 197-102. In this fiber, graphite was detected by x-ray diffraction and not by metallography. This would seem to indicate that the

Table XIV

DEPOSITION CONDITIONS AND FIBER CHARACTERISTICS FOR TITANIUM CARBIDE FIBERS PRODUCED USING CCl_4

Fiber No.	Pressure mm Hg	Temp. °C	Deposition Time, min	Total Flow cc/min	Gas Composition Mole Ratio CCl_4:$TiCl_4$	Gas Composition Mole Ratio H_2:$TiCl_4$	Substrate	Fiber Diameter mils	X-Ray Analysis Results (1)	Tensile Strength kpsi	Metallography	Remarks
197-101	10-15	1300	30	475	0.5	1.67	3 mil Ta	3.1	Not Run	Not Run	No sample	
103	10-15	1600	5	460	0.5	1.79	3 mil Ta	4.0 - 5.0	TiC, TaC	34	No graphite layer	Trap froze at end of run
104	10-15	1600	15	475	0.5	1.67	3 mil Ta	8.5 - 9.0	TiC	4.2	Graphite layer between TiC layers	Trap froze after 2 minutes (2)
105	10-15	1600	23	475	0.5	1.67	3 mil Ta	4.0 - 4.5	TiC, TaC, C	28	No graphite layer	Trap froze at end of run
102	10-15	1600	30	520	0.5	1.39	3 mil Ta	3.8	TiC, TaC, C	34.5	No sample	Trap froze at 8 minutes
107	10-15	1750	6	475	0.5	1.67	2 mil Ta	11.5-12.0	TiC	nil	No graphite layer	
108	10-15	1750	13	475	0.5	1.67	2 mil Ta	2.1	TaC	35.2	No graphite layer	
106	10-15	1775	4	475	0.5	1.67	2 mil Ta	5.5 - 6.0	TiC, C	17	Graphite layer over TiC	
197-115	20-25	1300	4	775	0.5	3.68	2 mil Ta	2.5	TiC, TaC	66	No graphite layer	
116	20-25	1300	23	775	0.5	3.68	2 mil Ta	3.0	TiC, TaC	44.8	No graphite layer	
120	20-25	1300	24	775	0.5	3.68	2 mil Ta	2.5	TaC	56.6	--	
119	20-25	1300	24	820	0.5	3.04	2 mil Ta	4.0	TiC	26.5	No graphite layer	
121	20-25	1400	22	775	0.5	3.68	2 mil Ta	3.5	TiC	28.8	--	
118	20-25	1500	20	685	0.5	6.07	2 mil Ta	19.0-21.0	TiC	nil	No graphite layer	
113	20-25	15/1600	9	775	0.5	3.68	2 mil Ta	19.0-20.0	TiC (powdered)	nil	No graphite layer	
123	20-25	15/1600	13	775	0.5	3.68	2 mil Ta	20.0-22.0	TiC	2.1	No graphite layer	
112	20-25	1600	2	775	0.5	3.68	2 mil Ta	8.0	TiC	8.1	No graphite layer	
125	20-25	1600	2	775	0.5	3.68	1.5 mil W	4.5 - 5.0	TiC	nil	--	
111	20-25	1600	3	775	0.5	3.68	2 mil Ta	11.0-12.5	Ta, TiC, TaC (powdered)	nil	No graphite layer	Trap froze at end of run
110	20-25	1600	4	775	0.5	3.68	2 mil Ta	10.5	TiC	2.5	No graphite layer	Trap froze at end of run
114	20-25	1600	6	775	0.5	3.68	2 mil Ta	16.5-17.5	TiC	nil	No graphite layer	Trap froze at end of run
109	20-25	1750	1	475	0.5	1.67	2 mil Ta	6.0 - 6.5	TiC (powdered)	11.2	--	
197-130	760	11/1200	20	775	0.5	3.68	2 mil Ta	3.5 - 6.5	TiC, C	15.3	Graphite layer over TiC	
86-2	760	12/1300	15	154	1.0	3.71	1.5 mil W	11.0-13.0	TiC	nil	No graphite layer	
98	760	1300	15	440	1.0	0.26	3 mil Ta	10.0-14.0	C, TaC, Ta_2C (powdered)	3.2	Graphite layer over TiC	
99	760	1300	20	295	0.5	0.77	3 mil Ta	20.0-23.0	TiC, C	nil	Graphite layer over TiC	
97	760	1300	30	160	1.0	0.92	3 mil Ta	12.0-15.0	TiC, C	7.5	Graphite layer over TiC	
95	760	1350	30	100	1.0	2.00	3 mil Ta	12.0-16.0	TiC	2	No graphite layer	
96	760	1350/1325	30	100	1.0	2.00	3 mil Ta	3.5	TaC, Ta_2C	9.2	--	
94	760	1350/1500	30	100	1.0	2.00	3 mil Ta	20.0	TiC, C	2.9	Graphite layer over TiC	
93	760	1500	8	100	1.0	2.00	3 mil Ta	12.5-14.0	TiC	7.4	No graphite layer	
87-2	760	1500	25	154	1.0	3.68	3 mil Ta	13.5-20.0	TiC, C	12.8	Graphite layer over TiC	
92	760	1500	30	160	1.0	0.92	3 milTa	26.5-31.5	TiC, C	7.6	Graphite layer over TiC	
89	760	1500	30	154	1.0	3.68	3 mil Ta	12.5-13.5	TiC, C	7.4	Graphite layer over TiC	
90	760	1500	30	204	1.0	5.57	3 mil Ta	4.5	TiC, C	26.6	Graphite layer over TiC	

(1) X-ray performed on fiber as-produced unless noted otherwise.
(2) Run stopped and nitrogen in cold trap replaced with dry ice + alcohol mixture. Run resumed.

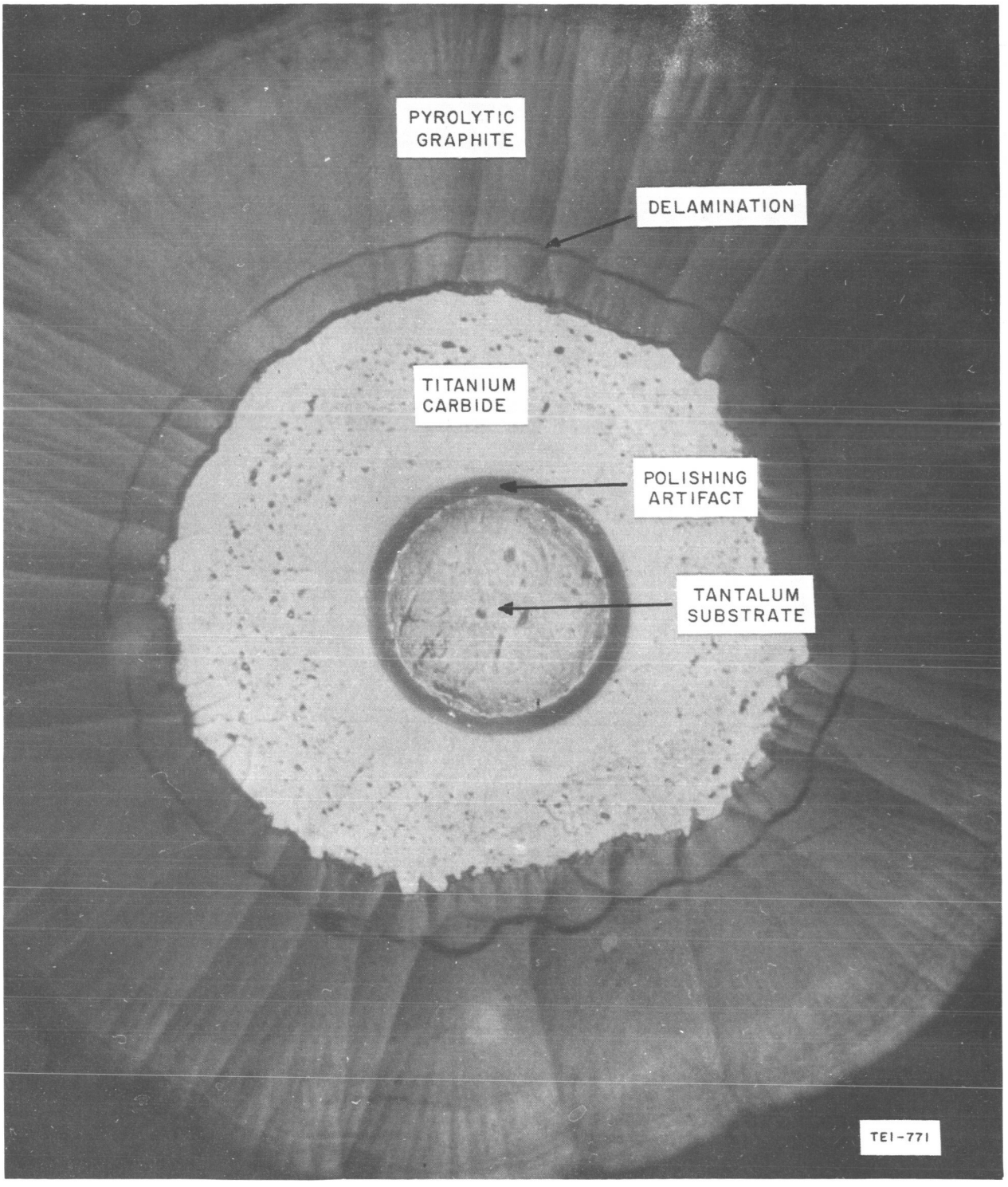

Fig. 21 TiC Fiber No. 197-87-2. Polished Cross Section. (Halo around substrate due to substrate being in relief) (Magnified 200 X, enlarged 2-1/4 X)

experiment was terminated a short while after the trap froze. In general, after the traps were thawed and the pressure was reduced again, graphite deposition appeared to continue. This clearly indicates the strong tendency to deposit graphite rather than TiC when CCl_4-$TiCl_4$ mixtures are used.

Although the foregoing would seem to indicate that graphite layering is associated with high deposition pressures, examination of the atmospheric pressure experiments shows that this is not always the case. For example, fibers 197-94 and 197-95 were produced under the same conditions, but one had a graphite layer and the other did not. The same can be said about fibers 197-89 and 197-93. These observations suggest that the simultaneous deposition of carbon and titanium is difficult to control at atmospheric pressure with the experimental procedures and deposition conditions employed. It was also noted that heavy sooting and polymerization occurred in the same experiments in which graphite layering occurred.

In an effort to reduce the tendency to produce graphite layers, the composition of the plating gas and the total gas flow were varied. The total gas flow was believed to be a possible variable because the velocity of the plating gases could affect the degree of backwash of HCl and other reaction by-products over the fiber. Backwash is caused by heat convection which sets up eddy currents of the gases on opposite sides of the fiber.

The atmospheric pressure experiments were conducted first using relatively low total gas flows that were arbitrarily selected (generally 100 to 300 cc/min). Two of the experiments were conducted with CCl_4:$TiCl_4$ mole ratio of 0.5 and the other had a mole ratio of 1. The mole ratio of H_2:$TiCl_4$ was varied from 0.26 to 5.57. In the stoichiometric equation for the reactions involved, one mole of CCl_4, one mole of $TiCl_4$, and four moles of hydrogen combine to yield one mole of TiC and eight moles of HCl. No trends were observed and graphite layers were produced at all temperatures (1100 to 1500°C) over the range of gas flows investigated.

In the 10 to 15-mm pressure experiments, the total gas flow was increased to 475 cc/min. This was the capacity of the pump at 10 to 15-mm pressure. The CCl_4:$TiCl_4$ mole ratio was held constant at 0.5, but the mole ratio of H_2:$TiCl_4$ was varied from 1.39 to 1.79. In the 20 to 25-mm pressure experiments, the total gas flow was increased to about 775 cc. min., largely by increasing the flow of hydrogen. The CCl_4:$TiCl_4$ mole ratio was held constant at 0.5, but the ratio of H_2:$TiCl_4$ was varied from 1.67 to 6.07. With the exception that graphite layering was suppressed at reduced pressures, no trends were apparent insofar as the effect of these variables on fiber quality is concerned.

It is interesting to note the drastic change in the average deposition rate at about 1400 to 1500°C in the 20 to 25-mm pressure experiments. Also some idea of the growth rate of TiC at 20 to 25-mm pressure and 1600°C can be

derived from Fig. 22. The growth rate of the fiber decreases as the diameter increases. This same phenomenon has been observed for other fiber systems.

In addition to the erratic deposition behavior of graphite, there apparently was some other factor or factors that prevented repeatability of experiments. This is made evident by comparing the fibers produced in the 197-107 and 197-108 experiments. Although these fibers were prepared using the same deposition conditions, the nucleation and growth of 197-108 was stymied, but 197-107 grew about 12 mils in diameter in one-half the deposition time. Another example is the variation in diameter of the fibers produced at 20-25 mm pressure and 1300°C. The thickness of these deposits varied by a factor of four; yet they were produced using the same deposition conditions. Unfortunately, the data give no clue as to the possible cause of these discrepancies.

None of these experiments produced good quality titanium carbide fibers. The fibers that were free of graphite layers had highly crystalline surfaces. At the higher deposition temperature, crystallite protrusions were commonplace. Figures 23 and 24 (same magnification) illustrate the extremes in crystallite size. In an effort to reduce the crystallite size, attempts were made to reduce the deposition temperature below 1300°C, but this met with little or no success. The deposition rate at 1100/1200°C was very low, and the resulting deposit was mostly graphite.

The tensile strengths of the TiC fibers produced from CCl_4 were quite low. Excluding those fibers containing graphite layers and those in which the deposit comprises less than 50 percent of the fiber volume, the highest strength TiC fiber produced from CCl_4 was No. 197-119, which had a tensile strength of 26,500 psi. In general, however, the tensile strength of this group of fibers was less than 10 kpsi and about one-half of the fibers had negligible strengths. Our inability to control carbon deposition from CCl_4 and the acute problem of experiment repeatability caused us to abandon further experiments with CCl_4.

(2) Deposition from Acetylene-$TiCl_4$ Mixtures

A brief look was given acetylene as the carbon precursor. In these experiments, an attempt was made to co-deposit carbon and titanium at the lowest practical temperature on the premise that low temperatures are conducive to fine-crystallite structures. One experiment showed that acetylene will decompose at 1200°C. On the basis of this experiment, the temperature of the codeposition experiments was set at 1200°C. Table XV is a compilation of the experimental conditions. These experiments produced either no deposits or pyrolytic graphite. In the

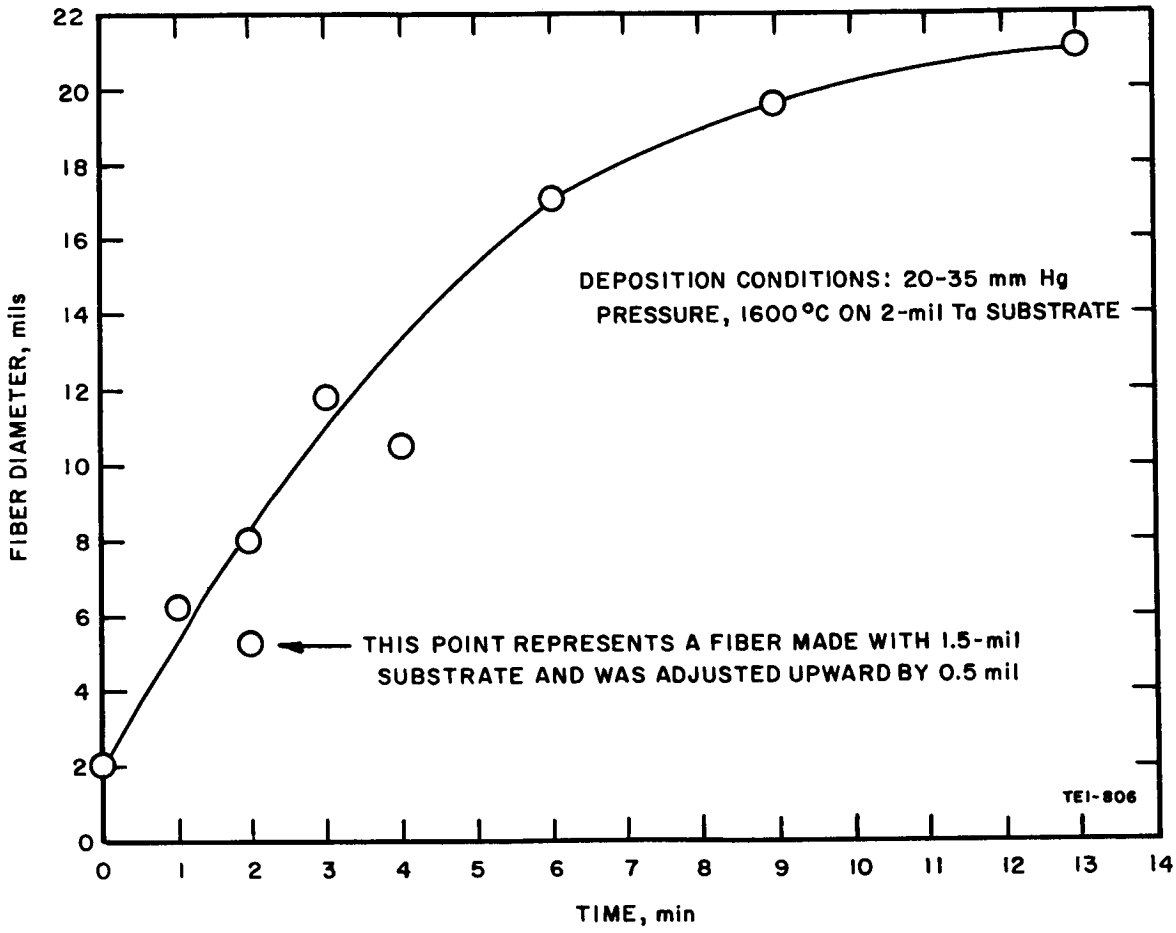

Fig. 22 Plot of Fiber Diameter versus Time - TiC

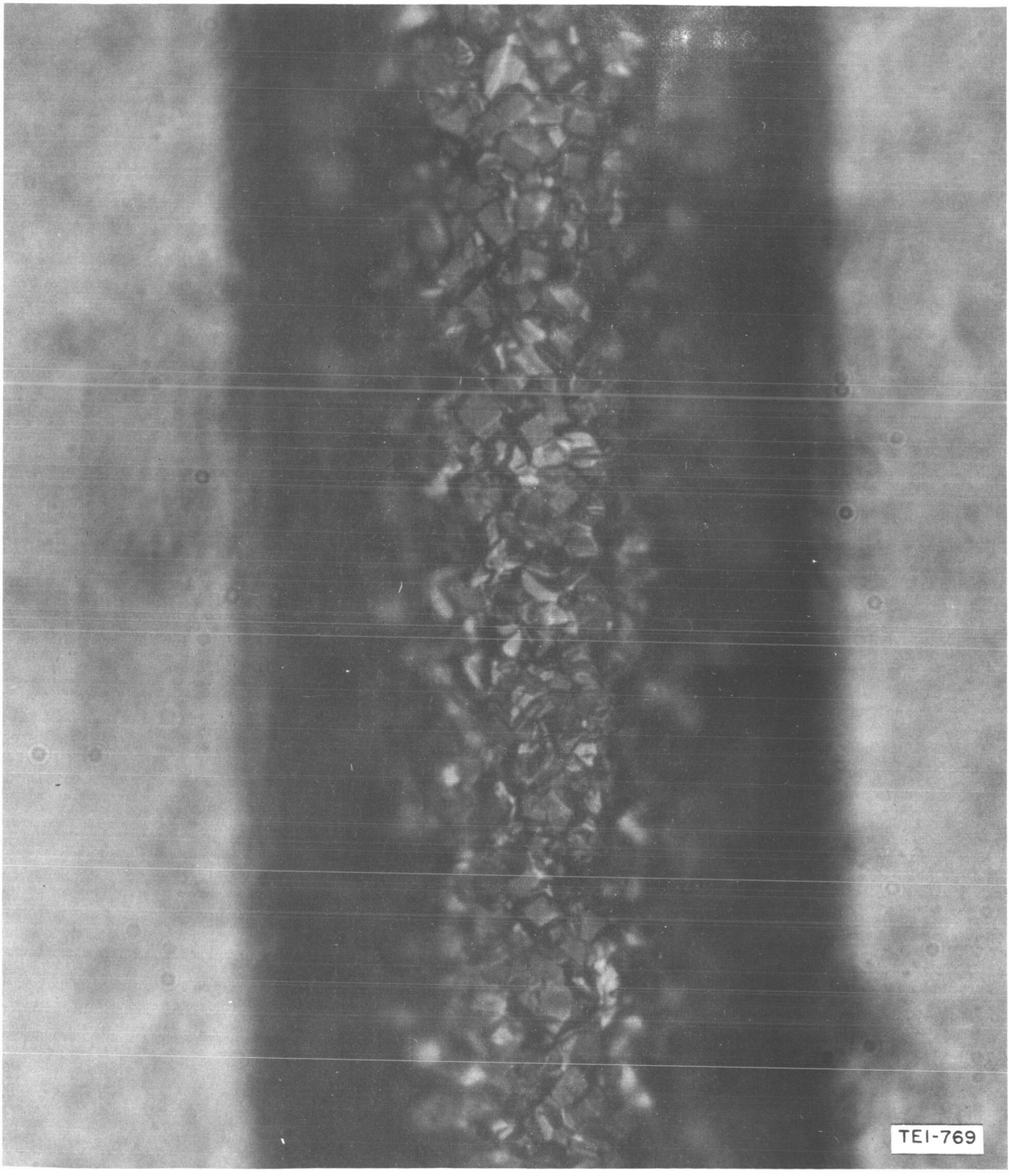

Fig. 23 TiC Fiber No. 197-116. Photograph of Surface, (Magnified 500 X, enlarged 2-1/4 X)

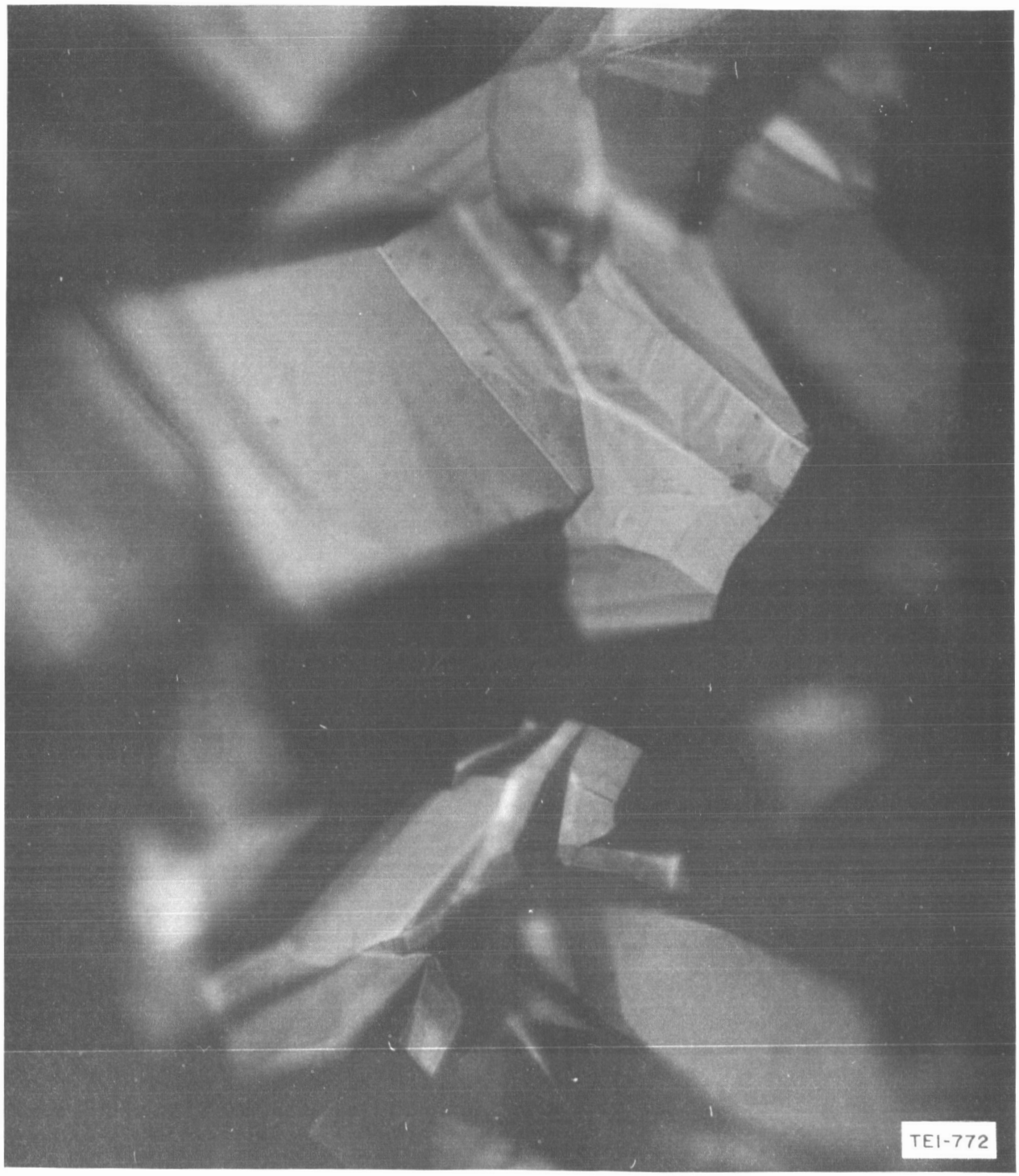

Fig. 24 TiC Fiber No. 197-110. Photograph of Surface, (Magnified 500 X, enlarged 2-1/4 X)

Table XV

DEPOSITION CONDITIONS FOR TITANIUM CARBIDE FIBERS
PRODUCED USING ACETYLENE AT 760 mm Hg PRESSURE

Fiber No.	Temp. °C	Substrate	Gas Flow, cc/min				Time min	Fiber Dia. mils	Remarks
			C_2H_4	H_2	$TiCl_4$	Ar			
222-4	1200	1.5 W	100	480	400	1700	-	-	Argon line plugged and run was terminated
222-5	1200	1.5 W	100	480	400	1700	20	1.7 - 2.0	Deposit had poor adherence. All graphite
222-6 *	1200	1.5 W	55	500	400	1000	14	1.5	--
222-7 *	1300	1.5 W	55	500	400	1000	7	1.5	After 7 minutes, the H_2 flow was increased to 1500 cc/min and fiber began to grow rapidly. Temperature was reduced to 1250°C and rapid growth continued. Fiber was graphite and brittle.
222-8	1250	1.5 W	55	1500	400	1000	4	1.5	--
222-12	1250	1.5 W	15-20	600	245	-	15	2.0 - 3.5	Graphite deposit
222-13	1250	1.5 W	10	600	245	-	7	1.6 - 2.2	--

* In these experiments, the substrate was pretreated by heating 2 minutes in hydrogen at 1200°C.

222-7 experiment, no deposit was evident after seven minutes, but when the hydrogen flow was increased from 500 to 1500 cc/min, rapid deposition of graphite occurred. Experiment 222-8 was an attempt to repeat 222-7 using the high hydrogen flow, but no growth was observed during four minutes of deposition time. In the 222-4 experiment, the argon flow ceased when the line became plugged. Immediately, heavy sooting was noted and the experiment was terminated. This illustrates the effectiveness of a diluent such as argon in suppressing vapor phase reaction.

(3) Deposition from C_2H_5Br-$TiCl_4$ Mixtures

The deposition conditions and properties of titanium carbide fibers produced from titanium tetrachloride - ethyl bromide mixtures are tabulated in Table XVI. Our prior experience indicated that the quality of titanium diboride fibers was improved when the deposition temperature was decreased. With this in mind, the primary emphasis in these experiments was placed on depositing titanium carbide at the lowest possible temperature. This was accomplished by varying the temperature during the initial stage of the experiment and noting the temperature at which deposition initiated or terminated. Changes in the ammeter reading were assumed to indicate deposition was occurring while no change over a short period (1 to 2 minutes) was taken to mean that no deposition was taking place.

Figure 25 illustrates the temperature changes that were made and their effect on deposition. These experiments show that deposition cannot be initiated until a temperature of 1350 to 1400°C is reached, but that after initiation is achieved, the temperature can be reduced to about 1250°C and deposition will continue. Heating directly to 1250°C will not initiate deposition except in the case of the 8:1 mole ratio of $TiCl_4$-C_2H_5Br. Also it appears that a graphite substrate offers no improvement insofar as lowering the deposition temperature is concerned.

Two additional experiments were conducted in an attempt to reduce the deposition temperature. In the preparation of pyrolytic graphite, it was noted that BCl_3 accelerated the decomposition of acetylene. With this in mind, BCl_3 was added to the gas mixture in experiment 197-149. Deposition was not noted until a temperature of 1425°C was reached. The temperature was held momentarily at 1250°C, while the argon flow was reduced incrementally from 1700 cc/min to 100 cc/min to observe the effect of argon flow on deposition. Deposition was not initiated at 1250°C regardless of the argon flow. In another experiment (197-150), the tungsten substrate was pre-coated with about 0.2 mil of boron. No deposition of TiC was noted up to 1300°C even after six minutes at this temperature.

Table XVI

DEPOSITION CONDITIONS AND PROPERTIES OF TITANIUM CARBIDE FIBERS PRODUCED FROM TITANIUM TETRACHLORIDE - ETHYL BORMIDE MIXTURES (1)

Fiber No.	Mole Ratios $TiCl_4$:C_2H_5Br	H_2:$TiCl_4$	Total Gas Flow cc/min	Argon Flow cc/min	Temp °C	Deposition Time min	Fiber Dia., mils	X-ray (2)	Tensile Strength psi	Surface
197-134	2.0	1.84	600	100	1250 (5)	5	8.5	TiC, W_2C, W	(3)	Smooth
197-132	2.0	1.84	600	100	1275 (5)	6	8.7 - 9.3	TiC, Ta	63,000	Smooth
197-133	2.0	1.84	600	100	1300 (5)	7	10.3-11.5	TiC, Ta	3400	Crystalline
197-138	2.0	1.84	2700	1700	1240 (5)	5	8.0	--	--	Crystalline
197-139	2.0	1.84	2700	1700	1250 (5)	7	7.9	TiC, W_2C, W	(3)	Crystalline
197-140	2.0	1.84	2500	1000	1250 (5)	7	8.3 - 9.0	TiC, W_2C, W	(3)	Smooth
197-143	2.0	1.84	2700	1700	1250 (5)	30	19.8-20.1	TiC	(3)	Smooth
197-145	2.0	1.84	2700	1700	1250 (5)	6	6.5	TiC, W_2C, WC	--	Crystalline
197-147	2.0	1.84	2700	1700	1250 (5)	3	6.4 - 9.2	TiC, W_2C, WC	Fragile	Crystalline
197-150	2.0	1.84	2700	1700	1300	6	1.9	--	--	Boron Deposit
197-149	2.0	2.12	1235	100 (6)	1425	1	--	--	--	Very Rough
222-14	8.0	1.59	2025	1000	<1400 (4)	7	5.4 - 5.6	--	--	Crystalline
222-15	8.0	1.59	2025	1000	<1400 (4)	12	5.1	--	--	Crystalline
222-16	8.0	1.77	654	0	1250	7	4.8	TiC (7)	Weak	Crystalline
222-17	8.0	2.66	954	100	1250	6	3.4	--	--	Crystalline
222-18	8.0	2.66	954	100	1250	8	6.0	--	Weak	--

Note:

(1) All experiments conducted at 760 mm Hg pressure with 1.5 mil tungsten substrate except 197-132 and 197-133 which used 2.0 mil tantalum substrate.

(2) Powdered samples except where noted otherwise.

(3) Specimen broke while being mounted in tabs.

(4) $TiCl_3$ deposits on chamber wall precluded temperature measurement.

(5) Fiber was heated to 1350 to 1400°C to initiate deposition; then temperature was reduced to that shown.

(6) Flow varied from 100 to 1700 cc/min while at 1250°C. However, flow was 1700 cc/min while at 1425°C.

(7) Fiber as produced.

Substrate pretreated by heating 60 sec at 1400°C in 263 cc/min C_2H_2 at 22 mm Hg	7
Substrate pretreated by heating 5 min at 1500°C in 350 cc/min C_2H_2 at 25 mm Hg	8
Substrate pretreated by heating 10 min at 1400°C in 160 cc/min C_2H_2 at 14 mm Hg	9
Substrate pretreated by heating 30 sec in a H_2 + BCl_3 mixture at 1050°C	10
Gas also contained 50 cc/min BCl_3	11
Substrate pretreated by heating to 1400°C for 1 min in $TiCl_4$ and H_2	12
Substrate pretreated by heating to 1400°C for 1 min in $TiCl_4$ and H_2	13
Substrate held horizontally between electrodes which were lowered 6-in. in chamber	15

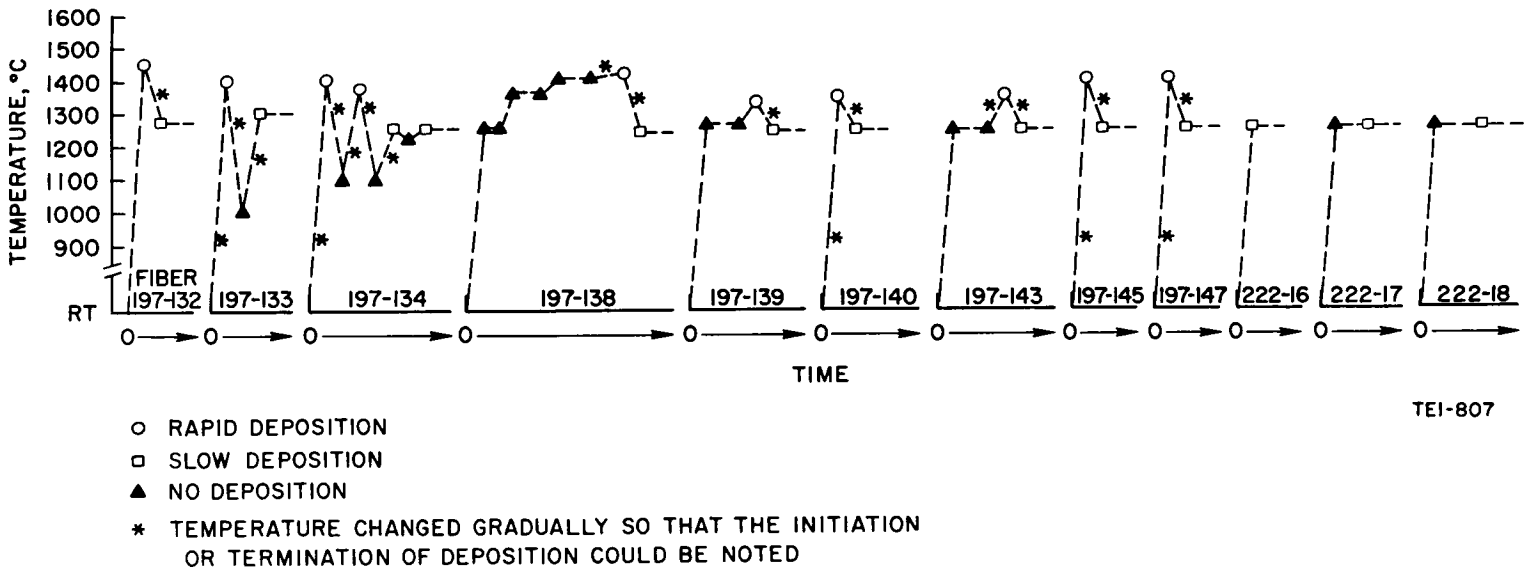

Fig. 25 Heating Program for Titanium Carbide Fibers Produced from $TiCl_4$-C_2H_5Br Mixture

With the exception of 197-132, none of the experiments produced TiC fibers with attractive tensile properties. Generally the fibers were too weak to tensile test or the specimen broke while being prepared for the test. Fiber No. 197-132 had a tensile strength of 63 kpsi and was by far the highest quality fiber produced. Experiments 197-133 and 197-134 were unsuccessful attempts to repeat 197-132. Unfortunately, our supply of tantalum substrate ran out after fiber 197-133 was prepared and tungsten had to be used in subsequent experiments. Therefore, we were not able to make additional attempts to repeat 197-132 using a tantalum substrate.

Figure 26 is a polished cross section of Fiber No. 197-132. Columnar grain structure and a radial crack are visible. The interface between the two layers in the deposit is tracible to an abrupt reduction in temperature made after growth was initiated at a slightly higher temperature. The non-concentricity of the substrate and deposit is difficult to explain but it could be related to the design of the deposition chamber. Careful analysis showed that the phenomenon is not due to the axis of the fiber being mounted at an angle other than 90° to the polished surface.

Only TiC was identified in the deposits of all of the fibers that were given x-ray examination. It is interesting to note that Ta but no TaC was identified in the two highest quality fibers (197-132 and 197-133). This is quite unusual because we normally identify constituents produced by the interaction of the deposit and the substrate. In the case of 197-143, only TiC was found. The reason for this is that the substrate volume (about 0.5 percent of the total volume) was too small for detection by the x-ray. It is also worthy of noting that only TiC was identified in the 222-16 fiber although a $TiCl_4$:C_2H_5 Br mole ratio of 8 was employed in its preparation. The fact that only TiC was identified in the deposits of fibers produced from $TiCl_4$:C_2H_5 Br mole ratios of 2 and 8 indicates that this parameter is not critical insofar as preparing the stoichiometric compound TiC is concerned. However, the data are far too sketchy to draw any conclusions in this regard.

In experiment 222-17, an attempt was made to see what influence the location and orientation of the fiber in the deposition chamber would have on TiC deposition. The electrodes were extended downward about 6 in. with 10-mil tungsten wire in order to displace the fiber further from the upper cover flange. Then the substrate was suspended in a horizontal position between the lower ends of the 10-mil tungsten wire. With this arrangement, it was found that the temperature for initiation of deposition was unchanged and that the deposit was crystalline. No evaluation was made on the fiber produced.

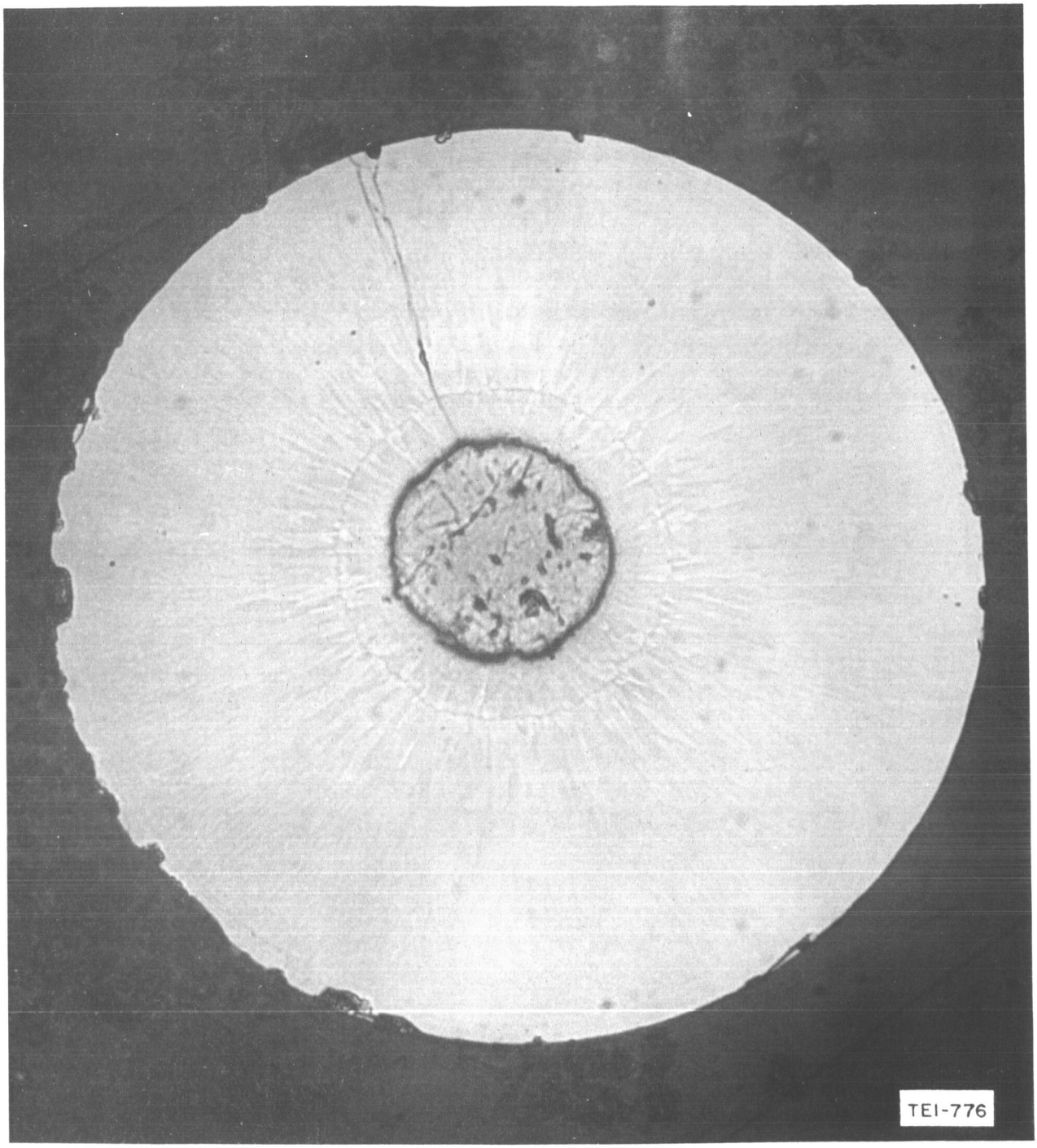

Fig. 26 TiC Fiber No. 197-132. Polished Cross Section, (Magnified 250 X, enlarged 2-1/4 X)

It is not possible to obtain growth rates (fiber diameter as a function of time) for these deposition experiments but it does appear that 4- or 5-mil fibers can be made in less than 5 minutes with a $TiCl_4$:C_2H_5Br mole ratio of 2. In general the deposition rates with the 8 mole ratio appear to be less than one half the rates of the 2 mole ratio.

(4) Deposition from C_4H_{10} - $TiCl_4$ Mixtures

Table XVII is a tabulation of the deposition conditions and the pertinent properties of fibers produced from mixtures of n-butane and titanium tetrachloride. In these experiments, emphasis was again placed on depositing TiC at the lowest possible temperature. In each experiment, the temperature was gradually increased until deposition was indicated by a small change in the electric current. Unfortunately, the accuracy of the reported temperature is not very high due to condensation of $TiCl_3$ on the chamber. The temperature reported for 229-18 is probably the most reliable of the lot because $TiCl_3$ condensation was minimal.

The argon concentration and the mole ratios of $TiCl_4$:C_4H_{10} and H_2:$TiCl_4$ were varied. The largest variations were made to the hydrogen and argon concentrations. In one experiment (229-12), the $TiCl_4$:C_4H_{10} ratio was lowered by about 30 percent. No trends are evident insofar as the effects of these variations on fiber properties are concerned. It is interesting to note, however, that TiC deposits were produced in all of the experiments even though the gas composition was varied.

The repeatability of experiments leaves something to be desired. Experiments 229-11 and 229-16 were conducted under the same conditions but the latter fiber had a crystalline surface and was quite brittle whereas the other fiber had a smooth surface and had a tensile strength of 51 kpsi. Another example involves fibers 229-9, 10, 13, and 14. Although these fibers had similar preparation histories, deposition times were different by a factor of two but their diameters were the same. The cause of this lack of repeatability is not evident but it could possibly be tied in with atmospheric contamination of the chamber experiments and subsequent offgassing during subsequent experiments. Another possible cause is that the actual temperatures were significantly different from those reported due to condensation of $TiCl_3$ on the chamber. The best fiber produced was No. 229-11. It had a tensile strength of 51.4 kpsi and a elastic modulus of 6.56×10^6 psi. The modulus is so far below the measured modulus of bulk TiC ($\sim 65 \times 10^6$ psi) that we seriously doubt its meaning.

Table XVII

DEPOSITION CONDITIONS AND PROPERTIES OF TITANIUM CARBIDE FIBERS PRODUCED FROM n-BUTANE-TITANIUM TETRACHLORIDE MIXTURES (1)

Fiber No.	Temp. °C	Mole Ratio $TiCl_4:C_4H_{10}$	Mole Ratio $H_2:TiCl_4$	Argon Flow cc/min	Total Gas Flow cc/min	Time min	Dia. mils	Surface Appearance	X-ray (4)	Tensile Strength psi	Remarks
229-18	1050 (2)	1.22	2.22	1700	2610	11	5.1	Crystalline	TiC	Weak	
229-12	1200 (3)	0.81	6.0	2000	3235	7.5	6.6	Smooth	TiC	Brittle	
229-15	1200 (3)	1.22	2.22	500	1410	6.5	6.6	Smooth with few crystal protrusions	TiC		
229-8	1200 (3)	1.22	2.22	2000	2910	3	4.9	Smooth	TiC	Weak	Exhaust line plugged
229-10	1200 (3)	1.22	2.22	2000	2910	7	6.3	Smooth	TiC	Brittle	
229-14	1250 (3)	1.22	2.22	2000	2910	7	6.0	Smooth with few crystal protrusions	No test	Weak	
229-13	1200 (3)	1.22	2.22	2000	2910	14	6.2	Smooth	TiC	Weak	
229-9	1200 (3)	1.22	2.22	2000	2910	15	6.1	Smooth	No test	Brittle	
229-16	1200 (3)	1.22	4.0	500	1810	5	4.6	Crystalline	TiC	Brittle	
229-11	1200 (3)	1.22	4.0	500	1810	10	6.1	Smooth	TiC	51,400	
229-17	1175 (3)	1.22	4.0	2000	3310	11	3.3	Smooth	TiC	Brittle	Exhaust line plugged

Notes:

(1) All deposition made at 760-mmHg pressure on 1.5-mil diameter tungsten substrate which was preconditioned by heating 2 minutes in hydrogen at 1200°C. All depositions were in Chamber 'C' except 229-18 which was made in Chamber 'B' modified as described in text.

(2) Actual temperature may have been slightly higher due to slight condensation in the chamber.

(3) $TiCl_3$ condensation on chamber was moderate.

(4) All x-ray performed on fiber as produced.

It does appear that n-C_4H_{10} - $TiCl_4$ mixtures will produce TiC deposits at slightly lower temperatures than the C_2H_5 Br - TiC_4 mixtures. In general, the appearance of the deposits made from n-butane was smoother and less crystalline. However, no high quality TiC fibers were produced.

(5) Deposition from C_5H_{12} - $TiCl_4$ Mixtures

In our search for a carbon precursor that would permit preparation of TiC fibers at the lowest possible temperature, a brief look was given to neo-pentane. The deposition conditions and properties of the fibers produced are given in Table XVIII. The $TiCl_4$:C_5H_{12} mole ratio was held constant throughout the experiments while large variations in hydrogen concentration were made. Argon was used as a diluent in all but one experiment.

In these experiments, the electric current drawn by the fiber while maintaining a constant temperature was recorded as a function of time. Deposition was terminated when the current increased to about 1.75 amperes. This procedure was largely responsible for the diameters of the fibers being so similar. It is interesting to note the variation in deposition time required to produce a given diameter fiber although the deposition conditions were nearly the same (i.e., Fibers 229-20, 21, 22, and 23). The apparent lack of correlation between the deposition time and fiber diameter suggests that the experiment repeatability was poor.

In general, the accuracy of the reported temperatures is better than in the case of the n-butane experiments because the jets of argon that were used to keep small areas of the chamber free of $TiCl_3$ condensate were quite effective. It appears that the minimum temperature for deposition of TiC from C_5H_{12}-$TiCl_4$ mixtures may be lower than for C_4H_{10}-$TiCl_4$ mixtures.

X-ray analysis identified only TiC in the deposits. With the exception of Fiber 229-20, the fibers were brittle and highly crystalline. Fiber 229-20, on the other hand, was smooth and had a tensile strength of 22.8 kpsi. The reason for the observed difference in properties is not apparent but it may be that the actual deposition temperature was significantly lower for Fiber 229-20 than in other experiments. As suggested in the butane experiments, atmospheric contamination may be an important factor.

Examination of experiment 229-25 suggests that a large excess of hydrogen and/or the absence of argon significantly reduces the rate of deposition. This fiber had the smallest diameter yet the longest deposition time of the lot.

Table XVIII

DEPOSITION CONDITIONS AND PROPERTIES OF TITANIUM CARBIDE FIBERS PRODUCED FROM NEOPENTANE - TITANIUM TETRACHLORIDE MIXTURES (1)

Fiber No.	Temp. °C	Mole Ratios $TiCl_4:C_5H_{12}$	Mole Ratios $H_2:TiCl_4$	Argon Flow cc/min	Total Gas Flow cc/min	Time min	Dia. mils	Surface Appearance	X-ray (3)	Tensile Strength psi
229-23	1125 (4)	1.28	2.17	1700	2155	8	6.25	Crystalline	TiC	Brittle
229-21	1030 (2)	1.29	2.22	1700	2600	14	5.8	Crystalline	TiC	Brittle
229-20	1050 (2)	1.29	2.22	1700	2600	16	6.1	Smooth	TiC	22,800
229-22	1150	1.29	2.22	1700	2600	20	5.8	Crystalline	TiC	Broke during mounting
229-24	1125 (4)	1.28	4.35	1700	2405	17	6.4	Crystalline	TiC	Brittle
229-25	1125	1.29	9.78	0	2600	23	4.0	Crystalline	TiC	Brittle

Notes:

(1) All depositions made at 760 mm Hg pressure on 1.5-mil diameter tungsten substrate which was preconditioned by heating 2 minutes in hydrogen at 1200°C. All depositions were made in Chamber B modified as described in the text.

(2) Actual temperature may have been slightly higher due to condensation of $TiCl_3$ on chamber.

(3) All x-ray performed on fiber as produced.

(4) Deposition initiated at 1200°C then temperature was reduced.

(6) Summary on Titanium Carbide Fiber

The highest quality titanium carbide fiber was prepared from ethyl bromide-carbon tetrachloride mixtures. This fiber had a tensile strength of 63 kpsi. Attempts to produce additional good fibers by the same procedure were unsuccessful.

In general, experiment repeatability was very poor in all of the TiC preparations. Carbon deposition from CCl_4 seems difficult to control. Minimum deposition temperatures were experienced with n-butane and neo-pentane.

C. Tungsten-Coated Boron Fibers

Three deposition gases, tungsten hexacarbonyl, tungsten hexachloride, and tungsten hexafluoride were used to deposit tungsten on boron substrates. The $W(CO)_6$ and WCl_6 were used to deposit tungsten on pre-prepared boron substrates. Later tungsten-coated boron fibers were produced by first producing a boron fiber and, as soon as deposition of boron was terminated, immediately depositing tungsten from the reduction of WF_6.

The experimental procedure for the $W(CO)_6$ and WCl_6 depositions consisted of placing a length of boron between the electrodes in deposition chamber 'A' (Fig. 14a), admitting argon into the chamber at the desired flow rate through a sublimer containing the volatile tungsten compound, evacuating the chamber to 1- or 10-mm Hg, heating the tungsten-containing solid in the sublimer to the desired temperature, and then heating the boron fiber to 800°C. The design of the sublimer was similar to the vaporizer used in deposition chamber 'B' (Fig. 14b). The substrate temperature was maintained at 800°C. In order to minimize recrystallization of the boron, the temperature must be below about 1100°C, but, on the other hand, it must be high enough to be read on the optical pyrometer.

The first coatings were attempted using $W(CO)_6$ as the deposition gas. A typical coating consisted of carbon and WO_2. The results clearly indicate that the substrate temperature was sufficiently high to decompose CO present in the $W(CO)_6$. According to Lander and Germer (17), the decomposition of CO can be eliminated at a temperature between 400 and 600°C by the addition of water vapor to the reacting gas according to the reaction:

$$CO + H_2O = H_2 + CO_2$$

Since we did not have a suitable means of determining substrate temperatures below about 800°C, the decomposition of $W(CO)_6$ below 800°C was not evaluated. Gold (18) also mentions the use of water to prevent carbon or carbide formation in the decomposition of pure $W(CO)_6$ at 0.025 to 0.200-mm Hg on substrates at 800 to 1500°C. An x-ray analysis of his deposits was not given. Although these reports clearly indicate the advantages of including water vapor in the feed gases when depositing tungsten from $W(CO)_6$, the oxidation of the boron substrate by the water vapor may be as deleterious to the final fiber as the decomposition of CO. The oxidation of boron at high temperatures has been reported (19). Thus, decomposition temperatures above 800°C were not attempted.

The conditions of preparation and properties of fibers reacted with $W(CO)_6$ are given in Table XIX. The tensile strength of all these fibers is considerably lower than the strength of the substrate boron. This may be due to the decomposition of CO to give oxides and possibly carbides of tungsten on the boron surface.

The second compound used as a tungsten precursor was WCl_6. Experiments were made at total chamber pressures ranging from 1- to 760-mm Hg. Hydrogen was used in some runs to chemically reduce WCl_6 to tungsten on the substrate. Conditions for preparing the fibers and their properties are given in Table XIX.

More than one-half of the fibers processed had considerably lower tensile strengths than the original boron fiber used as a substrate. However, fiber No. 193-87-3 showed a considerable increase in strength with no apparent increase in diameter. This fiber gave test strengths of 503×10^3 and 796×10^3 psi for an average of 650×10^3 psi, as compared with an average of 265×10^3 psi for the boron substrate. It should be noted in Table XIX that fiber No. 193-87-2, processed under similar conditions, did not show an increase in strength. It is most probable that the two test values for 193-87-3 are within the spread of values for the boron substrate and, therefore, do not represent an improvement in strength.

A tungsten-containing fiber was obtained by decomposing WCl_6 on the hot boron substrate at a chamber pressure of 10-mm Hg. A run of 90 minutes duration resulted in a 4.4-mil fiber (coating thickness about 0.2 mil) which appears to contain, not free tungsten, but a new tungsten boride, WB_2. Additional fibers produced by the same procedure also contained WB_2. Similar results were obtained at less deposition time, but variations in the sublimer temperature produced variations in the diameter of the fibers.

Figure 27 is a photograph of the fracture surface of a tungsten-coated boron fiber. The degradation in strength of the boron is most likely due to the gross pores which are formed beneath the tungsten/tungsten-boride layer. The mechanism by which these pores are formed is not understood, but their round shape, as observed in Fig. 27, suggests that they were formed by some sort of mass transport phenomenon.

Subsequent tungsten coatings were made by decomposition of WF_6, which is a gas at room temperature. Other experimenters (20) report that crackfree, adherent coatings can be made at temperatures of only 500°C. Deposition at such a low temperature should minimize tungsten-boron interactions.

Table XIX

TUNGSTEN-COATED BORON FIBERS
$W(CO)_6$ AND WCl_6 DEPOSITION

Fiber	Plating Gas	Hydrogen Flow Rate cc/min	Sublimer Temp, °C	Argon Flow Rate cc/min	Total Chamber Pressure mm Hg	Time min	Fiber[e] Dia mils	Tensile Strength[a] psi	X-ray Analysis[b]
193-85-1	$W(CO)_6$		150	200	10[c]	50		d	
193-85-2	$W(CO)_6$		100	500	10	20	6.3	d	
193-86-1	$W(CO)_6$		100	100	1	15	7.0	38,000	
193-86-2	$W(CO)_6$		100	100	1	15	4.0	34,000	WO_2, unidentifiable
193-87-1	WCl_6		200	300	760	30	3.9	d	
193-92-2	WCl_6		200	300	10	18	3.9	d	WB_2
193-91-2	WCl_6		200	300	10	20		d	WB_2, W
193-93-1	WCl_6		200	300	10	27	4.0	d	WB_2
193-87-4	WCl_6		200	300	10	30	4.0	29,000	W
193-91-3	WCl_6		200	300	10	67		d	WB_2
193-88-1	WCl_6		200	300	10	90	4.4	28,000	WB_2
193-92-1	WCl_6		200	300	10	120		d	W
193-88-4	WCl_6		200	100	2	32	4.0	322,000	
193-89-1	WCl_6		200	100	3	10	4.0	303,000	
193-87-2	WCl_6	200	200	300	760	3 min in Ar 3 min in Ar + H_2	4.0	272,000	
193-87-3	WCl_6	200	200	300	760	5 min in Ar 1 min in Ar + H_2	3.9	650,000	
193-88-2	WCl_6	200	200	300	10	2 min in Ar 5 min in Ar + H_2	4.0	317,000	
193-88-3	WCl_6	200	200	-	10	5 min in Ar 10 min in Ar + H_2	3.8	d	
193-89-2	WCl_6	25	250	25	1 1	50 50	4.1 4.1	100,000 100,000	
193-89-3	WCl_6		250	50	1	28		143,000	Unchanged

a. Average tensile strength of the boron used = 265×10^3 psi
b. Analysis only on fibers indicated. Substrate patterns present in all fibers
c. Pressure increased during run
d. Fiber too brittle to test
e. Boron substrate diameter 3.9 mils

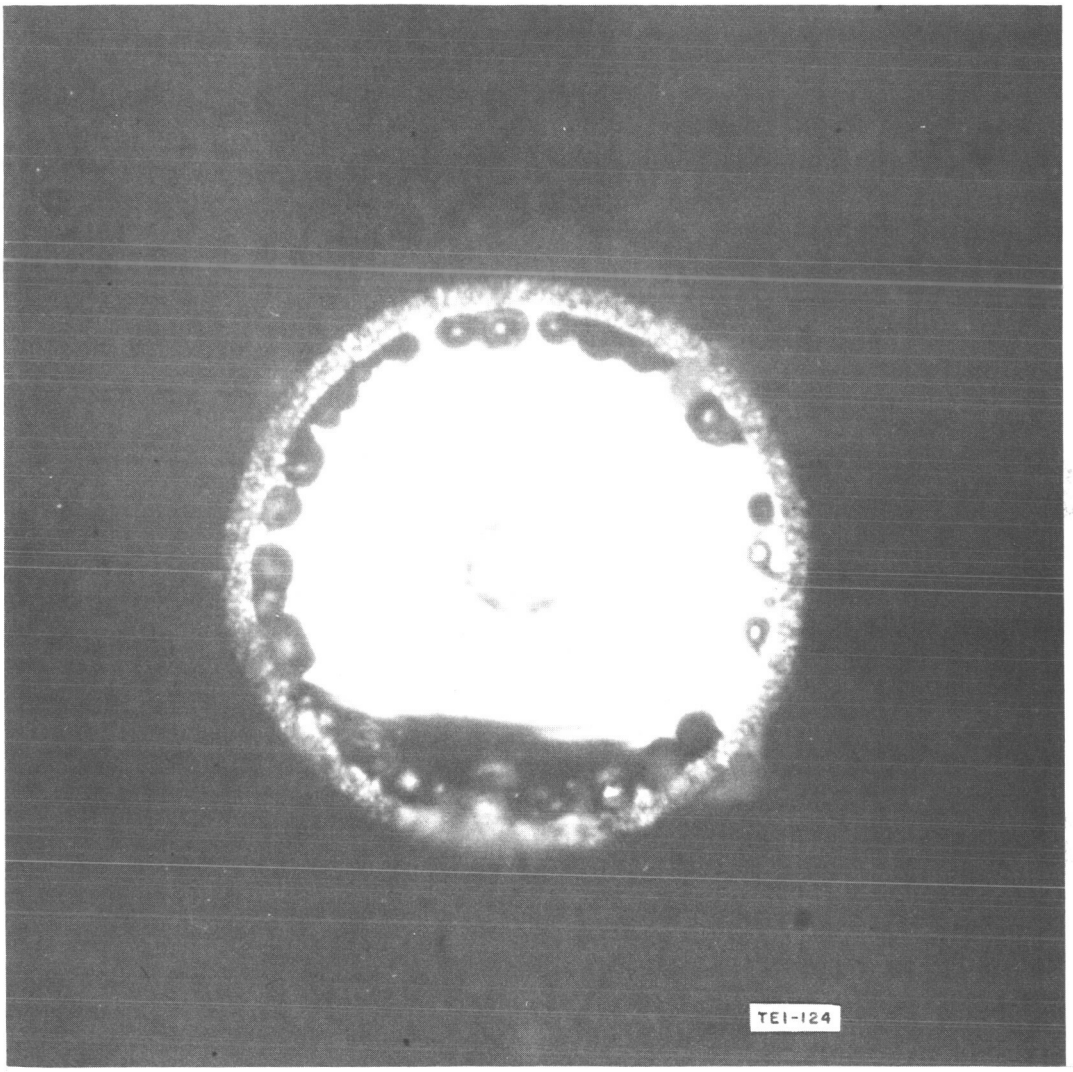

Fig. 27 Tungsten Coated Boron Fiber No. 193-88-1 as Fractured Surface, (Magnified 400 X, enlarged 1.8X)

An integral plating process was used in which the boron substrate was formed first, followed by immediate reduction of WF_6 to produce the tungsten coating. The idea here was to maintain the boron substrate at or near its plating temperature to avoid excessive cracking which may occur during the cooling, and to begin tungsten plating on a freshly deposited boron substrate. In addition to the tungsten-coated boron fibers, several boron fibers were produced to serve as control samples.

The experimental procedure for the WF_6 decompositions made at atmospheric pressure consisted of placing a length of 0.5-mil diameter tungsten wire between the electrodes in deposition chamber 'A' (Fig. 14a), admitting hydrogen and BCl_3 at the desired flow rates and heating the tungsten substrate to 1050°C. At the end of the prescribed deposition time, the BCl_3 flow was terminated, and the hydrogen flow was adjusted for the WF_6 decomposition. The temperature was then reduced to faint redness (room darkened) which is about 500-600°C and the WF_6 was admitted. At the end of the deposition time, the WF_6 flow was terminated and the temperature was gradually reduced to room temperature. Table XX lists the deposition conditions and pertinent results on fiber characterization.

All of the boron control fibers, 193-116-1, 117-1, 118-1, 119-1, and 120-1 were of good quality. They had the typical corn-cob surface appearance and were quite flexible. The flexibility of fiber 193-123-1 (Ta substrate) was not as good as the other control samples.

The tungsten-coated fiber, 193-119-1, had good flexibility, but the tensile strength was only 66 percent of the average tensile strengths of the control fibers. In addition, the thickness of the tungsten layer was probably less than a few hundredths of a mil because of the short deposition time. This is borne out by the appearance of the surface which is only slightly different from the surface of the boron.

Fiber 193-121-1 was brittle and its flexibility was low. Its surface was smoother than the surface of the boron fiber, but outlines of the corn-cob appearance were still evident. X-ray showed the presence of tungsten and tungsten boride. Fiber 193-124-1 had no significant flexibility and was somewhat brittle. The tungsten coating was badly exfoliated.

In an effort to reduce cracking and exfoliation of the deposits, tungsten depositions were then made at reduced pressure. Prior work by other investigators (21) indicated that low pressures and temperatures were conducive to adherent

Table XX

TUNGSTEN-COATED BORON FIBERS

BCl_3 AND WF_6 DEPOSITION

Fiber No.	Boron Deposition[1] Time, °C	Time, min	Tungsten Deposition Time, min	Fiber Dia, mils	Tensile Strength kpsi	X-ray Results	Remarks
193-120-1(4)	950	2.0		3.4-3.5	192	WB_4, B, W_2B_5	Could not reach temp
193-117-1(4)	1010	2.5		4.4-4.7	510		Run as planned
193-113-1(4)	1050	1.0		4.8-5.1			Fiber broke before WF_6 was admitted
193-116-1(4)	1050	1.5		3.8-4.5	98		Fiber broke
193-136-1(4)	1050	2.0		9.5-11.0			Fiber broke before WF_6 was admitted
193-138-1(4)	1050	2.0		6.2-6.7			Fiber broke before WF_6 was admitted
193-118-1(4)	1000/1150	2.5		7.3-7.6	445		Run as planned
193-119-1(4)	1050	2.5	<0.1(3)	5.8-6.2	232		Fiber broke when WF_6 was admitted
193-137-1(4)	1050	2.0	0.7(2)	6.0-6.8	18.1		Fiber broke
193-139-1(4)	1050	2.0	1.0(2)	8.7-10.0	Too brittle		Run as planned
193-121-1(4)	1050	3.0	1.5(3)	5.1-5.2	147	B, W_2B_5, W, WB_4	Run as planned
193-123-1(5)	~ 1050	2.5		12.1	28	B, TaB_2	Run as planned
193-141-1(5)	1050	2.0	2.0(2)	8.8-9.2	Too brittle	W	Run as planned
193-142-1(5)	1050	2.0	2.0(2)	10.0-10.6	88.7	W	Run as planned
193-143-1(5)	1050	2.0	3.0(2)	9.8-10.1	82.4	W	Run as planned
193-140-1(5)	1050	2.0	3.0(2)	9.0-9.3	44/68.4	W	Run as planned

(1) Boron Deposition - 400 cc/min BCl_3
600 cc/min H_2
760 mm Hg

(2) Tungsten Deposition - 460 cc/min WF_6
900 cc/min H_2
5 mm Hg
~ 500 °C (Faint redness in dark room)

(3) Tungsten Deposition - 460 cc/min WF_6
900 cc/min H_2
760 mm Hg
~ 500°C (Faint redness in dark room)

(4) 0.5 mil W Substrate

(5) 3.0 mil Ta Substrate

tungsten deposits made from WF_6.

Referring to Table XX, the experimental procedure for Fiber Nos. 193-140-1, 141-1, 142-1, and 143-1 consisted of placing a length of the desired substrate (tungsten or tantalum) between the electrodes in deposition chamber 'A', admitting hydrogen and BCl_3 at the desired flow rates, and heating the substrate to 1050°C. At the end of the prescribed deposition time, the BCl_3 flow was terminated, the temperature was reduced to about 500°C, and the pressure was reduced to 5-mm Hg. After the hydrogen and WF_6 flows were adjusted for the tungsten deposition, final adjustments were made to the temperature and pressure. At the end of the deposition time, the WF_6 flow was terminated, and the temperature was gradually reduced to room temperature. Fiber No. 193-137-1 was produced by essentially the same procedure except that after the BCl_3 flow was terminated, the hydrogen and WF_6 flows were adjusted, then the pressure was reduced to 5-mm Hg and the temperature was reduced to about 500°C. The reason for the slightly different sequence of procedures is that difficulty was experienced in keeping the boron temperature below 1050°C during the pump-down period and during the period that the hydrogen and WF_6 flows were being adjusted on Fiber No. 193-137-1. The difficulty was due to the changing heat transfer conditions in the deposition chamber while these adjustments were being made. Therefore, the temperature was decreased prior to the pressure and gas-flow adjustments for Fibers 140-1 through 193-143-1, in order to minimize temperature surges.

Fibers 193-140-1, 141-1, 142-1, and 143-1 were produced by the same procedure and deposition conditions. The large variation in fiber diameter is most likely due to differences in the time-temperature relationships during deposition. For example, assuming that all of the variation is due to the diameter of the boron deposits, a difference of 10 seconds in reaching the plating temperature and 10 seconds in terminating the BCl_3 flow would account for all of the variation.

The thickness of the tungsten coating varied between the three fibers (0.24 to 0.30 mils). However, the thickness of the coating on any one of the fibers was quite uniform. There was no evidence of significant interaction between the boron and the tungsten, and x-ray diffraction patterns of the as-produced fibers revealed only tungsten to be present. This indicates that the diffusion of boron into tungsten is quite slow at the deposition temperature (500°C). Figure 28 is a photomicrograph of the as-fractured surface of Fiber 193-142-1.

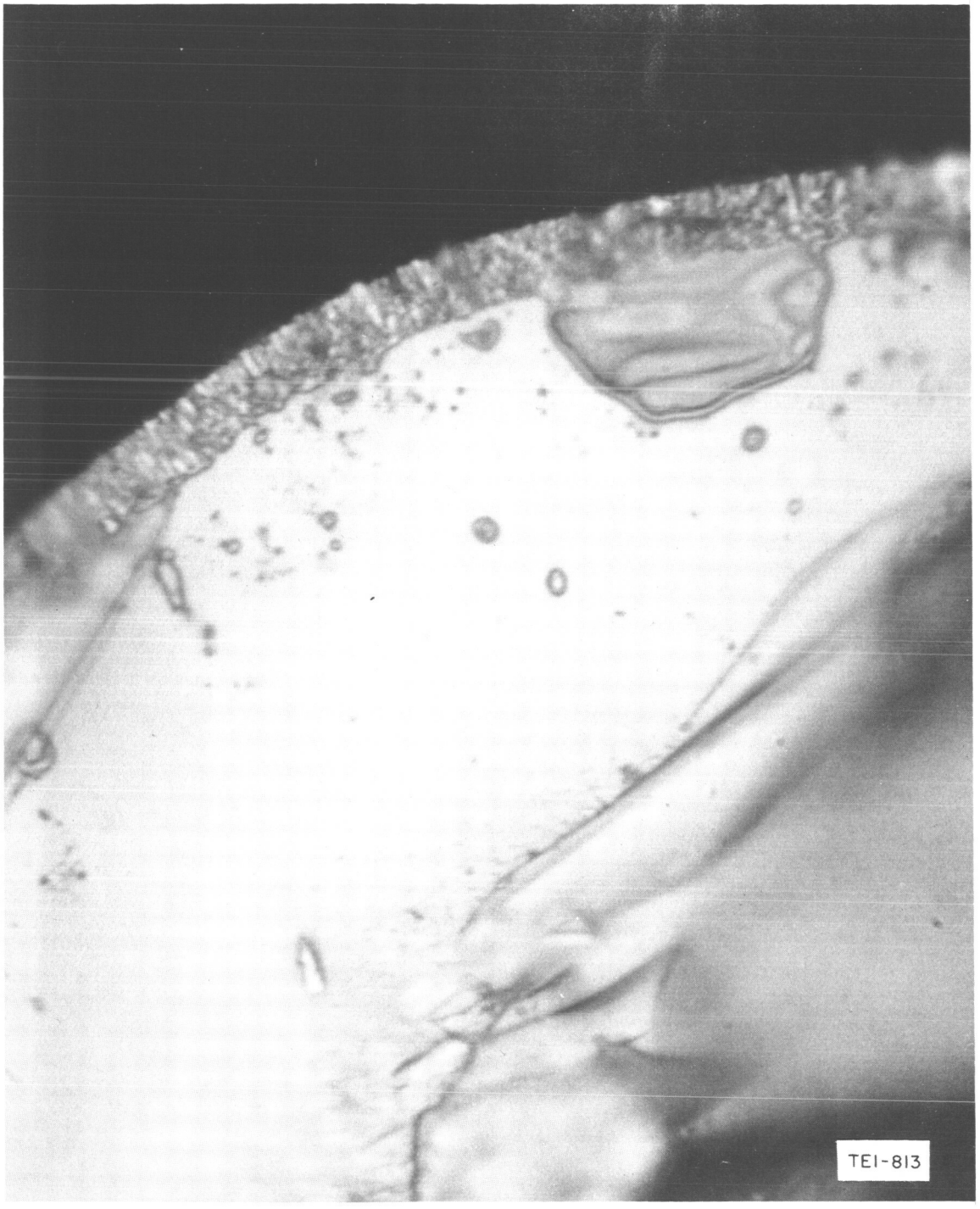

Fig. 28 Tungsten Coated Boron Fiber No. 193-142-1 as Fractured Surface, (Magnified 1200 X, enlarged 1.4 X)

The tensile strengths of Fibers 193-142-1 and 143-1 were about the same, but were quite low compared to boron filament strengths. Fiber 193-141-1 was too brittle to test. The difference in tensile behavior of the three fibers may be related to the surface roughness. Fiber 193-141-1 has a nodular surface, whereas the other two fibers have comparatively smooth surfaces. Since the tensile results represent single values for each fiber, it is quite possible that these values are not representative of the strength of fibers produced by this procedure.

In summary, tungsten coated boron fibers were successfully produced by the hydrogen reduction of WF_6 on a boron substrate at 5-mm Hg pressure. These fibers had tensile strengths in the range of 44 to 89 kpsi but the statistics are so poor that it is highly probable that higher strengths could be realized by additional testing.

D. Pyrolytic Graphite Fibers

Graphite fibers were prepared by the pyrolysis of acetylene on hot tungsten wire substrates. Acetylene was chosen as the carbon-containing gas because: (a) the reaction $C_2H_2 = 2C + H_2$ does not produce a net change in the number of gas molecules, and thus, the deposition chamber pressure should remain essentially constant, and (b) evidence has been presented that some hydrocarbons are pyrolyzed to acetylene before forming the final products, solid carbon and hydrogen (22 and 23).

In these experiments the deposition pressure was varied from 5- to 100-mm Hg while the temperature was varied from 1000 to 2000°C. The acetylene flow was held constant at 263 cc/min (measured at 760-mm Hg) with the exception of one experiment (193-36-1) which had an acetylene flow of 150 cc/min. Deposition times were varied from 5 to 240 minutes. All fibers were prepared in deposition chamber 'A' (see Fig. 14a). The deposition conditions and properties of each fiber produced are presented in Table XXI.

Attempts were made to correlate tensile strength with deposition temperature and pressure but only weak trends are evident. The difficulty of establishing correlations with tensile strength lies in the fact that a large scatter normally occurs in the tensile test results of fibers. This scatter is largely due to the variation of the type, size, and number of defects in the specimens. Some specimens have more severe defects than others or they may have a higher population of them. Thus, a large number of tests are needed in order to establish representative tensile strengths. The tensile strengths reported in Table XXI represent single tests on each fiber and, therefore, may or may not be representative values. Another factor that has been found to affect the strength of fibers is the fiber diameter. It is usually found that the strength of fibers increases as their diameters decrease, although this is not a hard and fast conclusion. Examination of Table XXI shows a wide variation in diameters for a given temperature and/or pressure. This variation is due primarily to the variation in deposition time.

In spite of these difficulties, two weak trends are noted. At a deposition temperature of 1500°C, there is an indication that tensile strength increases as the pressure decreases. This trend is shown below:

Pressure, mm Hg	Tensile Strength, kpsi	Diameter, mils
100	14.9	6.5
50	15.8	8.8

Table XXI

DEPOSITION CONDITIONS AND PROPERTIES OF GRAPHITE FIBERS PRODUCED BY PYROLYSIS OF ACETYLENE

Fiber[1][3]	Chamber Pressure mm Hg	Substrate Temp, °C	Time min	Final Dia, mils	Density g/cc	Tensile Strength Kpsi	Elastic Modulus Million psi
193-74-9	5	1400	60	5.4	2.10	58.4	9.3
193-72-1	10	1000	60	1.2	-	-	
193-74-1	10	1050	240	0.9	>2.90	-	
193-72-2	10	1200	60	3.4	2.45	27.0	
193-74-2	10	1200	100	2.0	> 2.90	-	
193-73-1	10	1400	10	2.1	> 2.70	-	
193-73-10	10	1400	15	3.6	2.28	54.2	18.9
193-73-2	10	1400	20	4.1	2.29		
193-73-3	10	1400	30	5.0	2.22		
193-72-3	10	1400	30	4.25	2.18	46.5	8.7
193-74-3	10	1400	36	5.4	2.08	56.3	8.0
193-73-4	10	1400	45	4.8	2.09		
193-73-5	10	1400	60	6.0	1.93		
193-73-6	10	1400	90	7.2	1.82	47.3	14.2
193-73-7	10	1400	120	8.8	1.77	33.4	
193-73-8	10	1400	150	8.6	1.73	44.7	
193-73-9[2]	10	1400	150	10.4	1.72	47.5	
193-37-2[2]	≃ 10	1500	20	4.8	-	50.0	
193-72-7	10	1550	60	14.0	2.07	27.8	
193-74-4	10	1600	13	9.5	2.11	22.3	
193-72-4	10	1600	30	10.25	2.10	29.4	
193-74-5	10	1700	12	10.3	2.11	24.1	
193-74-6	10	1700	24	16.6	2.10	31.5	
193-74-7	10	1800	10	12.5	2.11	32.0	
193-74-8	10	1800	18	17.0	2.11	18.5	
193-72-6[2]	10	2000	10	4.10	2.35	-	
193-37-1[2]	20	1500	20	8.1	2.3	23.6	
193-71-1	34	1000	30	1.05	>2.70		
193-71-2	34	1200	30	1.6	>2.70		
193-71-4	34	1400	30	7.0	1.80	48.0	
193-71-3	34	1600	30	17.3	2.06	10.6	
193-71-5	34	1800	5	12.8	1.70	19.3	
193-36-1[2][4]	50	1500	15	8.4	-	-	
193-36-2[2]	50	1500	20	8.8	2.0	15.8	
193-29-1[2]	100	1200	120	2.5	> 3.4	-	
193-29-2[2]	100	1500	20	6.5	2.4	14.9	

Notes:
1. Substrate was 0.5 mil tungsten unless noted otherwise
2. Substrate was 1.5 mil tungsten
3. C_2H_2 flow rate was 263 cc/min at 1 atm unless noted otherwise
4. C_2H_2 flow rate was 150 cc/min

Pressure, mm Hg	Tensile Strength, kpsi	Diameter, mils
20	23.6	8.1
10	27.8	14.0
10	50	4.8

The large difference in tensile strength of the two fibers produced at 10 mm pressure may be due to the large difference in their diameters. This trend is consistent with observations made on the surface appearance of these fibers. Qualitatively, the total composite of these data indicates that the surfaces get smoother with fewer nodules as the deposition pressure is decreased.

Another trend involves the effect of deposition temperature on tensile strength at 10-mm Hg pressure. Tensile strength appears to increase as the temperature is decreased. Again, this is in general agreement with observations made on surface roughness (i.e. smoother fibers were produced at the lower temperatures). The trend is shown below:

Temperature, °C	Average Tensile Strength, kpsi	Fiber Nos.	Diameter, mils
1800	25.2	193-74-7	12.5
		193-74-8	17.0
1700	27.8	193-74-5	10.3
		193-74-6	16.6
1600	25.8	193-74-4	9.5
		193-72-4	10.25
1500	38.9	193-37-2	4.8
		193-72-7	14.0
1400	47.1	193-73-6	7.2
		193-73-7	8.8
		193-73-8	8.6
		193-73-9	10.4
1200	27	193-72-2	3.4

It should be noted that fiber diameter also trends to decrease as the temperature decreases and that this casts some doubt on the validity of the suggested trend.

In summary, it does appear that the highest strength and smoothest fibers were

produced at the lower pressures and lower temperatures (down to 1400°C) but that the effect of temperature is somewhat uncertain. Fibers with tensile strengths up to 58 kpsi were produced.

The rate of change of fiber diameter with deposition time is shown in Fig. 29 for fibers prepared at 10-mm Hg pressure and 1400, 1600, 1700, and 1800°C. The curves for 1400, 1700, and 1800°C are produced from the data in Table XXI while the growth curve for 1600°C was determined by another technique. In this technique, a fiber was photographed periodically as the decomposition of C_2H_2 proceeded. After the film was processed, the negatives were projected onto a screen with a multiplication of 50X and the growth of the fiber was determined (by diameter increase) as a function of time. The weight used to hold the substrate in tension during deposition was used as a calibrating marker. This weight consisted of a section of rhenium wire, 10.3-mils diameter, looped around the substrate. The weight, which was cooler than the fiber, appeared on the negative as a discontinuity in the fiber. The width of this discontinuity is directly proportional to the diameter of the weight or, 10.3 mils.

Based on the linearity of the 1600°C plot and the fact that the curve intersects the ordinate at about 0.6 mil (the calculated diameter of the expanded WC core), we used two experimental points and forced linear curves through these points and another point at 0.6 mil and zero time to produce the curves at 1700 and 1800°C.

As the growth curve for 1400°C clearly shows, the rate of diameter increase in the early stages decreases as deposition proceeds but, that after this initial period, the rate is linear. Unfortunately, the growth rates during the early part of the curve are not readily determinable for several reasons.

(1) Small diameter measurements at short times may be influenced by the starting technique. This provides for heating the substrate below 1200°C for several minutes in the presence of the acetylene until hot spots in the wire are "cured". Although the deposition rate at this temperature is generally quite low, some growth may occur. The temperature is then raised to 1400°C, and this is taken as the starting time for the experiment.

(2) The core diameter is altered by the change from tungsten to tungsten carbide (as shown by x-ray analysis).

(3) There probably are catalytic effects of the initial metal substrate.

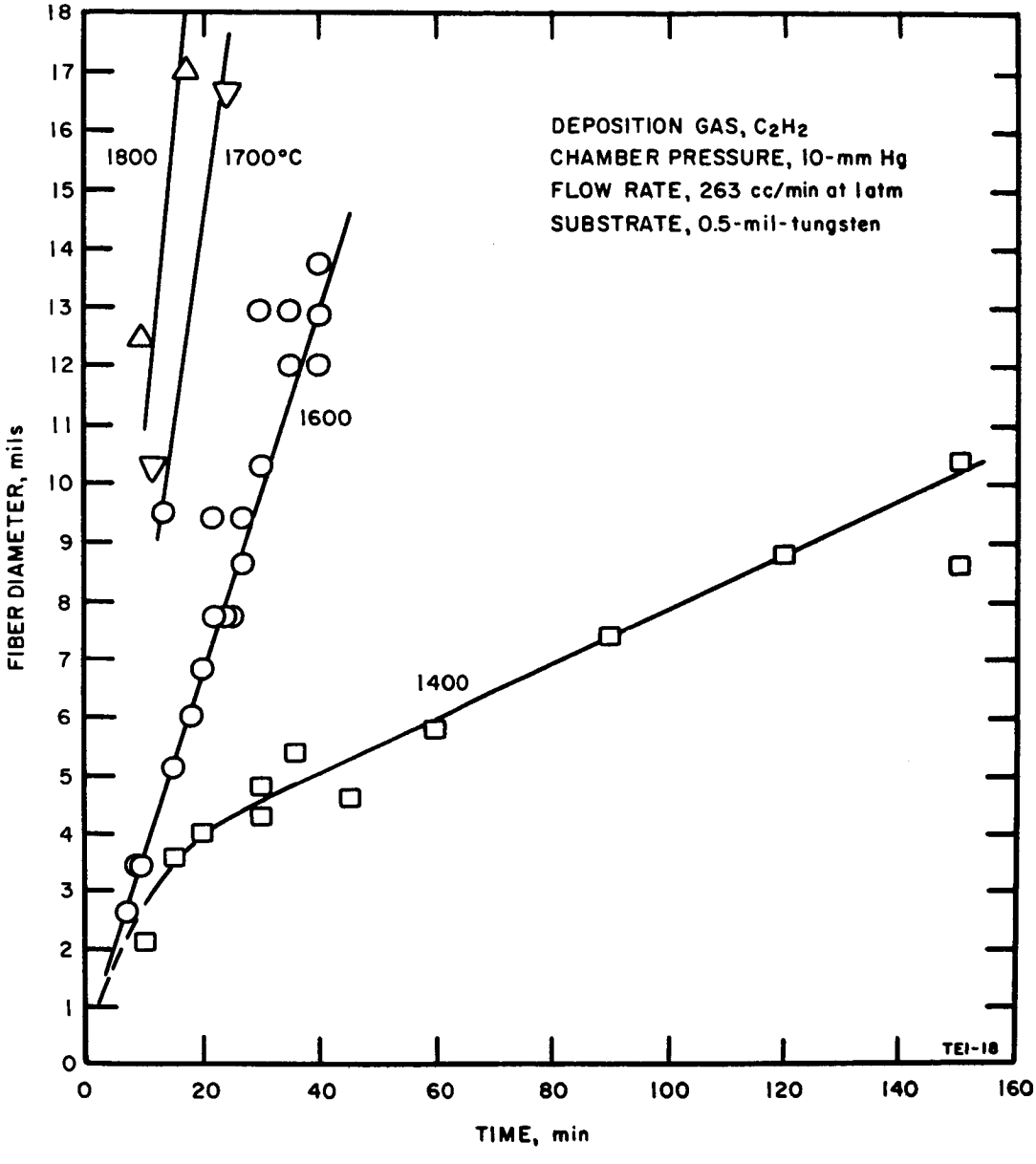

Fig. 29 Growth Curve for Pyrolytic Graphite Fibers

(4) The true surface temperature of the substance does not vary the same as the apparent surface temperature (determined with the pyrometer) since the substrate emissivity varies from 0.45 for tungsten to 0.93 for carbon.

After the initial period, however, the rate of diameter increase is definitely linear and is a strong indication that the deposition is a function of the fiber surface area and that, under the processing conditions used, the deposition rate is not limited by mass transport of reactants or products.

The slopes of the linear portions of the curves of Fig. 29 are shown as an Arrhenius plot in Fig. 30. The rate increases rapidly with temperature and, if it is assumed that the specific rate constant is proportional to the growth rate under these conditions, an activation energy of 25.0 K cal/mole for the deposition of graphite from C_2H_2 is obtained. This value for the activation energy compares with a value of 26K cal/mole (24) and 30 K cal/mole (23) for the first-order homogeneous pyrolysis of C_2H_2 in this temperature range.

The effects of pressure as well as temperature on rate are not clearly shown over the entire range of data of Table XXI. However, in the range between 1400 and 1600°C, the effects can be seen in summary below, where it is apparent that the rates are substantially higher at 34 than at 10-mm Hg.

Flow Rate cc/min at 1 atm	Chamber Pressure mm Hg	Substrate Temp, °C	Time min	Final Diameter mils
263	34	1400	30	7.0
		1600	30	17.3
263	10	1400	30	4.25-5.0
		1600	30	10.25

Results at 1800 and 2000°C are not as well defined because the rates are so high that only short runs are possible, and they cannot be compared directly with those at 1400 to 1600°C.

It is noted in Table XXI that the density of the graphite fiber varies with substrate temperature and with the diameter of the fiber. Under constant plating conditions the density appears to decrease with increased diameter. This is illustrated by the data on fibers 193-72-3 and 193-73-1 through 193-73-9, all of which were prepared at 1400°C. The density data are shown graphically in Fig. 31. Calculations, based on the smooth curve in this figure, show that the decreased density is brought about by the reduced

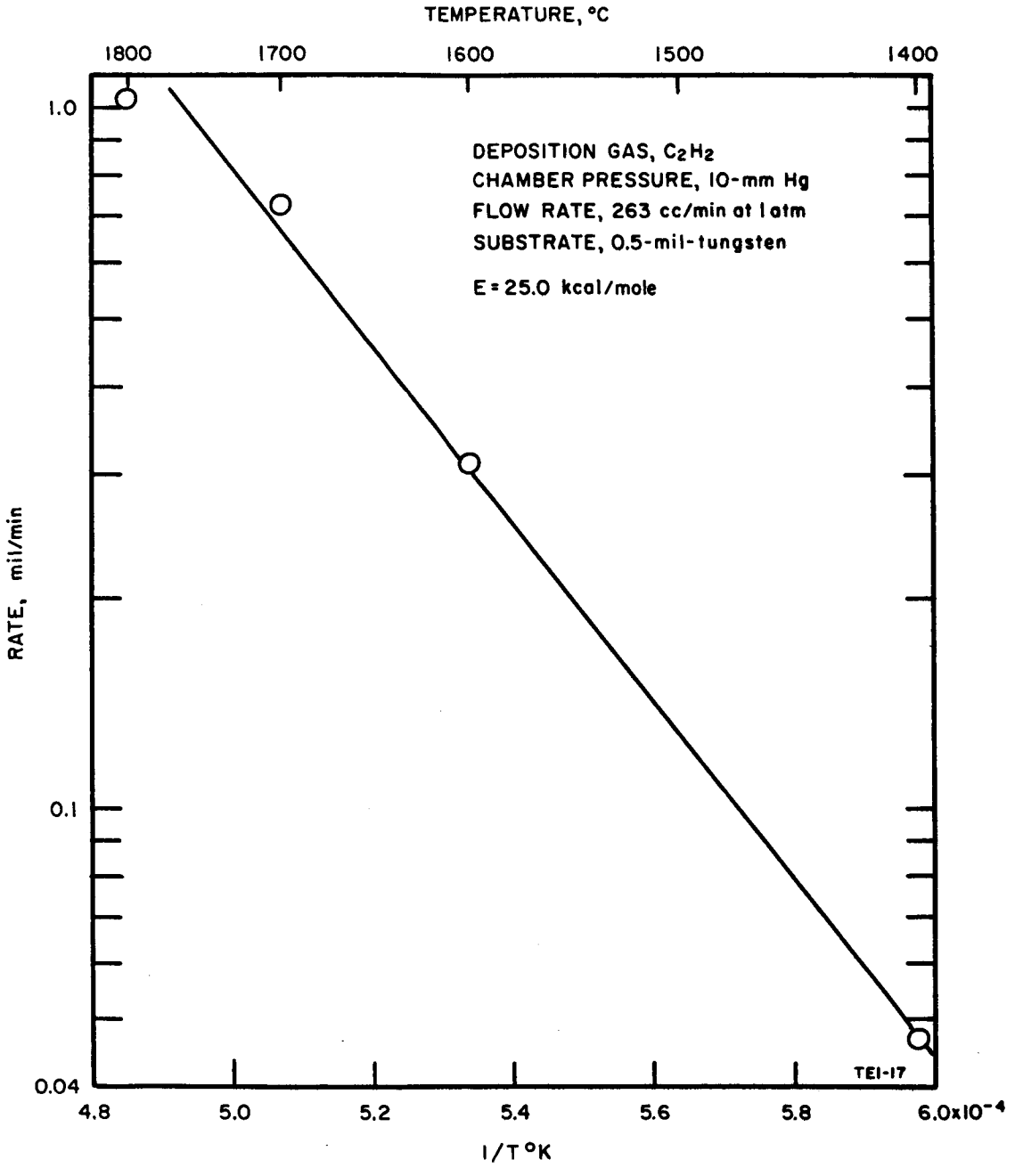

Fig. 30 Growth Rate Vs 1/T for Graphite Fibers

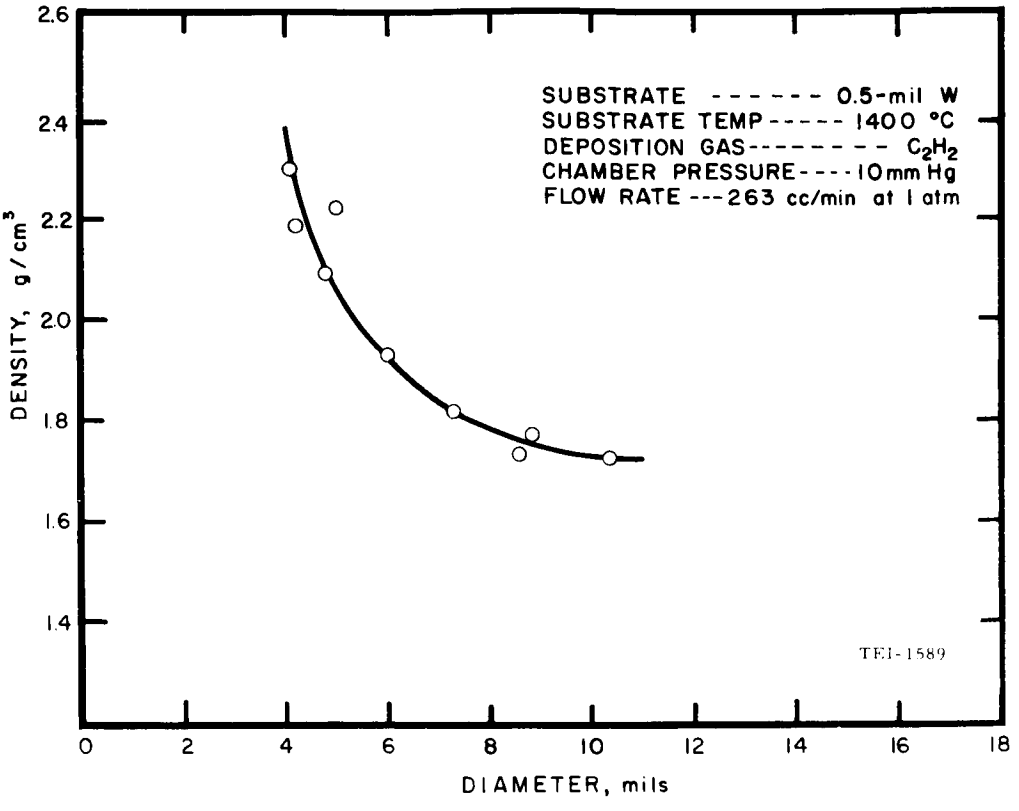

Fig. 31 Density Variation of Pyrolytic Graphite Fibers

effect of core material on the final density as the volume of the graphite increases. It may be seen in the calculations of Table XXII that each mil increment of graphite laid down has about the same density. These average 1.63 g/cc, and this is believed to be representative of graphite made under these conditions. Further calculations (not shown), based on these results, give some indication of the core weight, volume, and diameter. Based on densities of 1.63 for the graphite, and 15.7 for a tungsten carbide (WC by x-ray) core, the values are 59.0×10^{-6} gm/cm, 3.76×10^{-6} cc/cm and 0.86 mils, respectively.

Higher density material (in the range of 2 to 2.05 grams cc after correcting for the cores) can be made by carrying out deposition at 1550-1600°C, but the density remains essentially constant above these temperatures. Higgs, et al (25), depositing from 5 percent methane and 95 percent argon at 1 atmosphere, show a decrease of density from around 1.58 at 1650°C to a minimum of 1.23 at about 1900°, and then a rapid increase to about 2.2 to 2100°C. The reason for the dip in the curve is not given, and such a dip is not found in our work with C_2H_2.

To determine a representative composition of the pyrolytic carbon fibers, an x-ray analysis of fiber No. 193-71-4 was made with a powder camera. The analysis showed only the presence of graphite and tungsten carbide (WC). No free tungsten or other tungsten carbides were observed.

Figure 32 is a photomicrograph of the cross section of fiber No. 193-71-4. The photomicrograph shows clearly the columnar grains (cones) and the delaminations which are typical of pyrolytic graphite. Harvey, et al (26), propose that the cone growth is due to selective nucleation of the deposit at irregularities along the surface of the substrate. As the diameter increases, the cones originating at the larger substrate irregularities overlap those which originate at the smaller irrequlrities, thus causing the wrinkled appearance of the cross section. The area surrounding the core appears to have less cone growth and irregular structure. This may be due to the partial graphitization or annealing of the material around the core which is probably at a higher temperature. Diefendorf, et al (27), suggest that the delaminations are caused by anisotropy in the coefficients of thermal expansion of pyrolytic graphite. The delaminations could have occurred either when the temperature of the fiber was adjusted during the experiment or when the fiber was cooled after the experiment was terminated. The crack which follows one of the delaminations and extends to the outside of the fiber was probably caused by the breaking of the fiber and is not part of its structure.

Table XXII

DETERMINATION OF GRAPHITE DENSITY FROM FIBER DENSITY AND DIAMETER

Assumed Fiber Diameter, mils	Fiber Density g/cc*	Specific Vol (V) cc/cm x 10^{-4}	Specific Mass (ρ V) g/cm x 10^{-4}	Incremental Values for each mil deposited		
				ΔV x 10^{-4}	ΔM x 10^{-4}	$\frac{\Delta M}{\Delta V} = \rho$
10	1.735	5.067	8.791			
				0.963	1.568	1.628
9	1.76	4.104	7.223			
				0.861	1.418	1.647
8	1.79	3.243	5.805			
				0.760	1.236	1.626
7	1.84	2.483	4.569			
				0.659	1.067	1.619
6	1.92	1.824	3.502			
				0.557	0.898	1.612
5	2.055	1.267	2.604			
Average						1.626 ≅ 1.6

* Data are based on smooth curves of Fig. 30.

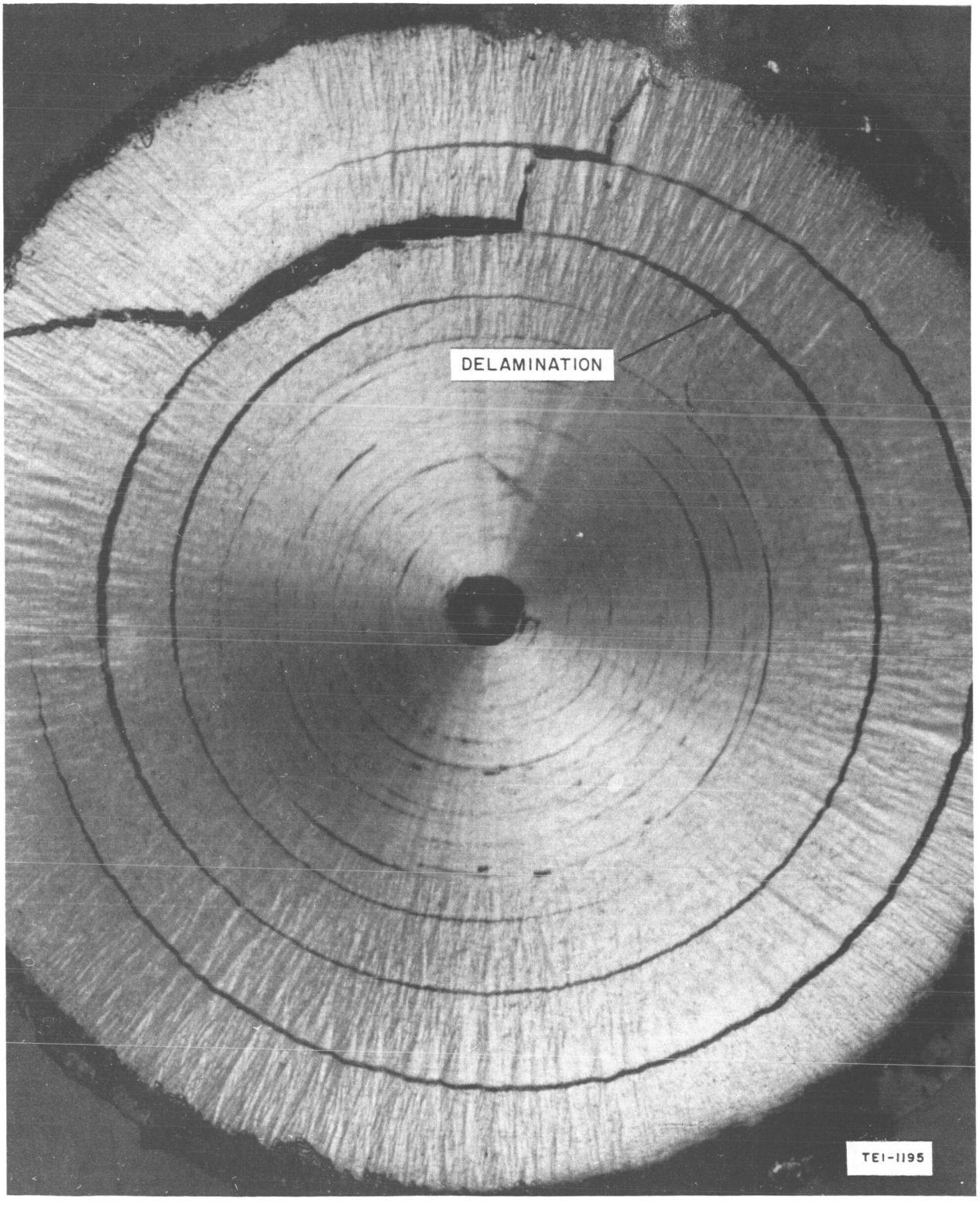

Fig. 32 Pyrolytic Graphite Fiber No. 193-71-4. Polished Cross Section, (Magnified 200 X, enlarged 1.7 X)

Baker (28), has presented evidence that the structure of graphite whiskers consists of cylindrical or prismatic layers of graphite in the form of a scroll. It is interesting to note that the inner delaminations of fiber 193-71-4 shown in Fig. 32 do not meet on themselves, but, instead, tend to wind around as a scroll would do.

It has been reported that the strength of bulk graphite is improved by the inclusion of a small percentage of boron, and, for this reason, codeposition of boron along with pyrolytic graphite was attempted. The conditions of preparation and the properties of the fibers are given in Table XXIII. Although the decomposition of BCl_3 is not favorable thermodynamically at 1400°C, the hydrogen produced by the decomposition of acetylene is available to reduce some of the BCl_3 to boron.

Two striking results of the addition of BCl_3 to the plating atmosphere are: (1) that the deposition rate of graphite is about twice that obtained with pure C_2H_2 under similar conditions, and (2) the fiber density is nearly the theoretical density of graphite. The high fiber density also results in a very smooth fiber surface with only an occasional whisker. Since a similar increase in graphite density and deposition rate was noticed when less than 1 percent Cl_2 was used in the pyrolysis of CH_4 on a hot substrate (29), the effects observed in our experiments may result from the presence of chlorine in BCl_3 and not boron.

The fiber strength remained good with a maximum value of 73 kpsi, but we observed in this series of experiments no increase in the general level of tensile strength of the graphite fibers due to the addition of boron to the plating gas.

Table XXIII

PREPARATION AND PROPERTIES OF BORON DOPED GRAPHITE FIBERS

Fiber	Gas	Flow Rate, cc/min at 1 atm	Chamber Pressure mm/Hg	Tungsten Substrate Dia, mil	Substrate Temp, °C	Time min	Final Dia, mil	Density g/cc	Density Corrected For core	Tensile Strength	X-ray Analysis
193-90-1	C_2H_2 BCl_3	100 25	*	1.5	1400	15	7.8	2.66	2.03	73×10^3 50	WC, graphite
193-90-2	C_2H_2 BCl_3	100 25	*	1.5	1400	30	6.2	> 2.90	> 1.80	30 30	
193-90-3	C_2H_2 BCl_3	100 25	10	0.5	1400	45	10.7	2.19	2.17	51 44	WC, WB graphite Slight B_4C
193-91-1	C_2H_2 BCl_3	100 25	10	0.5	1400	45	10.6	2.18	2.15	52 66	

* Pressure increased from 10 to over 100 mm Hg

E. Zirconium Diboride Fibers

Several possible routes for the preparation of zirconium diboride fibers by chemical vapor plating were screened by computing the free-energy changes for the proposed reactions. The $\Delta F°$ for each reaction was computed at 1227 and 1727°C (1500 and 2000°K), using published values for the free energies of formation for the compounds involved. The methods of preparation, the primary reactions involved, and the free-energy changes are tabulated in Table XXIV. Thermodynamically, reactions 1A and 2A are not favorable.

The primary advantages of reaction 1B and 2B are that a vaporizer is not required, and that only two gas systems are involved; namely, BCl_3 (or BBr_3) and argon (used as a carrier gas and for purging). In addition, the diameter of the substrate is approximately the same size as the fiber so that substrate heating difficulties, such as are experienced with smaller diameter substrates, are minimized. A potential disadvantage with this approach is that $ZrCl_4$, a reaction product, condenses at 330°C so that fogging occurs in the reaction chamber if the temperature of the gases within the chamber is less than 330°C.

Reactions 3A and 3B are quite favorable thermodynamically. Vapor condensation should not be a problem. However, we believe that ZrH_2 will form initially, because the diffusion rate of hydrogen in zirconium should be greater than that of boron. The presence of ZrH_2 was confirmed in a fiber that was produced by this method. However, subsequent reaction between boron and the hydride should occur to produce ZrB_2, but this intermediate reaction may unduly slow the formation of ZrB_2. This approach involves three gas systems.

Reactions 4A and 4B are probably the most difficult from an operational standpoint. Four gas systems are involved, and provisions must be made to sublime the $ZrCl_4$. These two approaches have been used successfully by other experiments to produce ZrB_2 coatings.

(1) Reduction of BCl_3 on Zirconium Substrates

Based on the considerations discussed above, we decided to proceed initially with the reduction of BCl_3 by a zirconium substrate. Experimentally, the approach appeared to be the easiest and most desirable from a future production standpoint. All experiments were conducted in deposition diameter 'A'.

Initially, three plating runs were attempted at substrate temperatures of 1400 and 1500°C. Premature burnout of the substrate occurred and no

Table XXIV

CHEMICAL VAPOR PLATING METHODS FOR ZrB_2

Method and Equations	$\Delta F°$, K cal/mole 1500°K	2000°K
1. Reduction of BCl_3 by Zr Substrate Followed by Diffusion		
A. $Zr + 2BCl_3 \rightarrow ZrB_2 + 3Cl_2$	+ 93.2	+ 84.3
B. $5Zr + 4\ BCl_3 \rightarrow 2ZrB_2 + 3ZrCl_4$	-320.2	-288.3
2. Reduction of BBr_3 by Zr Substrate Followed by Diffusion		
A. $Zr + 2BBr_3 \rightarrow ZrB_2 + 3Br_2$	+ 21.6	+ 3.5
B. $5Zr + 4BBr_3 \rightarrow 2ZrB_2 + 3ZrBr_4$	-339.2	-314.7
3. Reduction of Boron Halides by H_2 on Zr Substrate Followed by Diffusion		
A. $Zr + 2BCl_3 + 3H_2 \rightarrow ZrB_2 + 6HCl$	- 55.6	- 68.7
B. $Zr + 2BBr_3 + 3H_2 \rightarrow ZrB_2 + 6HBr$	- 69.4	- 81.9
4. Co-reduction of Boron Halide and $ZrCl_4$ by H_2 on W Substrate		
A. $ZrCl_4 + 2BCl_3 + 5H_2 \rightarrow ZrB_2 + 10\ HCl$	- 11.3	- 18.3
B. $ZrCl_4 + 2BBr_3 + 5H_2 \rightarrow ZrB_2 + 4HCl + 6HBr$	- 2.4	- 31.6

satisfactory fibers were made. In order to reduce the possibility of burnout, the substrate temperature in subsequent experiments was lowered to below 1200°C.

Table XXV is a tabulation of the fibers made by the reduction of BCl_3 on zirconium substrates. The preparation procedure employed for these fibers is as follows. The zirconium substrate was degreased in acetone, and was lightly etched in a room-temperature bath of nitric-hydrofluoric acid. The substrate was strung-up on the electrodes, and, after the electrode assembly was installed, the system was pumped down to an ultimate vacuum of usually less than 40 microns. The leak rate was determined and the argon flow was adjusted. Flow was maintained a few minutes prior to heating the substrate to temperature. After the substrate temperature was adjusted, BCl_3 was introduced and, after the prescribed plating time, the temperature of the fiber was gradually reduced to room temperature in flowing argon.

Condensation of the $ZrCl_4$ product turned out to be a minor problem. The condensed vapor filled the reaction chamber and plated-out on the reaction chamber tube. After this occurred, the temperature measurements were meaningless. The problem was circumvented by heating the deposition chamber with heater tapes.

Initially, fibers 193-101-1 and 101-2 were prepared. They were brittle and could not be bent, even to the slightest degree. Metallographic examination proved quite interesting in that both fibers had axial central holes of a fairly uniform diameter. Figure 33, a photomicrograph of the cross section of Fiber No. 193-101-2, shows the tube shape. The ZrB_2 appears to have a large amount of porosity. Closer examination of these fibers revealed that the center hole ran through their entire length and that a 4-mil diameter wire could be inserted through it. A black powdery material was found in the hole. The outside of the fiber was covered with a 0.5-mil thick layer of a black granular material which could be scraped off the tube quite easily (Fig. 34). The outside diameter of the fibers was only slightly smaller than the original zirconium substrate.

In an effort to establish how the tubes are formed, fibers 193-102-2 through 193-105-3 were prepared. Preparation conditions were the same as for fibers 193-101-1 and 101-2 except deposition times were varied from 1 to 12 minutes. Photomicrographs of transverse sections of fibers are presented in Figs. 34 and 35. Figure 36 is a photomicrograph of the zirconium substrate which was heated to 1200°C for five minutes in high purity argon.

Table XXV

DEPOSITION CONDITIONS AND PROPERTIES OF ZIRCONIUM DIBORIDE FIBER PREPARED BY THE REDUCTION OF BCl_3 ON ZIRCONIUM SUBSTRATE [1]

Fiber	Zirconium Substrate Temp, °C	Deposition Time min	Substrate Diameter	Fiber mils	Diameter Change mils	X-Ray Diffraction Analysis	Properties of Fiber
193-115-1	600	18	9.4	5.1	-4.3		Brittle
193-111-1	800	15	9.2	9.1	-0.1		Brittle
193-109-1	800	30	8.8	8.5	-0.3		Spalls easily, brittle
193-108-1	1000	15	9.1	15.	+6	ZrB_2[3]	Spalls easily, brittle
193-110-1	1000	15	8.8	9.2	+0.4		Bends, fragile
193-112-1	1000	23	9.3	8.8	-0.5	ZrB_2[9] -Zr[5]	Spalls easily, bends
193-114-1	1100	4[2]	9.5	8.3	-1.2	ZrB_2[4] -Zr[5]	Spalls, fragile
193-113-1	1200	13[2]	9.5	8.7	-0.8		Spalls easily, bends
193-103-2	1200	1	9.1	8.9	-0.2	ZrB_2 + Zr[7]	Bends
193-105-3	1200	2	9.1	9.14	+0.04		Spalls easily, bends
193-102-1	1200	3	9.2	9.1	-0.1	ZrB_2 + Zr[7]	Brittle
193-102-2	1200	12	9.0	9.08	+0.08	ZrB_2 + B Zr[7] ZrB_2[6] ZrB_2[8]	Spalls easily, brittle
193-101-1	1200	15	9.3	8.7	-0.6	ZrB_2[7]	Brittle
193-101-2	1200	30	9.1	8.8	-0.3	ZrB_2[7] ZrB_2 + unidentifiable[4] ZrB_2[6]	Spalls easily, brittle
193-99-2	1400	10	9.3	9.2	-0.1		

Notes:

1. Deposition conditions
   Substrate material - zirconium
   Plating gas, BCl_3; Flow, 100 cc/min
   Carrier gas, argon; Flow, 900 cc/min
   Pressure, 760 mm Hg

2. Interrupted deposition. Series of one minute deposition periods separated by two minute intervals of no deposition. Temperature constant throughout experiment. The deposition times shown are the sums of the one minute deposition periods.

3. Powdered sample of entire fiber

4. Granular deposit on OD

5. Core only

6. Fiber with OD deposit removed

7. As-deposited fiber

8. OD deposits and core residue removed

9. Core removed

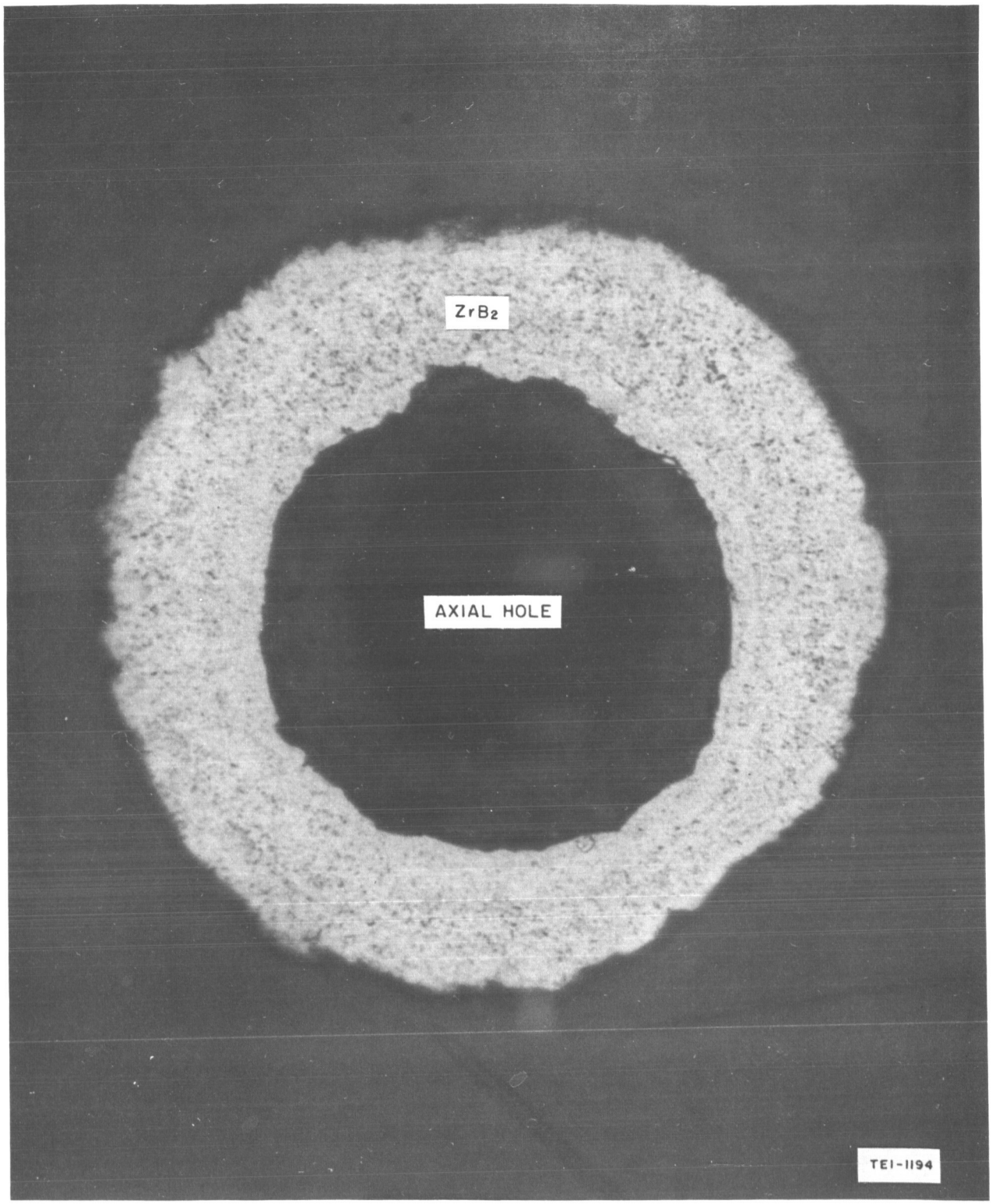

Fig. 33 ZrB_2 Fiber No. 193-101-2. As polished Cross Section, (Magnified 250 X, enlarged 2-1/4 X)

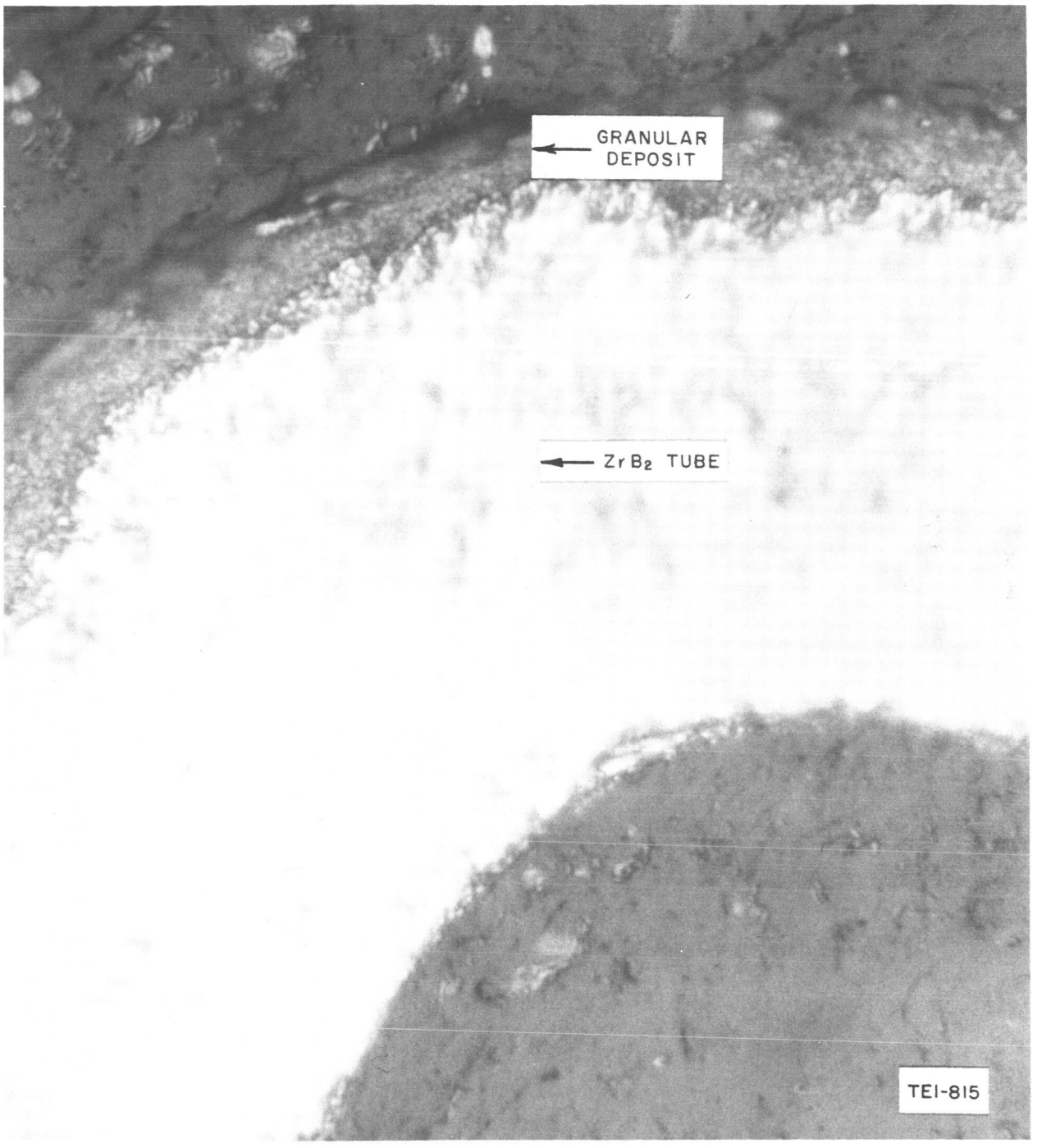

Fig. 34 ZrB_2 Fiber No. 193-102-2. Polished Cross Section, (Magnified 800 X, enlarged 2 X)

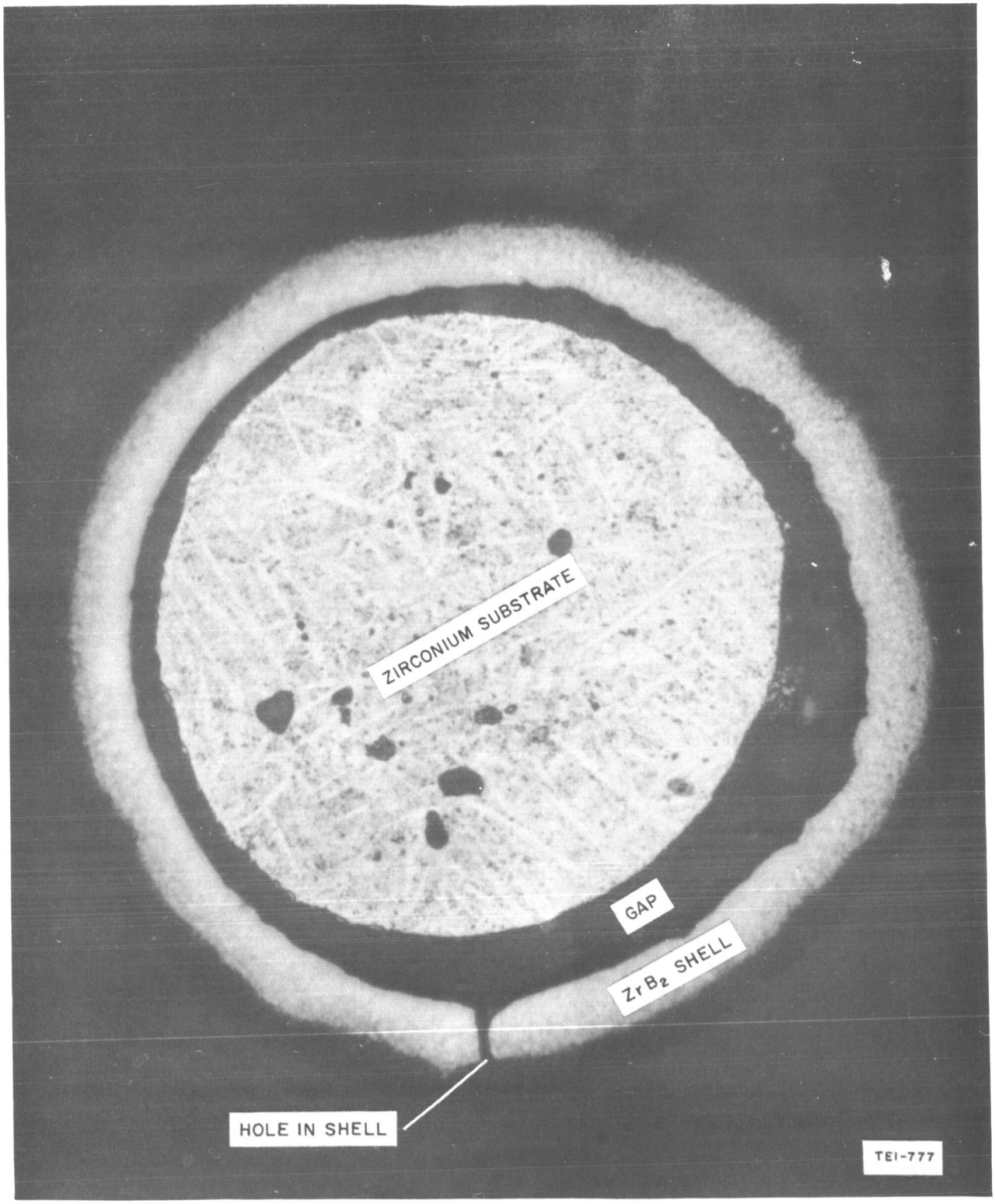

Fig. 35 ZrB_2 Fiber No. 193-105-3. As Polished Cross Section, (Magnified 250 X, enlarged 2-1/4 X)

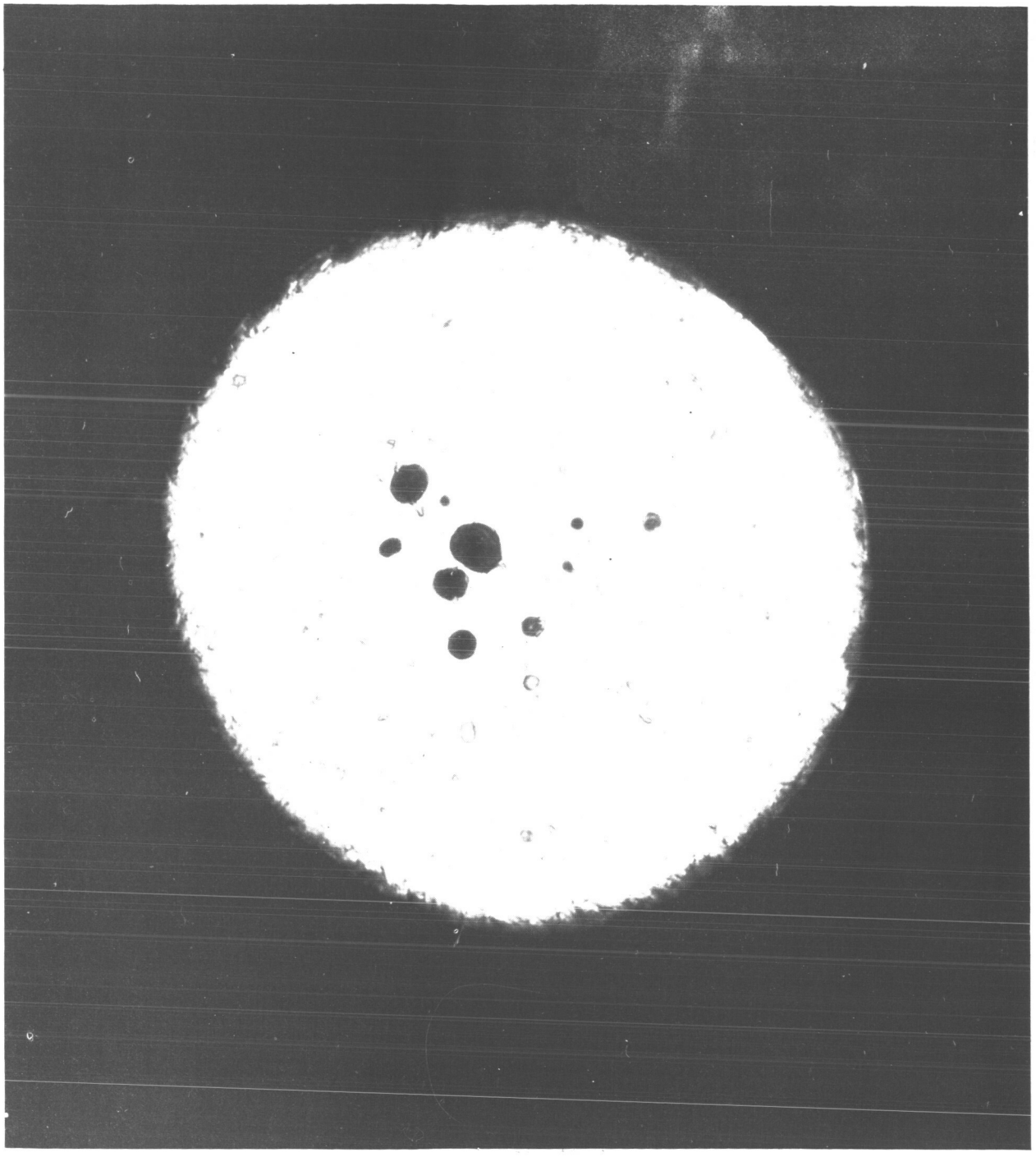

TEI-285

Fig. 36 Zirconium Substrate - Heated 5 minutes at 1200°C in Argon. Polished and etched Cross Section, (Magnified 250 X, enlarged 2.1 X)

All photomicrographs were prepared in the same manner. The diameter of the fibers reported in Table XXV were measured with the filar eye piece after light polishing but before the edges of the speciment became excessively rounded. Considerable difficulty was experienced in polishing the fibers because of the granular outside layer which fragmented very easily. By the time a final polish was accomplished, the layer was wasted away and the unsupported edge of the underlying material was fragmented.

The 1-minute sample has a layer of the black granular material on the surface of the zirconium core. At the interface between the layer and the zirconium core, there appear to be numerous small voids. Comparison with the unreacted zirconium substrate indicates that the microstructure of the core of the 1-minutes sample has not been altered significantly by the reaction with BCl_3.

The 2-minute sample (Fig. 35) consists of a shell of metallic-like material separated from the zirconium core by a finite gap of fairly uniform thickness. The shell has an outside layer of the black granular material and is harder than the zirconium core. The shell material has radial holes which penetrate its entire thickness. The 3-minute sample consists of a shell of hard material separated from the zirconium core by a finite gap. No outside layer of the granular material is evident. Radial holes are present in the shell. X-ray diffraction of the as-produced fiber shows only ZrB_2 and alpha-zirconium.

The 12-minute sample (Fig. 34) is a fully developed tube of hard material surrounded by a layer of the granular material. X-ray diffraction analysis of the as-produced fiber shows ZrB_2 and beta-zirconium to be present. X-ray tests of the tube with the granular deposit removed, and of the tube with both the granular deposit and the residue inside the tube removed, showed only ZrB_2 in both cases.

Based on the metallographic observations and the results of the x-ray diffraction analyses, the following mechanism is proposed for the formation of the ZrB_2 tubes. The BCl_3 reacts with the surface of the zirconium substrate, penetrating to a depth of about 0.5 mil and forming a porous granular layer of ZrB_2. There is a decrease in diameter of about 0.2 mils, average. This reduction can be explained by the fact that 60 percent of the zirconium atoms which react with BCl_3 are vaporized as $ZrCl_4$. During this initial reaction period, there is a gradual filling of the porosity in the reaction layer by zirconium atoms, some of which react with BCl_3 to form more ZrB_2. Transport of the

zirconium atoms is accomplished by disproportionation of $ZrCl_2$ which is suggested as an intermediate in the reaction. Filling of the porosity by transport of zirconium atoms from the zirconium/ZrB_2 interface causes depletion of zirconium atoms, formation of voids and, ultimately, a finite gap between the zirconium core and the ZrB_2 shell (Fig. 35). The shell is sufficiently porous to allow ample penetration of BCl_3 and $ZrCl_4$ reaction product. Evidence of porosity is shown in Fig. 37 which is a view of the inside surface of the shell showing two possible holes with halos (probably condensed $ZrCl_4$). These holes are probably the same as those observed in the shell shown in Fig. 35. When the gap is created, the temperature of the zirconium core is increased because of the lower conductance of the gases in the gap. Thus, over a very short time span, following the initial reaction, the reaction rate is greatly increased. The shell continues to increase in thickness as zirconium atoms are transported across the gap as $ZrCl_2$, which disproportionates in the gap or on the inside surface of the shell. The rapid increase in reaction rate is evidenced by a sudden appearance of copious quantities of condensed $ZrCl_4$ vapor after about one minute of reaction time. While the zirconium core continues to be consumed, free zirconium in the outer portion of the shell reacts with BCl_3 and increases the thickness of the layer of porous granular material on the OD. At some point in time, the power generation in the zirconium core ceases, and consumption of the remainder of the zirconium occurs isothermally. It is suggested that the black powdery residue in the tube ID is the ZrB_2 which formed during the isothermal reaction. The volume of zirconium consumed during this isothermal reaction period is probably equivalent to a volume slightly less than the ID volume of the final tube.

Although the tubular fibers are intriguing and perhaps have some interesting applications, no further work was done on them since our goal was to produce solid fibers. We decided to try to produce solid ZrB_2 fibers by reacting BCl_3 and zirconium at temperatures below 1200°C. We believed that the lower reaction rates and the lower vapor pressure of $ZrCl_2$ (vapor pressure 760 mm at about 1500°C) at the lower temperatures may favor formation of a solid fiber. Three fibers were produced at 1000°C, two at 800°C and one at 600°C. Preparation procedures were the same as those previously used for the 1200°C fibers. In addition, two fibers were produced at 1100 and 1200°C, respectively, by an interrupted deposition scheme. Deposition was carried out in 1-minute intervals, each separated by a 2-minute period of no deposition. Temperature was held constant throughout the experiment. The purpose of the interrupted deposition was to try to eliminate the formation of the gap beneath the reaction products by permitting time for diffusion of boron into the zirconium core. It

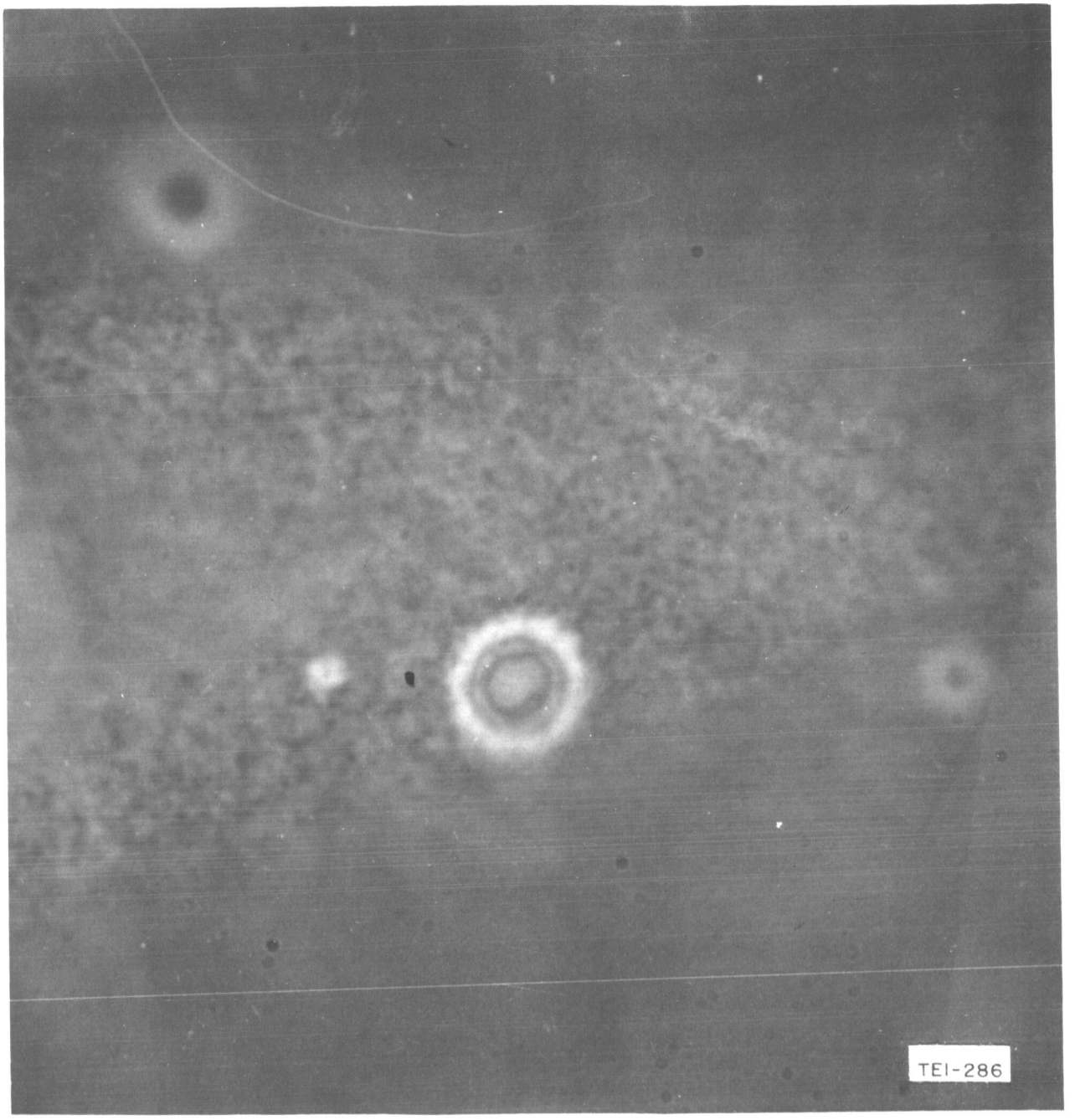

Fig. 37 ZrB_2 Fiber No. 193-114-1. Photograph of Inside Surface of Shell, (Magnified 1600 X, enlarged 2-1/4 X)

was hoped that the diameter of the fiber would gradually decrease as the deposited boron diffused into the core, thereby forming a solid fiber.

The preparation conditions for all of these fibers are tabulated in Table XXV. No satisfactory fibers were produced under any of the conditions employed.

Fiber 193-115-1 (18 min at 600°C) has no trace of a reaction layer on its outside surface. The structure of the zirconium is unchanged. However the diameter of the zirconium was reduced about 5.1 mils. Fiber 193-111-1 (15 minutes at 800°C) was very porous and no evidence of tube formation was apparent. However, fiber 193-109-1 (30 minutes at 800°C), had a shell of material surrounding a very porous core and the shell had an outer layer of porous, granular material. The appearance of the core was very similar to the companion fiber. The two fibers produced by heating 15 min at 1000°C were quite different. A possible explanation for this difference is that local temperatures, where the samples were taken, may have been significantly different. One of these fibers, 195-110-1, was quite interesting in that two concentric tubes were formed. The companion fiber showed no evidence of tube formation and consists of porous, granular material which was identified as ZrB_2 by x-ray diffraction of a powder sample of the entire fiber. Gross porosity near the surface and narrow rings of a metallic-like material were evident. The fiber produced by heating 23 min at 1000°C was too fragile for metallography. The fiber consisted of a tube and a core which could be separated easily. The tube was identified as ZrB_2 and the core alpha-zirconium by x-ray diffraction of samples of each.

The two fibers produced by the interrupted deposition scheme (193-113-1 and 114-1) consisted of a shell surrounding a core. The shell and core could be easily separated. There was no evidence of a layer of black granular material on the OD of the shell. The reduction in diameter was slightly greater than that observed for the fibers produced by uninterrupted deposition. X-ray diffraction analysis of the shell and core separately show only ZrB_2 and alpha-zirconium, respectively. The next attempts to produce zirconium diboride fibers involved the codeposition of zirconium and boron by hydrogen reduction of BCl_3 and $ZrCl_4$ on tungsten and tantalum substrates.

(2) Codeposition of Zirconium and Boron

Zirconium diboride fibers were prepared by the codeposition of zirconium and boron from $ZrCl_4$ and BCl_3 at atmospheric pressure. Because of the chemical similarity of titanium and zirconium, the deposition conditions investigated

for ZrB_2 preparation were made similarto those used for the successful TiB_2 preparation. All experiments were performed in deposition chamber 'D' (Fig. 16). Powdered $ZrCl_4$ was loaded in the sublimer (Fig. 17) which was connected to the mixing chamber of the deposition chamber. The sublimer was maintained at a predetermined temperature while a flow of argon (500 cc/min) was passed through the powdered $ZrCl_4$. The temperature of the deposition chamber and all of the piping carrying $ZrCl_4$ was maintained above 350°C to keep the $ZrCl_4$ vaporized.

Calculations based on saturation of the argon carrier with $ZrCl_4$ vapor predicted a $ZrCl_4$ flow of 200 cc/min when the sublimer was maintained at a temperature of 300°C, but this flow was never achieved in any of the experiments. Samples of the effluent gas were collected in a cold trap to establish the average $ZiCl_4$ flow over a flow period of 3 to 5 minutes. These tests showed that the $ZrCl_4$ flow was only a fraction of the desired flow. No more than about 0.4 grams of $ZrCl_4$ werecollected over a 3-minute period. This corresponds to a $ZrCl_4$ flow rate of about 0.1 cc/min. Even when the sublimer temperature was increased to 450°C, the flow seemed to be unchanged. This strongly suggests that the sublimation rate was limited by the surface area of the $ZrCl_4$ particles and that in future experiments, a sublimer that would expose a much larger surface area of $ZrCl_4$ to the argon carrier gas would be required.

Even though the desired $ZrCl_4$ flow was not attained, fibers containing ZrB_2 were produced. Table XXVI shows the deposition conditions and properties of the fibers prepared. Zirconium diboride was found by x-ray diffraction analysis in all of the deposits tested. In four of the fibers, only ZrB_2 and ZrB were found, but in the remainder of the fibers, boron was present along with the ZrB_2.

The densities of the deposits were well below the density of ZrB_2 but somewhat above the density of boron. This suggests that the deposits were predominantly composed of boron. Assuming that no porosity existed in the deposits and that the deposits consisted of boron and ZrB_2, the volume content of boron was calculated to be 70 to 92 percent.

Off hand, the results of the x-ray and density analysis look inconsistent, but actually they are not. Although there was a large volume fraction of boron present in the deposits for which densities were determined, boron was identified by x-ray analysis in only one fiber (219-79), the one with the highest boron content. No trace of boron was seen in the other deposits. The apparent reason for this is that x-ray exposures of about 4 hours minimum are required

Table XXVI

DEPOSITION CONDITIONS AND PROPERTIES OF ZIRCONIUM DIBORIDE FIBERS PRODUCED BY CODEPOSITION[1]

Fiber No.	Flow - cc/min BCl_3	H_2	Argon Chamber	Argon Sublimer	$ZrCl_4$ Sublimer Temp, °C	Temp °C	Time min	Substrate (7)	Dia, mils	X-ray[4]	Tensile Strength psi	Density of Deposit g/cc	Composition[6] % ZrB_2	B
219-62	185	325	1100	500	300	1000-1150	19	1.5 W	4.7	ZrB_2, W_2B_5	-	3.23	24.5	75.5
219-63	185	325	2200	500	300	950-1050	20	2.0 Ta	4.1-7.1	ZrB_2	-	-		
219-65	185	325	2200	500	295	1010-1065	23	1.5 W	6.0-6.8	ZrB_2, ZrB	-	3.45	30.4	69.6
219-66	185	325	2200	500	300	1000-1200	15	1.5 W[2,3]	6.6	ZrB_2, ZrB[5]	-	-		
219-82-2	200	950	4000	500	385	1010-1090	6	1.5 W[2]	7.0	No Test	-	-		
219-67	415	800	2200	500	300	1040-1170	12	1.5 W	6.6-8.1	ZrB_2, ZrB	-	-		
219-68	415	950	2500	500	300	1070-1115	9	2.0 Ta	4.1-5.4	ZrB_2, ZrB	-	2.89	15.5	84.5
219-69	415	950	2500	500	305	1040-1100	8	1.5 W	6.1	ZrB_2, WB_4, W_2B_5	-	-		
219-70	415	950	2500	500	300	1050-1100	7	1.5 W[2]	3.8-4.7	ZrB_2, WB, W_2B_5[6]	59,600	3.42	29.6	70.4
219-71	415	950	2500	500	300	1050-1160	5	1.5 W	2.4-4.0	ZrB_2[5]	26,600	-		
219-76-1	415	950	2500	500	310	1035-1080	7	1.5 W[2]	9.2	No Test	-	-		
219-76-2	415	950	4000	500	300	1040-1100	7	1.5 W[2]	6.1	ZrB_2, B, WB_4, W_2B_5	10,200		-	
219-77-1	415	950	4000	500	305	1030-1100	7	1.5 W[2]	5.2	ZrB_2, B, WB_4, W_2B_5, W	29,200		-	
219-79	415	950	4000	500	310	1100-1120	7	0.75 W[2]	6.4	B, WB_4, W_2B_5, ZrB_2	166,000	2.62	8.5	91.5
219-81	415	950	4000	500	340	1070-1120	7	1.5 W[2]	2.7	No Test	-			

Notes:
1. Pressure - 760 mm Hg
2. Substrate pretreated by heating 3 to 9 minutes in hydrogen at 1200°C
3. Substrate coated with boron by heating 1.5 min at 1050°C in 390 cc/min BCl_3, 600 cc/min H_2
4. X-Ray performed on powdered sample under noted otherwise
5. X-Ray performed on fiber as produced
6. Computed from density assuming no porosity and only ZrB_2 and B in deposit
7. Numbers refer to the diameter of the substrate in mils. W and Ta are the material symbols

to show up boron on samples of pure boron, whereas the exposures in these instances were less than 2.5 hours on samples containing 70 to 85 volume percent boron.

More puzzling, however, is the identification of ZrB in these deposits. Identification in this instance was made by lattice constant since the x-ray lines for ZrB have apparently not been published. Table XXVII lists the lines produced from a powdered sample of fiber No. 219-68 and the identifications made. The lattice constant calculated from those lines tentatively identified as ZrB_2 was 4.63. This value compares well with the published value of 4.65 (30).

Normally, a deficiency of boron would be required to form ZrB, whereas, in these experiments, an excess of boron was available. In one fiber (219-66), ZrB was found by x-ray of the as-produced fiber, and visual examination of the fiber surface revealed a few large cubic crystals protruding from an otherwise corn-cob type (boron) surface. This suggests that the ZrB phase was highly localized in the predominantly boron deposits. Since the plating gases passed through the lower plenum which was filled with glass beads, it is difficult to see how variation in gas composition could account for the highly heterogeneous deposit. Other possibilities seem rather obscure.

The diameters of the fibers produced were in the range of 4 to 9 mils. Difficulty was experienced with uneven nucleation when 1.5-mil tungsten was used as the substrate. Numerous long thin areas, which were elongated in the axial direction of the substrate, failed to foster nucleation, thereby leaving deep holes of the same shape in the deposit. No such difficulty was encountered with the tantalum or 0.75-mil (electrolytically etched) tungsten substrate.

In future experiments involving $ZrCl_4$, it is apparent that an improved $ZrCl_4$ supply must be developed initially. An improved sublimer would be one approach, but there are two other possibilities that merit close scrutiny. One method involves the preparation of $ZrCl_4$ by the chlorination of zirconium metal in a reactor that would effect complete reaction of the chlorine gas. If such is realized, the $ZrCl_4$ flow would be proportional to the chlorine flow which is easily measurable. Another method would be to react silver or copper chloride with zirconium metal chips in a "bomb". Since the vapor pressure of $ZrCl_4$ is orders of magnitude greater than the vapor pressure of the other possible vapor species in the system at the reaction temperature, a cylinder of high-purity $ZrCl_4$ would be formed. Both of these methods of producing $ZrCl_4$ vapor "in situ" have a decisive advantage over the $ZrCl_4$ sublimation method in that

Table XXVII

X-RAY DIFFRACTION PATTERN OF FIBER 219-68

Intensity (1)	d	Identification
VS	3.28	ZrB
VVS	2.74	ZrB_2
VVS	2.32	ZrB
M	2.17	ZrB_2
VVS	2.08	ZrB
VW	1.90	ZrB
VW	1.75	ZrB_2
M	1.65	ZrB
VVW	1.58	ZrB_2
M	1.54	ZrB
W	1.49	ZrB_2
W	1.44	ZrB_2 + ZrB
VS	1.39	ZrB
S	1.35	ZrB_2 + ZrB
W	1.275	ZrB_2 + ZrB
M	1.17	ZrB_2
M	1.12	ZrB
W	1.08	ZrB_2
M	1.06	ZrB_2
M	1.03	ZrB_2 + ZrB

(1) S = Strong
VS = Very strong
VVS = Very very strong
M = Medium
VW = Very weak
VVW = Very very weak
W = Weak

none of the reactants require the special handling required for $ZrCl_4$. Zirconium tetrachloride, because of its high reactivity with moisture and the atmosphere, must be handled in an inert atmosphere, particularly when it is in powdered form.

(3) Zirconium Diborane Preparation by Diffusion

A series of 10 samples was prepared by plating boron at low temperatures (below 700°C) from diborane onto a 3-mil zirconium substrate. The low temperature process was chosen to minimize diffusion during deposition so that the subsequent effect of time and temperature for diffusion could be studied. The boron was plated to a total diameter of 3.8 mils to give a calculated quantity equal to stoichiometric ZrB_2 if completely diffused into the zirconium substrate. The diffusion, at about 830°C for 10 minutes, produced ZrB_2 but resulted in fluffy growth and a weak fiber. Diffusion at about 750°C for 5, 15, and 30 minutes gave increasing amounts of ZrB_2 with time. Tensile strengths (37.1 - 48.5 kpsi) were approximately those of the substrate (43.2 - 53.6 kpsi) but adherences were not good. At the tensile breaks, the substrate appeared to be stripped out of the diffused zone.

Although the formation of ZrB_2 by boron deposition and diffusion can be readily carried out, it appears that the resulting fiber will not be satisfactory from a strength and adherence standpoint, and no additional work is justified at this time.

(4) Summary

Fibers of zirconium diboride were produced by three approaches: (1) reduction of BCl_3 on zirconium substrate, (2) codeposition from $ZrCl_4$ and BCl_3, and (3) deposition of boron from diborane on the surface of zirconium substrate, followed by diffusion heat treatment. The reduction of BCl_3 on zirconium substrate produced tubular fibers of ZrB_2 that were porous and quite fragile. The codeposition experiments were only partially successful because the $ZrCl_4$ flow possible with the sublimer used in this program was inadequate. Deposits of only 15 to 30 percent ZrB_2 by volume (balance boron) were obtained. Although the formation of ZrB_2 by deposition of boron from diborane and subsequent diffusion heat treatment can be readily carried out, the ZrB_2 deposits so produced have poor adherence and are quite fragile.

F. Evaluation of Fibers with the Plasma Arc

The chemical resistance of fibers produced in this program were evaluated by exposing specimens to high velocity gas streams containing gases of oxygen or fluorine compounds. The gases were heated to temperatures of 1500°C and above by means of a Thermal Dynamics Model F-40 40 KW plasma torch. Argon was employed as the plasma gas and the oxidizing gases were injected in controlled concentrations into the plasma gas stream at the torch nozzle.

A test chamber was built for use in conjunction with the plasma arc testing. The test chamber and the plasma torch are shown in Fig. 38 and illustrated schematically in Fig. 39. The chamber was made from a heavy-wall 304-SS tube 2 in. in diameter. The nozzle of the plasma torch fits inside of an "O" ring seal in the right end of the test chamber. The fiber support mechanism shown on the left side of the Figure contains three stainless steel tubes which house thermocouples, and, with the help of W-3% Re wire,, support the test fibers. Vacuum couplings welded to the endplate of the chamber allow the tubes to be moved to various positions inside the chamber. The endplate is fastened to the chamber by a coupling containing a teflon seal. Large test samples were supported by the W-Re wire only, while small fibers were mounted in a tapered molybdenum holder supported by the W-Re wires. Four samples were mounted in the holder for a single test.

The sample support mechanism held the samples in the left end of the chamber while the power to the torch and the gas flows were adjusted. Then the SS tubes were pushed into the chamber until the samples were in test position.

Sample temperatures were measured with a Pyro Model No. 95 micro-optical pyrometer by observing the sample through a vycor window on the test chamber or by W-5% Re/W-26% Re thermocouples located in close proximity of the samples. Temperatures were recorded on a Varian Model No. 6-11A temperature recorder.

When H_2O was used as an oxidizing gas, its flow was measured as water with an Ace Glass Co. Type 1A-15-1 rotameter. The H_2O was introduced into the torch nozzle as steam produced by passing the water through a heated stainless steel coil. The BF_3 and HF flows were measured as gases with a Schutte and Koerting type 1852 kel-F rotameter. These gases were obtained in pressure cylinders from The Matheson Co. Inc.

Prior to fiber evaluation, the operability of the test apparatus was demonstrated by heating carbon rods 1/16 in. in diameter and 4 in. long in each of the following

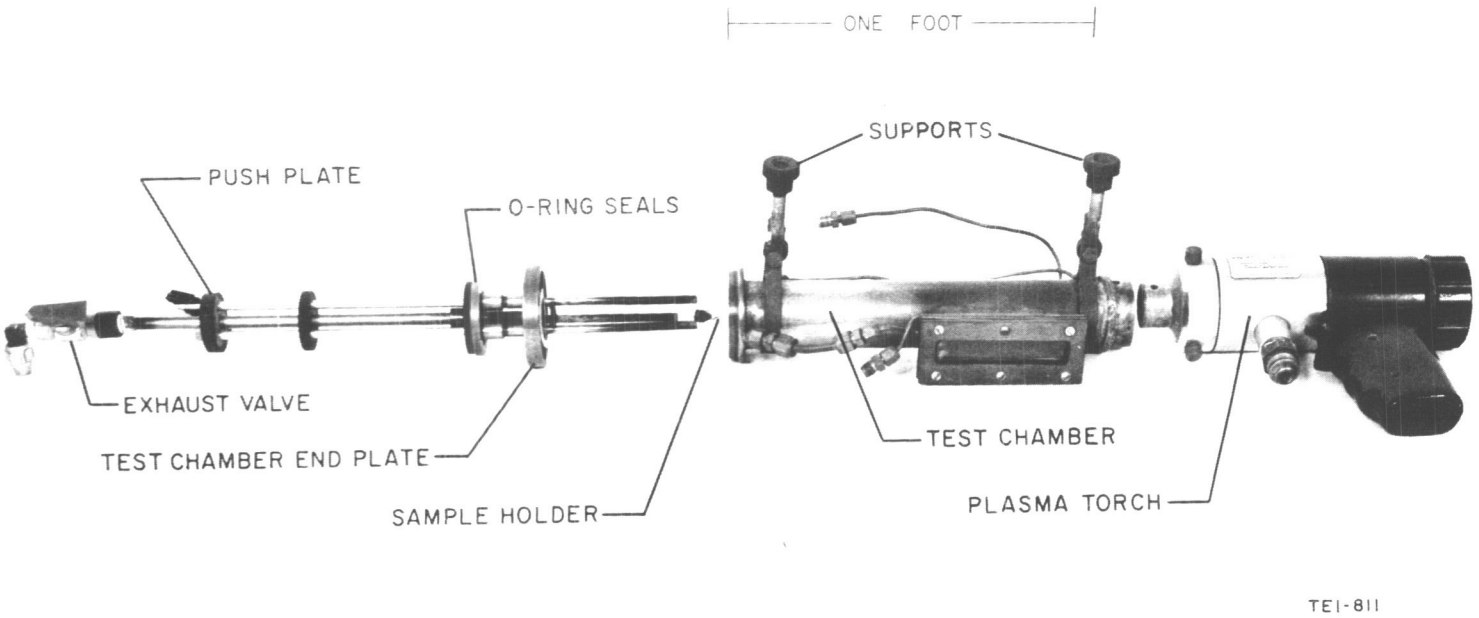

Fig. 38 Photograph of Plasma Arc Test Equipment

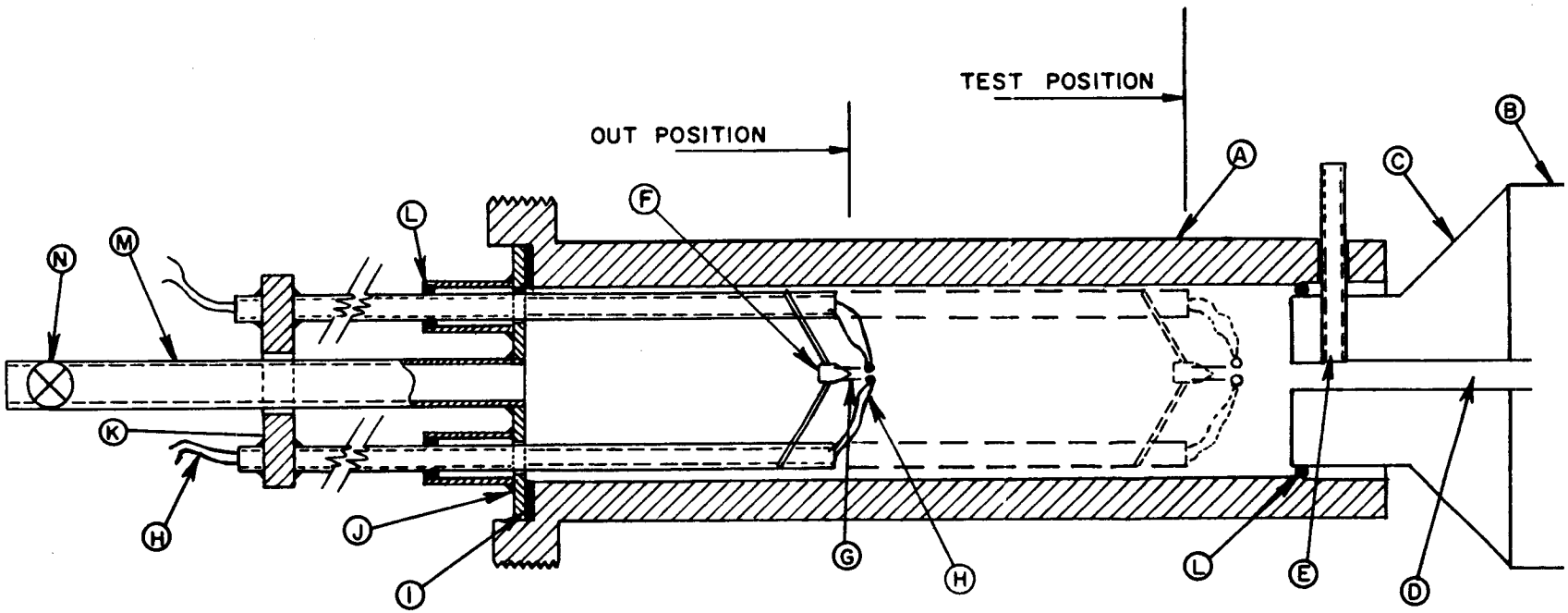

A. TEST CHAMBER
B. PLASMA TORCH
C. PLASMA TORCH NOZZLE
D. ARGON INLET
E. OXIDIZING GAS INLET
F. MOLYBDENUM SAMPLE HOLDER
G. FIBER TEST SAMPLES
H. THERMOCOUPLES
I. TEFLON SEAL
J. TEST CHAMBER ENDPLATE
K. PUSH PLATE
L. "O" RING SEAL
M. EXHAUST LINE
N. EXHAUST VALVE

TEI-760

Fig. 39 Schematic of Plasma Arc Test Equipment

oxidizing media: argon-0.5 vol percent H_2O, argon-5 vol percent BF_3 and argon - 5 vol percent HF. The temperature of the rods in each test varied from 2000°C on the end of the rod nearest the plasma flame to 1500°C on the opposite end. The weight losses of the rods were 27, 23, and 17 percent respectively. No difficulties were experienced in these tests and equipment operability was good.

The fiber samples which were evaluated in the test chamber varied in diameter from 0.006 to 0.020 in. The length of fiber exposed to the oxidizing media was about 1/2 in. W-3% Re wire was evaluated in several tests along with three fibers for comparison purposes. The conditions and results of these tests are summarized in Table XXVIII.

From the tests it can be concluded that H_2O in the oxidizing media is extremely corrosive at the test temperatures employed. In oxidizing media containing BF_3, the carbon fibers showed good resistance in all of the tests. The TiC fibers, although comparatively weak in tensile strength, did show reasonably good resistance to BF_3. The TiB_2, when a sample of high tensile strength was used (219-37), showed good resistance to BF_3, but the sample weakened and failed structurally. A later test in argon alone at 2200°C on a similar TiB_2 fiber also resulted in structural deterioration of the fiber. Both of the TiB_2 fibers were slightly enriched with titanium. It is believed that their structural degradation was probably caused by aglomeration of the excess titanium at the grain boundaries. The test temperature was well above the melting temperature of titanium so that grain boundary weakening probably occurred. No suitable tests were made on tungsten coated boron because the samples failed structurally when the boron melted.

Table XXVIII

PLASMA ARC TEST RESULTS

Fiber No.*	Material	Diameter in.	Duration of test sec	Oxidizing Gas Medium	% Weight Loss of Sample
222-23	W-3% Re	0.020	5	Argon 5% H_2O	12.5
193-72-4	C	0.010	5	Argon 5% H_2O	100
219-36	TiB_2	0.008	5	Argon 5% H_2O	100
219-79-1	ZrB_2	0.007	5	Argon 5% H_2O	100
222-27	W-3% Re	0.020	5	Argon 5% BF_3	2.2
219-5	TiB_2	0.016	5	Argon 5% BF_3	10.3
197-143	TiC	0.020	5	Argon 5% BF_3	2.4
193-25-1	C	0.020	5	Argon 5% BF_3	2.8
222-28	W-3% Re	0.020	2	Argon 5% BF_3	10.2
219-6	TiB_2	0.017	2	Argon 5% BF_3	77.5
197-143	TiC	0.021	2	Argon 5% BF_3	21.0
193-125-1	C	0.017	2	Argon 5% BF_3	16.5
229-33	C	0.008	5	Argon 5% BF_3	14.0
219-37	TiB_2	0.008	5	Argon 5% BF_3	23.5**
197-132	TiC	0.009	5	Argon 5% BF_3	46.5
193-140-1	W coated B	0.009	5	Argon 5% BF_3	100 ***

* Temperature of Fibers = 2150 ± 100°C

** % Volume loss. Sample broke during cooling and an accurate weight loss was not obtained

*** Sample melted during test.

IV. RECOMMENDATION OF FIBERS FOR FURTHER DEVELOPMENT

It is the object of this task to select for further development the most promising fibers investigated in this program. Selection for further work depends on many factors including fiber physical properties and the ability to resist chemical attack during ablative use. Also of importance are the adaptability to scale up from batch to continuous preparation and the problems involved in future production. Before discussing the merits of the individual fibers, it is well to indicate the problems of conversion to continuous processing and and to illustrate certain problem areas in preparation and in use.

1. Problems Involved in Continuous Fiber Preparation

The problems of continuous preparation will differ for each fiber, but, in general, they concern six major points: (1) the deposition rate; (2) the temperature gradient along the filament during plating; (3) the control of multiple components to obtain stoichiometric deposit in co-plating operations; (4) the addition and control of feed components which are liquids or solids rather than gases; (5) the handling of low volatility reaction products; and (6) the use of controlled low pressure where required.

a. Deposition Rates

Deposition rates affect the number and length of deposition chambers required for a given filament production rate. As a first approximation, the required length of chamber is inversely proportional to the deposition rate. However, in the case of a parallel-flow apparatus (i.e., gas flow parallel to the filament), limitations on maximum chamber length may be imposed by the buildup of reaction products in the stream of plating gases or the length of filament which can be heated to a uniform reaction temperature. Moreover, previous studies at TEI on another filament system suggest that the initial few inches in a parallel-flow plating chamber account for most of the deposition. They also indicate that in successive chambers, the deposition rates are considerably higher near the entrance of each chamber compared to the rate at the tail end of the preceding chamber. This suggests that a series of short chambers is much more favorable, from a deposition rate standpoint, than a single, long chamber. However, it is not certain that this information is applicable to the systems of interest in this program and for this reason it will be assumed that chamber length is inversely proportional to the deposition rate in the ensuing discussions.

In the case of a cross-flow apparatus (i.e., gas flow being perpendicular to the filament), the chamber length may be limited by the temperature uniformity considerations, and also by the practical considerations of designing a system which would provide a uniform distribution of the reaction gases along the length of the filament.

Recent studies at TEI on another program have demonstrated an important consideration in chamber design. These studies have shown that the heated substrate causes eddy currents to develop on opposite sides of the filament in an otherwise laminar gas flow. The nature of the eddies is such that reaction products would tend to circulate over the filament and possibly affect the plating rate adversely. In a cross-flow apparatus, the location of the eddies relative to the filament can be changed by regulating the gas flow. At a certain flow, the eddies would be on each side of the filament and the adverse affects of back flow of the reaction products would be maximized. However, at higher flows the eddies are minimized. Thus, in order to keep the eddies away from the heated filament, cross-flow chambers must have a sufficiently large cross section so that the boundary of the chamber does not interfere with the eddies and, in addition, gas flows must be high enough to keep the eddies well above the filament.

A new concept in chamber design is currently being studied on another program at TEI which, in early testing, has shown considerable promise with regard to high deposition rates. The concept is based on a parallel-flow apparatus of circular cross section, in which the substrate is located laterally, off-center near the inside surface of the chamber. Convection currents off the heated substrate cause a circular flow of gas. In essence, this concept combines the desirable features of the parallel- and cross-flow deposition chambers.

The deposition rates for the several fibers investigated here will be low, at least initially, in any scale up to continuous operation. This is due partially to the fact that the best quality and strength has been obtained at lower temperatures where lower reaction rates are also experienced. After continuous processing has been worked out it may be possible to secure a better rate by close control of all conditions and by raising the temperatures until an optimum balance between quality and rate is obtained.

Rates may also be inherently low as in the case of graphite. However, as previously pointed out, additives such as BCl_3 in graphite plating may significantly improve the rates. Some work should be done to determine the continuous

deposition rate for each fiber system, before it is accepted or rejected, to determine its promise for future production and to serve as a guide for design of a processing unit.

b. Temperature Gradient

Another scale-up factor which must be considered is the electrical characteristics of the deposits. The fiber is a variable resistor in an electrical circuit because conduction is by the substrate initially; then by the altered substrate as the deposit reacts with the substrate; and finally, by the altered substrate and the deposit. The amount of change depends on the relative resistivities of the various components of the fiber and the heat losses from the filament. The net result of this is that in any chamber the incoming fiber, as it passes between the electrodes, may assume a temperature gradient. Thus, in order to maintain a relatively constant temperature in the fiber, the power may have to be varied to compensate for the changes in resistance and heat losses of the fiber. By using multiple short chambers with mercury contacts at each end, the power to each chamber could be regulated as required. Another method, adaptable to longer chambers, is the use of metallic sliding contacts spaced at predetermined intervals along the length of the chamber. This type of development has been underway at TEI for several months on another program, and results look encouraging for currents on the order of milliamperes. Most of the fibers made on this program, however, have required currents in the range from 0.5 to 1.3 amps so that additional testing and possible modification of the sliding contacts may be required. No ultimate difficulties are anticipated however.

The extent of the temperature gradient problem for each fiber should be surveyed experimentally so that proper arrangement of equipment and power sources can be made for a suitable production unit.

c. Control of Multicomponent Plating Gases

The complexity of scale up increases with the number of plating gases. For example, the production of both pyrolytic graphite and tungsten on boron utilizes gaseous plating chemicals and only a single element is deposited. By contrast, TiB_2, TiC, and ZrB_2 are much more complex because two components must be laid down in each, and the Ti or the Zr plating compounds are $TiCl_4$ (a liquid) and $ZrCl_4$ (a solid). Furthermore, in the case of titanium deposition, the plating chambers must be kept hot to prevent condensation of reduction product, $TiCl_3$, which has a very low volatility (discussed below).

The preparation of stabilized ZrO_2, which has not been attempted under this contract, is expected to be still more complicated. It will require co-plating of zirconium, oxygen, and another metal oxide (such as aluminum or magnesium) to serve as a stabilizer. Control of the plating gases is important but it can be accomplished by good engineering design of the plating equipment.

d. Addition and Control of Low Volatility Plating Materials

The volatility of the reactants affects, among other things, (1) the method of introducing the reactants to the deposition chamber, (2) measurement and control of the vapor flow, and (3) the temperature at which the equipment handling the vapor must be operated in order to keep the reactants volatile. The volatility of the reaction products may also affect the temperature at which the equipment must be operated. The use of materials such as BCl_3, C_2H_2, C_4H_{10}, WF_6, which are all gases at room temperature, permits easy control. Titanium tetrachloride, which boils at 136.4°C, and zirconium tetrachloride, which sublimes at 335°C, require special handling and control as previously indicated. The $TiCl_4$ can be effectively metered into the system and flash vaporized but the control of $ZrCl_4$ offers additional problems. A sublimer, maintained at a constant temperature and arranged for a carrier gas of known flow, can be used if precautions are taken to saturate the gas with $ZrCl_4$. However, control is difficult and two improved approaches have been conceived and should be considered in zirconium work. Both concepts are based on in-situ preparation of $ZrCl_4$.

(1) One approach would produce $ZrCl_4$ by passing chlorine gas over heated zirconium chips. Assuming that a suitable reaction column can be designed to react all of the chlorine, the $ZrCl_4$ flow would be proportional to the chlorine flow which could be determined by conventional metering devices. Argon could be used as a carrier gas for the $ZrCl_4$ vapor.

(2) Another approach would be to react silver chloride and zirconium metal chips in a pressure container at about 550°C. At this temperature, silver chloride is a liquid which should enhance the reaction. Since the vapor pressures of silver chloride, silver and zirconium and the dissociation vapor pressure of silver chloride are negligible compared to the vapor pressure of $ZrCl_4$, a cylinder of high-purity $ZrCl_4$ would be produced. Using a heated transfer line, the $ZrCl_4$ vapor would be bled into the deposition chamber through a calibrated orifice using a differential pressure indicator. Copper chloride, which is cheaper than silver chloride, could possibly be used.

e. Low Volatility Reaction Products

The problems resulting from the reduction of $TiCl_4$ to $TiCl_3$ have been made clear in earlier portions of the report. The $TiCl_3$ must be prevented from obscuring the chamber windows and, preferably, should be prevented from accumulating anywhere in the plating chamber. Failing this, it must be periodically removed by some method. Since $TiCl_3$ sublimes between 425 and 450°C depending on pressure, the maintenance of the plating chamber walls at or above 450°C should prevent condensation. Once outside the chamber, the $TiCl_3$ may be preferentially condensed out and separated from the other effluent gases. The $TiCl_3$ so separated may be kept in the anhydrous state or may be dissolved and subsequently recrystallized as the hydrate from water. A market exists for $TiCl_3$ as a catalyst for polymerization of olefins. Another possibility may be the chlorination back to $TiCl_4$ but no work has been done on this.

f. Low Pressure Operation

Low pressure operation has worked effectively for preparation of pyrolytic graphite and for plating tungsten on boron. The use of large quantities of argon (or other inert gas) as a diluent to permit operation at atmospheric pressure has shown much promise and should be further studied. In the event that reduced pressure remains a preferred route, it presents a minor problem regarding atmospheric seals on the substrate and fiber passing into and out of the chamber. Suitable methods, however, have been devised. Essentially, a seal is made by means of a long capillary through which the fiber is drawn. This creates a required pressure drop by controlled in-leakage of argon or helium, and with a suitable vacuum pump, excellent control of chamber pressures at any desired value down to tenths of a millimeter can be maintained.

2. Continuous-Plating Equipment

A continuous-plating chamber which would embody many of the features discussed in the previous section is shown schematically in Fig. 40. The design is based on a simple modification of Batch Unit 'D' (Fig. 16). This employs cross flow and is expected to give higher plating rates than a parallel-flow unit. The major change is the provision for handling the fiber on a continuous basis using a substrate let-off reel (not shown) and a take-up reel. The latter would also be equipped with a traverse (not shown) to wind the filament in layers across the width of the take-up reel without entanglement so that in subsequent use of the fibers for testing or composite preparation, the fiber

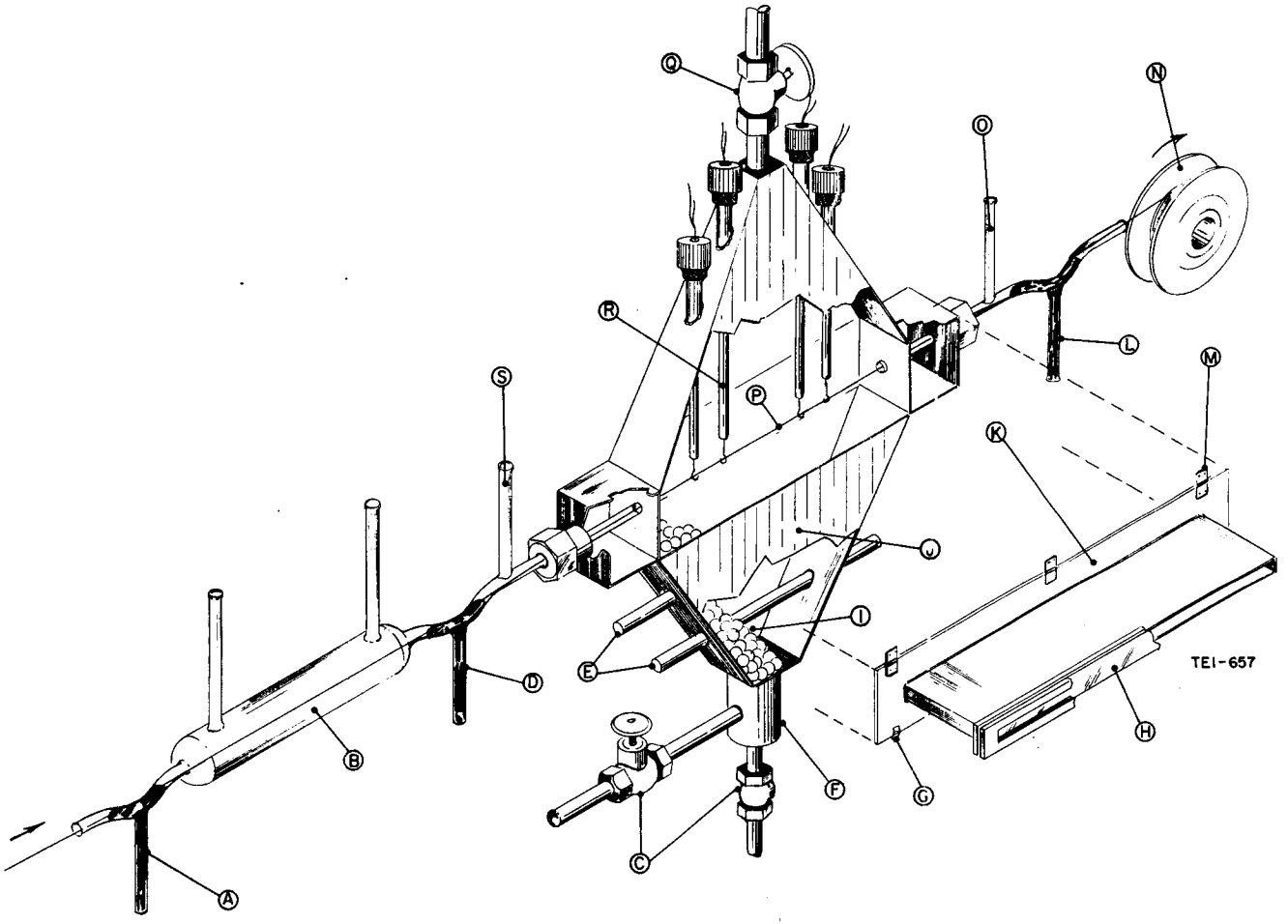

A - Hg Electrode
B - Hydrogen Pretreat Chamber
C - Gas Inlet Lines
D - Hg Electrode
E - Calrod Heater
F - Gas Mixing Chamber
G - Door Fastener
H - Pyrex Window
I - Metal Beads
J - Gas Dispersion Chamber
K - Door to Reaction Chamber
L - Hg Electrode
M - Door Hinge
N - Take-Up Reel
O - Argon
P - Filament
Q - Gas Exit
R - Sliding Electrical Contact (If Needed)
S - Argon

Fig. 40 Modifications of Batch to Continuous Unit

can be easily unwound. Fiber handling devices providing excellent control of linear velocity through the chamber and of maintaining constant tension are well established equipment. A hydrogen pretreat chamber is advisable for cleaning the tungsten substrate by removing any residual lubricant from the wire-drawing operation or any oxide that forms on the surface. The use of gas-cooled mercury electrodes at inlet and outlet permits resistance heating of the substrate. Provision is made to heat the chamber walls to 450°C where necessary to prevent condensation of the plating gases and reaction products. Argon flushed windows permit temperature measurement or automatic temperature control devices to function. Sliding electrical contacts are shown schematically: they can be used, if needed, to adjust the electric current over shorter sections of the fiber if the temperature gradient in the chamber is steep. Multiple chambers can also be added in tandem if the fiber plating rate is too low to attain the desired fiber diameter in a single chamber.

A conceptual design of an inexpensive, quartz plating chamber, capable of operation at 450°C wall temperature, is shown in Fig. 41. This design embodies the off-center location of the substrate to take advantage of increased plating rates permitted by the convection currents which cause a circular flow of plating gas through the chamber. Gas-cooled mercury electrodes provide the current for the substrate. The equipment walls are, by means of an oven, kept at desired temperatures up to 450°C to prevent condensation. There are no joints or seals in the high temperature zone, thus minimizing leakage of plating gases or influx of air which could cause trace oxide or nitride contamination. If used with $TiCl_4$ (for TiB_2 or TiC preparation) the exit for the gases is heated until they pass outside to a condenser arranged to collect the $TiCl_3$. Other effluent gases then pass to suitable traps for removal and recovery of $TiCl_4$ and BCl_3. This equipment could also be used for $ZrCl_4$ handling. Once again, multiple chambers could be arranged in tandem as required. A single-fiber handling system, of course, suffices for the tandem chambers.

3. Substrate For Fiber Preparation

It is recommended that all fibers be prepared on tungsten wire substrates since this is known to work exceptionally well. This will permit scale-up to continuous operation in the shortest time. However, in a long range picture, tungsten is a high-cost item and less expensive substrates would be desirable. Stainless steel, for example, offers some promise, but experience to date with other fiber deposit programs has not shown good adherence with this core

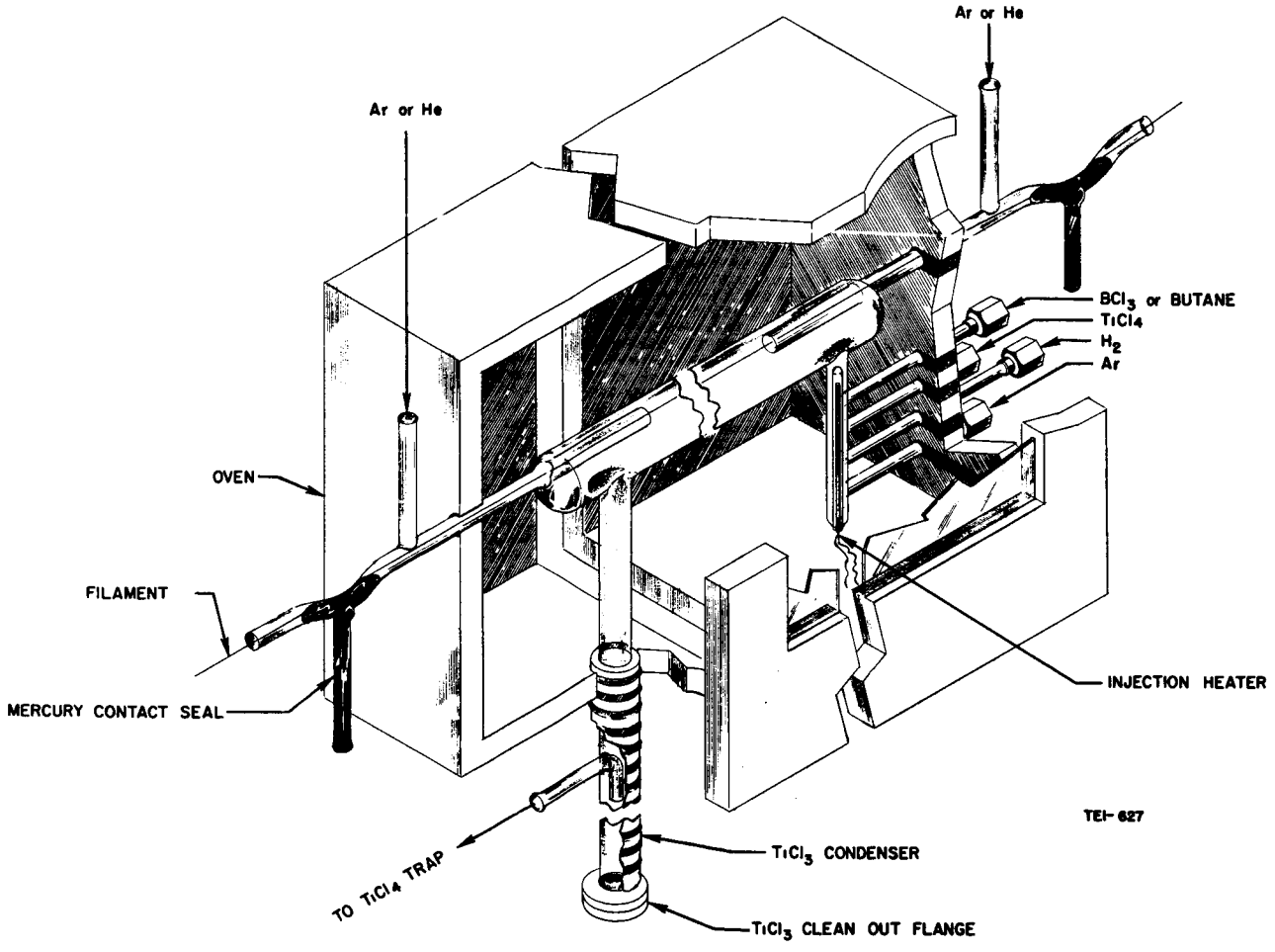

Fig. 41 Conceptual Design of Glass Continuous Unit for High Temperature Chemical Vapor Plating

and the low melting point of 1450 to 1500°C is a disadvantage.

A substrate made of carbon-coated silica has considerable price potential, but is limited in the maximum plating temperature (about 925°C) at which it can be used. Of the candidate materials studied, only the tungsten coated boron fiber could be made with this substrate where the boron is initially laid down on it. However, stabilized ZrO_2, if prepared from volatile zirconium - organic compounds such as the zirconium alkoxides or dicyclopentadienyl halides, may possibly be made at a low enough temperature for such a substrate to be employed. Other substrates, such as zirconium and tantalum, have been successfully used in batch fiber preparation and should be further considered in continuous preparation if thermal expansion matches with deposits are apparent; but no price advantage is expected.

An alternate to a wire substrate which merits consideration is a ribbon. Because of the large surface area compared to a wire of diameter equivalent to the ribbon thickness, a larger mass of deposit can be formed per unit time. The relative quantities are not simple relationships between surface areas. They differ from system to system depending on whether surface reactions, gas phase reactions or diffusion rates from gas to surface or other variables control the plating rate. Because of the greater quantity deposition on the ribbon, the cost per unit weight of deposit can be reduced. However, several disadvantages may result. Stresses at the edges of the ribbon tend to give poor adherence and reduced strength. It is possible that rounded edges may aleviate this in some degree and this would have to be experimentally verified. The ribbon would be quite stiff and would introduce problems in handling. Furthermore, it would contain a higher proportion of substrate material than a wire. However, ribbon plating is worthy of consideration for reducing the production cost.

4. Fiber Handling and Fabrication of Ablative Composites

Continuous fibers can be used to prepare ablative composites by a number of techniques which will be described in subsequent paragraphs. Of importance to the feasibility and ease of handling are the tensile strength and modulus of the fiber. These properties determine, to a large extent, the degree to which fibers can be bent and/or the axial load that can be exerted on the fiber during coiling, uncoiling, or winding. Using values for these properties obtained in the program, we computed the breaking load of 4-mil diameter fibers and the minimum winding diameter for the same size fiber. In these computations, the average tensile strength of the unetched fibers produced in the TiB_2 pilot run and the tensile strengths of the strongest TiC, tungsten-coated boron and pyrolytic graphite fibers were used. In the case of elastic moduli, the average modulus of the TiB_2 pilot run fibers and the highest modulus values of the other fibers were used with the exception of tungsten-coated boron which was assumed to have a modulus equal to that of boron.

The results of these calculations are given in Table XXIX. The fracture loading for all of the fibers is less than that of boron. Pyrolytic graphite, the weakest, has a fracture load only one-fifth (1/5) that of boron filament, while TiB_2, the strongest, has a fracture load one-half (1/2) that of boron. At TEI, 4-mil diameter boron filament is successfully wound, using tensile loads of only 30 grams (dry filament) to 100 grams (pre-preg filament). If the same winding loads were applied to the fibers produced in this program, the loadings would only be 10 to 30 percent of the fiber fracture loads. This margin of 70 to 90 percent would seem to be of an acceptable order of magnitude. Furthermore, it is quite possible that the tensile applied during winding can be reduced, thereby increasing the margin even further.

For a given diameter fiber, the minimum bend diameter is determined by the tensile strength and elastic modulus of the fiber. The low bend diameter for TiC is probably not correct because the measured modulus is far below that of bulk TiC. Using the modulus for bulk TiC (65×10^6 psi) given in Ref. 4, the minimum bend diameter for a stress of 10 percent of the tensile strength would be 41 in. Thus it would appear that the minimum bend diameters for the fibers produced in this program are 2 to 5 times larger than that of boron filament. However, the bend diameters do indicate that it is entirely feasible to coil the fibers on properly sized take-up reels during preparation and to unwind, rewind and otherwise handle the fibers. Increased tensile strength as the continuous fiber-preparation technique is developed for any fiber will, of course, permit smaller bend diameters and give more latitude in subsequent handling.

Table XXIX

TABULATION OF TENSILE PROPERTIES PERTINENT TO FIBER HANDLING

Fiber Material	Tensile Strength kpsi	Elastic Modulus psi	Minimum Bend Diameter, Inches (1) For σ (Fracture)	For 0.1σ (Fracture)	Tensile Fracture Load Grams
TiB_2	151	65×10^6	1.7	17.0	870
W on B	88.7	55×10^6 (2)	2.5	25.0	510
Graphite	58.4	19×10^6	1.3	13.0	340
TiC	63	6.6×10^6 65×10^6 (4)	0.4 4.1	4.0 41.0	360
B	300	55×10^6 (3)	0.75	7.5	1720

Notes:

(1) For 0.004 inch dia fiber

(2) Assumed to be same as boron

(3) Reference 35

(4) Reference 4

Each of the fibers under consideration is relatively stiff and, in the 3 to 5 mils diameter proposed, cannot be crimped. Therefore, they cannot be woven in the conventional sense where they would serve as both warp and woof. However, tapes or fabrics would be prepared if the fibers are laid unidirectional as either warp or woof, as desired, with a more flexible (although weaker) material running at right angles. These second materials, for example, may be glass, quartz, or pyrolyzed yarns whose principal function is to hold the stiff fibers in a weave for easier fabrication of a complex composite. After implacement, the mechanical reinforcement depends primarily on the strong, stiff fibers, but the glass, silica, or pyrolyzed yarn can take part in the heat-absorbing function during ablation.

The optimum use of filament reinforcement in rocket exhaust nozzles is a debatable question at this time. Continuous versus chopped fibers and the orientation of the fibers with respect to the ablating surface and direction of gas flow are important parameters to consider. In order to maximize the ability of the fibers to hold char in place, it is probably desirable to orient the fibers with their axis perpendicular to the motor axis or with the fiber axis sloped at an angle with the motor axis. One method of doing this is to make simple large-diameter hoop windings which may be cut into segments to make relatively straight-grained, end-on fiber blocks. These blocks may be arranged with their fibers oriented as desired and joined together by suitable resins. Two other possible methods of accomplishing this are shown in Figs. 42A and 42B. Figure 42A shows blocks built up to alternate layers at 90° to each other, with the nozzle hole of desired diameter and configuration drilled through. This would be satisfactory for smaller nozzles but would become more difficult and entail some waste with large nozzles. The Fig. 42B arrangement could be used for large or medium nozzles and consists of alternate layers of thin-hoop winding overlaid by a thin layer of end-on oriented fibers. The object of this configuration is to provide strength at the fiber roots by the hoop and to help dissipate heat conducted along the radial fibers. The diameter of the nozzle would be dictated by the allowable diameter of the hoop winding based on minimum bend diameter as discussed earlier.

Another important property to consider is the ability of the surface of the fibers to be "wet" by the matrix material. In general, high translation of fiber strength in a composite is accomplished when the matrix "wets" the fibers. This property can be determined only by experiment and, since we have had no compositing experience with the fibers produced in this program, we cannot assess the particular "wetting" behavior of these fibers. However, in further development this factor should be determined, both with phenolic resins and with any other new resin proposed for use with these fibers.

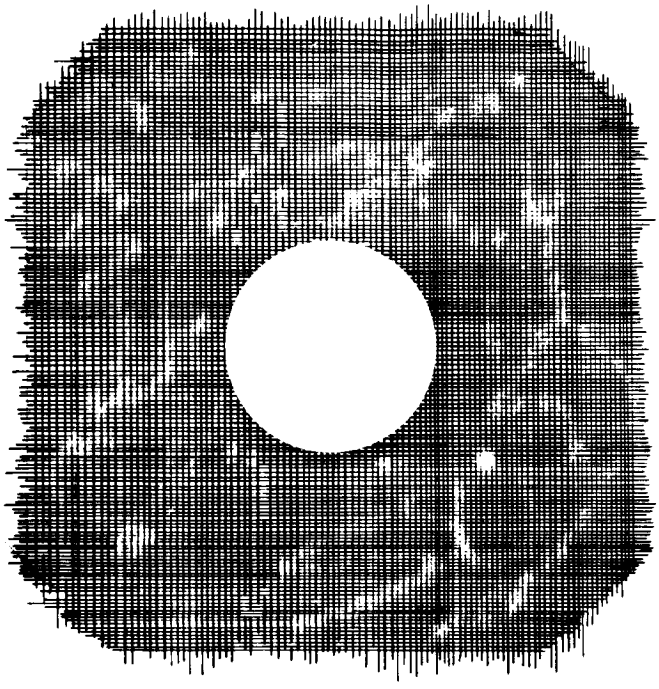

A. ALTERNATE LAYERS OF FIBERS AT 90° ORIENTATION

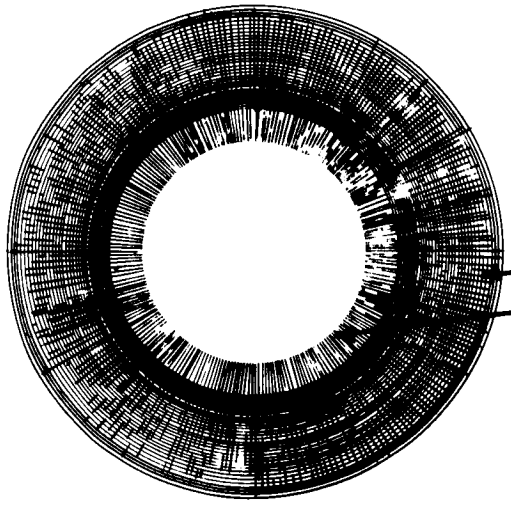

B. ALTERNATE LAYERS OF THIN HOOP WINDING AND END-ON FIBERS

TEI-639

Fig. 42 Fiber Arrangement for Rocket Nozzle Construction

In summary, it appears that conventional compositing techniques could be used for the fibers produced in this program. The application of the fibers to the composite will be improved as the strength of the fibers is increased and this should remain a goal of scale-up to continuous fiber preparation.

5. Fiber Evaluation in an Ablation Composite

One of the ultimate aims of the fiber development program is to determine how well the fiber works in an ablative application. There are at least two approaches which may be tried. One is to prepare and test small composites in an arc plasma and the second is to construct a small nozzle and either test-fire with an actual rocket-propellant combination or else use an arc plasma which closely simulates combustion product composition, enthalpy, and flow rate. The small-nozzle technique should be expected to give the most quantitative data and will, ultimately, be required for a final evaluation. However, such tests are expensive and the nozzle construction will require many thousands of feet of fiber.

Small composite rods, for example in the form of 1/8-in. diameter rods or 1/8 by 1/8-in. beams about 1-in. long, may be effectively examined in a small arc plasma such as used in this program. Ablation comparison to similar beams or rods made of quartz-phenolic as a standard should give an excellent preliminary measure of fiber effectiveness but requires only small quantities of material.

An alternative evaluation could be conducted in a large arc plasma unit more closely simulating combustion conditions. The fiber composite could be in the form of 1/2 by 1/2 by 1/2-in. cubes inserted into a two-dimensional nozzle as illustrated in Fig. 43.

The cubes could be normal to the nozzle axis or preferably "shingled" 60°. Slots recessed into the nozzle wall could be arranged to receive a graphite plug, a test specimen, another plug, a second specimen and a third plug. These could be held in place by suitable binding matrix material. As indicated in Fig. 43 as many as 8 specimens (4 on each side of the nozzle passage) could be evaluated at once. Fiber requirements for each would be only 400-500 feet, assuming 4-mil fibers with a 50 percent volume loading in the composite. Gross effects such as abnormal erosion, chemical reaction, char incompatibility, fiber weakening, or thermal shock could be noted. Corrective measures, either with the fiber or the matrix material, could be taken before a more extensive nozzle is built and tested.

6. Recommendation of Fibers

The batch process used during this work has been particularly useful in such

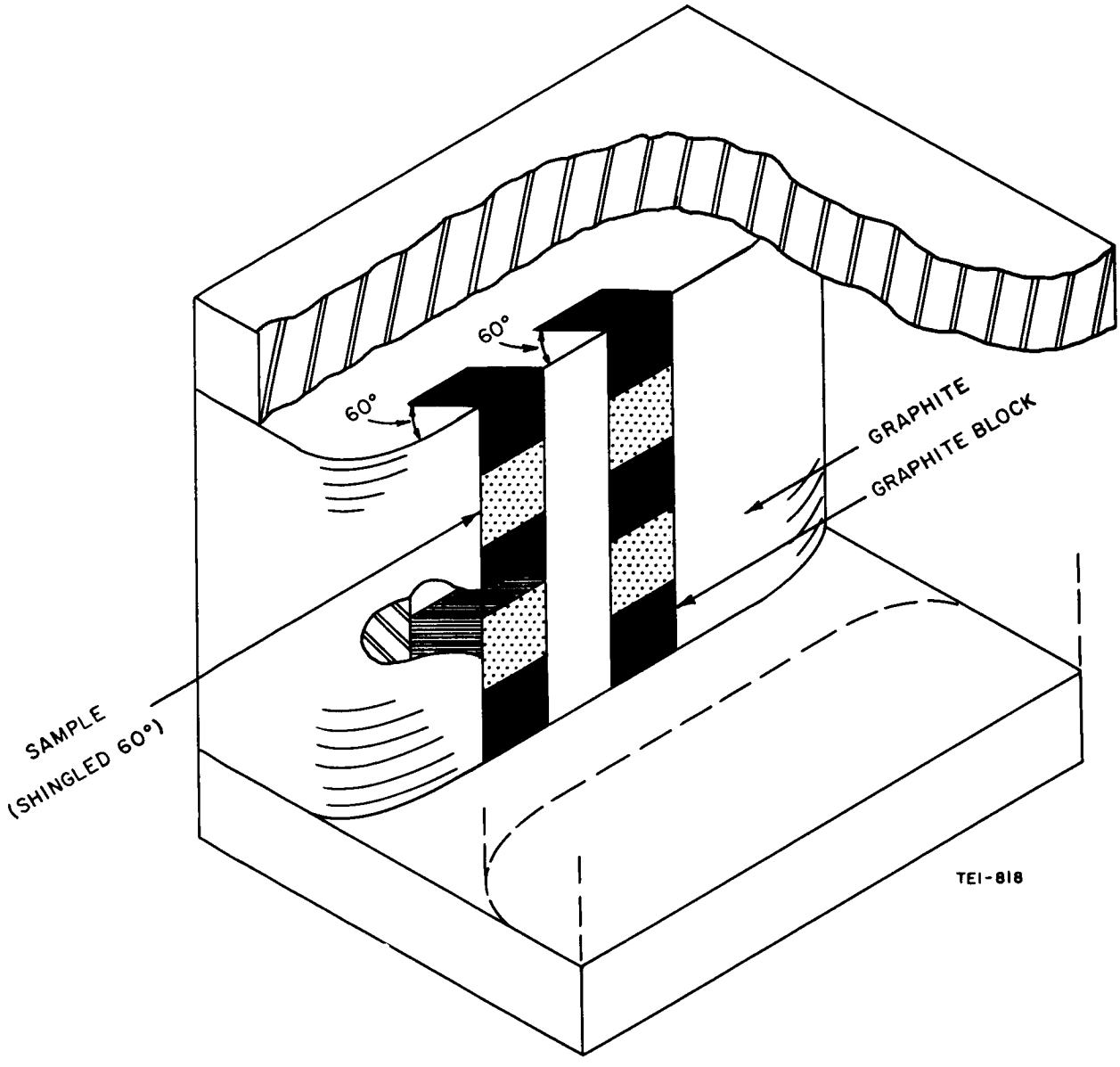

Fig. 43 Two Dimensional Nozzle for Arc Plasma Evaluations of Fiber Composite Specimens

a study since initial exploratory conditions often resulted in weak fibers which could not be effectively processed on continuous equipment. Once proper conditions were obtained, the resulting fiber strengths enable continuous processing to be undertaken. Based on other fiber experience at TEI, it is of interest to note that continuous preparation methods can normally be expected to improve both uniformity and strength over batch results. For this reason future work to convert to continuous operation is both feasible and desirable.

The strength and modulus of the materials should not be over emphasized but they remain useful criteria of quality and are important in the reinforcement role that the fibers are designed to play. All the fibers experimentally examined have theoretically outstanding strength and modulus values. This is illustrated in Table XXX. These values are given by Hjelm (Ref. 31).

Table XXX

CALCULATED MODULUS TO DENSITY RATING FOR SELECTED CRYSTALS*

Crystal	Calculated Elastic Modulus Million psi	Density lb/cu in.	Fig. of Merit Million in.	Theoretical Strength Million psi
Carbon	82	0.049	1673	4.0
B_4C	66	0.090	734	3.3
B	51**	0.083	615	2.6
TiB_2	94	0.162	580	4.7
TiC	72	0.177	406	3.6
ZrB_2	64	0.202	317	3.2
W	60	0.696	86	3.0

* Data from Hjelm (Ref. 31)

** Experimental values at TEI have been 55-60 which would indicate a theoretical strength for boron of up to 3.0×10^6 psi.

The theoretical tensile strength is based on the concept that it will be proportional to the calculated elastic modulus for the material (Ref. 32). This may vary from 3 to 17 percent (Ref. 33) and is taken as 5 percent by Hjelm.

It may be seen that on the basis of theoretical strength the materials might be rated in the following order: TiB_2, C, TiC, B_4C, ZrB_2, and W on B. Values for ZrO_2 are not available, but it is believed that it would show excellent potential strength. The problem is, of course, to what extent these values can be approached in fiber preparation.

The advantages and disadvantages of the various fibers will be discussed in the following sections:

a. Titanium Diboride

This fiber was the strongest fiber made in the program with values in the general range of 150 to 250 kpsi and individual values as high as 312 (unetched) and 378 kpsi (etched). It is expected that these values can be increased substantially in continuous preparation.

The resistance to chemical corrosion in the OF_2/B_2H_6 systems appears good both theoretically and by the experimental evaluation with the arc plasma at Vidya. The severe weakening observed in the TEI plasma test with BF_3 is not understood at the present. A possible explanation may be indicated by the TiB_2 analyses of the fiber which showed 73 percent Ti, a slight excess over the theoretical value of 68.9. It is possible that the excess Ti may have rapidly diffused to grain boundaries and weakened the structure. This indicates the necessity for controlling the process to make stoichiometric TiB_2. This factor should be investigated in future work. The strength of the TiB_2 fibers has not been studied at high temperature but Ramke and Latva (Ref. 6) report that the strength to weight ratio of bulk TiB_2 has not been exceeded by any other bulk material from 1600-2000°C.

The preparation of TiB_2 appears to have no outstanding problems which cannot be handled by good engineering practices. The necessity of maintaining a high temperature system to prevent condensation of $TiCl_3$ offers no unusual difficulty. It is recommended that TiB_2 be scaled up to continuous preparation.

b. Pyrolytic Graphite

Graphite ranks first among the materials studied in resistance to F_2/H_2 and OF_2/B_2H_6 combustion product corrosion. Graphite increases in strength at high temperatures. It has one of the best theoretical strengths, the highest melting

temperature (sublimation temperature) and is compatible with the carbon-forming ablating matrix. By all counts it is the preferred reinforcement material in this application if it can be made strong enough.

In this investigation, strengths in the range of 50 to 73 kpsi were obtained. These strengths are sufficient to make continuous production feasible. Plating rates have been low but the use of BCl_3 as an additive was found to double the rate. Early work required low pressure of about 5-mm Hg for effective preparation from C_2H_2. However, dilution with argon enabled satisfactory fibers to be made at atmospheric pressure with C_2H_2 and n-C_4H_{10}. Future work using argon and BCl_3 should be carried out on continuous equipment since strength, uniformity, and plating rate can all be expected to improve. The use of BCl_3 (with no added hydrogen) should particularly be studied since limited work done elsewhere at TEI on another fiber system has demonstrated that the rate of graphite deposition is directly proportional to the BCl_3 concentration.*

Graphite strength data from the literature have generally covered bulk pyrolytic graphite or pyrolyzed synthetic yarns. Those usually have been lower than the tensile values obtained in this program. However, Hough (Ref 34) prepared, on continuous apparatus, 0.8-mil graphite fibers starting with an 0.5-mil W substrate. He obtained tensile values of 118.2 and 145 kpsi. For these thin fibers the graphite was 61 vol percent and the tensile may have been influenced substantially by the substrate strength. In any event, he obtained relatively low specific strength because of the high density of the tungsten. He obtained a tensile value for a 4.04-mil graphite on 1.0-mil tungsten (94 percent graphite) of 66.4 kpsi.

Very impressive results have been reported for work done at Union Carbide Company (35) who have produced considerable amounts of fibers with 200 kpsi tensile and 6.9×10^6 psi modulus. In addition, preliminary properties of new laboratory scale fibers show 350 kpsi tensile with 30×10^6 psi modulus, a density of 1.4 g/cm^3 and fiber diameter (irregular cross section) of about 5 microns. This material is made by carefully controlled degradation of synthetic fibers such as rayon. They currently offer for sale pound quantities of 300 kpsi tensile material with a 20-30 million psi modulus. This is in the form of a 2-ply yarn with 720 ends.

It is clear the graphite fibers are desirable for reinforcing the ablation matrix but it is not so clear, on the limited information available, whether or not monofilaments made by chemical vapor plating (CVP) are competitive to the above

* Work done by the present group after expiration of NAS3-4196 has verified the rate increase given by BCl_3 and, during the writing of this report, has prepared at one atmosphere pressure a 5.9-mil graphite fiber on 1.5-mil W substrate (93.5 vol percent graphite) with values of 103.6 kpsi tensile and 17.8 million psi modulus.

fibers resulting from controlled pyrolysis of synthetic organics. The latter have the advantage of lower cost, currently higher strength and modulus and probably have the ability to be woven in two directions. However, they have the disadvantage of higher surface area with greater sensitivity to oxidation. They are slightly porous and absorb 5 to 6 percent water.

The monofilament such as prepared in this program has low porosity and surface area and should be more resistant to oxidation and corrosion. The strength conversion in a matrix has not been measured but, based on experience with other monofilaments, should be 100 percent.

Because of the high strength potential of graphite and the traditional improvement in making continuous over batch filaments, the strength of the CVP monofilaments may become very attractive. The continuous processing will be relatively simple since all plating materials are gases and are easy to control. No special equipment designs are required. Major questions to be answered will be the plating rate and the obtainable strength and modulus.

It is believed that, in view of the newness of the state-of-the-art, the potential of monofilament pyrolytic graphite should be examined briefly under continuous CVP conditions. If strengths in the range of 300 to 500 kpsi and modulus at 20 to 30 million psi or above can be attained in a relatively short time, then consideration for further development should be carefully made to see whether further gains might be achieved and whether these fibers will be competitive to the pyrolyzed yarns. If the above initial goals cannot be readily obtained, further development should be stopped.

c. Tungsten on Boron

Tungsten has been successfully plated on boron using WF_6. The process is simple and the major problems will be to improve the strength and to decide whether to plate on an existing boron substrate or to make a two-step process with the boron being freshly prepared before plating the tungsten. Temperature control offers a problem because the desired temperature of 500°C is at or below the range of an optical pyrometer. However, infrared devices can be used to maintain a constant and reproducible (although unmeasured) temperature.

Tungsten has shown excellent resistance to reaction with the propellant system. By plating it on the lighter substrate the combined fiber should be resistant to corrosion and have a more desirable density in the range of 5.5 to 6.5, depending on the thickness used. The main disadvantage is the melting point of 2040°C of the boron substrate. This, however, is more than a 1000°C above the softening point of glass and is over 300°C higher than the melting point of SiO_2, the main fibers in current use.

Further consideration should be given to the continuous preparation of tungsten of boron, but, because of its relatively low melting point, this fiber should receive a low priority.

d. Titanium Carbide

Titanium carbide has attractive properties with a high melting point (3250°C), high potential strength, and fair resistance to corrosion. Arc plasma tests on TiC fiber made in this program indicated that TiC has relatively good resistance to corrosion-erosion by an argon 5 percent BF_3 atmosphere. Titanium carbide, however, has not been prepared in a satisfactory form in this program. One fiber, using $TiCl_4$ and C_2H_5Br as the plating gases, gave a tensile strength of 63 kpsi. This was not duplicated in successive experiments. The temperature of 1250°C appears to be the best to use. Where TiC is formed it appears to be of high quality, without porosity, and having high microhardness. It is possible that other carbon precursors such as butane or neopentane will give better results. It is also possible that more constant temperatures and other operating conditions in a continuous process will give a more uniform fiber. It is believed that a limited program on a continuous unit is justified to see if the fiber can be made with reasonable quality. If so, further work would be highly justified. The complexity of preparation should be about that of the TiB_2 fiber, with provision being made for handling the low volatility $TiCl_3$ product.

e. Zirconium Diboride

Zirconium diboride is very desirable from the standpoint of resistance to corrosion and has potentially good strength. It is the most difficult to make of the fibers studied because of the low volatility of the $ZrCl_4$. The sublimer gave difficulty and the plating gas mixture was generally deficient in $ZrCl_4$. Therefore the plating conditions were not established but they are believed to be close to those used for TiB_2. The chief problems in scale up will be the design and operation of an effective sublimer or else the production of $ZrCl_4$ in-situ by chlorination of Zr metal or the generation of $ZrCl_4$ by reaction between AgCl or CuCl and Zr metal as discussed earlier. Plating equipment with high temperature walls similar to that used for TiB_2 would be required. No outstanding difficulties of other natures are expected. It is believed that a limited program of scale up is justified, as in the case of TiC, to ascertain whether or not, with the assurance of a constant supply of $ZrCl_4$, a good quality ZrB_2 fiber can be made. If results are encouraging, further development will be well justified.

f. Recommendations

It is recommended that scale up from a batch to a continuous process be carried

out for TiB_2 and pyrolytic graphite. Limited programs should be undertaken to determine the feasibility of scale up for TiC. If promising, TiC fibers should be further developed. The feasibility of preparing ZrB_2 fibers should be investigated further and, if feasibility can be demonstrated, scale-up to continuous preparation should be pursued. Scale up for tungsten on boron is feasible but should be given a lower priority than the other fibers because of the relatively low melting point of 2040°C.

It is also recommended that an investigation be conducted of the high temperature structural and chemical behavior of the recommended fibers. The effect of temperature and composition on metallurgical stability, mechanical properties, and chemical resistance to the oxidizing media should be investigated.

V. CONCLUSIONS

1. Pyrolytic graphite, titanium carbide, titanium diboride, boron carbide, zirconium dioxide, and zirconium diboride are strong candidate materials for fiber reinforcement of resins used for the thrust chamber liners of advanced liquid-fuel rocket engines. Tungsten coated boron and carbon coated boron also look attractive but the relatively low melting temperature of boron will restrict the application of these materials.

2. The preparation of pyrolytic graphite, titanium carbide, titanium diboride and tungsten coated boron fibers is feasible by chemical vapor plating.

3. The titanium diboride fibers produced in this investigation had the highest tensile strength and elastic modulus of all of the fiber materials investigated. The TiB_2 fibers had tensile strengths up to 378 kpsi and elastic moduli up to 84 million psi.

4. A reliable method of producing and measuring the desired flow rates of $ZrCl_4$ must be developed before a systematic and controlled investigation of ZrB_2 fiber preparation can be performed.

5. Future investigations into the preparation of these fibers should be performed on a continuous preparation basis rather than a batch basis in order to eliminate numerous experiment control difficulties associated with batch preparations. These investigations should try to optimize the preparation of these fibers from the standpoint of quality and rate of preparation.

6. An investigation of the high-temperature structural and chemical behavior of the candidate fibers should be conducted. This investigation should explore the effect of temperature and composition of the fibers on the metallurgical stability, mechanical properties and chemical resistance to the rocket engine exhaust gases.

APPENDIX

1. Calibration of Rotameters

The flows of the various gases used in this program were measured with Schutte and Koerting type rotameters. Calibrations for the rotameter tubes were obtained in one of the following three ways: (1) supplied by the manufacturer, (2) calibrated by TEI, using a conventional bubble flow meter or (3) estimated from the calibration chart of another gas using a conversion factor. The calibration curves derived from the TEI bubble flow-meter tests were usually averages of at least two determinations. In general, when more than one rotameter tube of a particular size was used, only one of the rotameter tubes was calibrated, and this calibration was used for the other rotameter tubes of the same size.

The rotameters for BCl_3 were calibrated by TEI using Freon 12. Acetylene, methane, and hydrogen rotameters were calibrated by TEI using the actual gases. Argon rotameters were calibrated by TEI using the actual gas except for flows above 1200 cc/min. Flows above 1200 cc/min were estimated as described below.

In some instances, the flow of a particular gas was estimated from the calibration chart of another gas by the following relationship:

$$F_2 = F_1 \sqrt{\frac{G_1}{G_2}}$$

where F_2 is the flow of the uncalibrated gas, F_1 is the flow of the calibrated gas at a particular rotameter setting and G_1 and G_2 are the specific gravities of the calibrated and uncalibrated gases, respectively. Using this approach, the flows of n-butane, neopentane, and WF_6 were estimated using existing calibrations for Freon 12. Also, this approach was used to estimate argon flows greater than 1200 cc/min using a calibration chart for HF furnished by the manufacturer.

In the TiC preparations, the flows of $TiCl_4$ and its solution with CCl_4 and ethyl bromide were measured using a Schutte and Koerting Co. rotameter that was calibrated in the following manner: the liquid was admitted to the rotameter from a calibrated reservoir pressurized with argon, and the depletion of the reservoir over a given time was measured for several rotameter settings. The average liquid flows for each setting were converted to gas flows by the following relationship

$$F_G = \frac{F_1 \quad \rho}{M} \times \qquad 22,400$$

where F_G is the gas flow, F_l is the liquid flow, ρ is the density of the liquid and M is the molecular weight of the liquid. When the desired flows differed from the calibration points, they were determined by interpolation or extrapolation. When solutions were calibrated, the liquid flow of each constituent compound was first determined from the composition of the solution, and then converted to gas flow by the above relationship. In some experiments, however, the rotameter was simply used to control and monitor the steadiness of the flow while the actual flow was determined from the rate of depletion of the reservoir.

2. Tensile Tests

The tensile strengths of fibers produced in this program were determined on a Model TM-L Instron tensile tester, using specimens of the fiber about 0.5-in. long. The ends of the specimen were glued to metal tabs with an epoxy such that a distance of 1/4 in. separated the tabs (1/4-in. gauge length). The tabs had slots in them to receive the fiber and to aid in alignment. After gluing, the specimen was placed in the tensile tester by hooking the tabs, which had holes in them, to the Instron clamps. The holes in the tabs were aligned axially with the specimen so that bending moments during testing were minimized.

The cross-head speed was set at 0.05 in. per minute. The load as a function of time was recorded using a chart speed of 20-in. per minute. The tensile strength was computed from the breaking load and the calculated cross-sectional area of the fiber specimen. The diameter of the specimen was determined as the average of several measurements made on an optical comparator.

Generally, only one test was made on each fiber.

3. Density Determinations

The densities of pyrolytic graphite fibers were determined using density gradient columns prepared in accordance with ASTM D 1505-63T in the range of 1.60 to 1.80 g/cc and 1.90 to 2.50 g/cc. The column in the range of 1.60 to 1.80 g/cc was prepared with carbon tetrachloride and carbon tetrabromide. Chloroform and carbon tetrabromide were used to prepare the column ranging from 1.90 to 2.50 g/cc. In preparing both columns, several solutions of the two liquids were prepared, such that each differed from the next heavier by the same number of grams per cubic centimeter. The gradient tubes were then filled by adding an equal volume of each solution to the column, starting with the heaviest. Standardized glass beads within the desired range of the

column were dropped into the column and settled to their own density levels. If a fairly uniform gradient was obtained, the glass beads floated at equal intervals within the tube. Pieces of the fiber were dropped into the columns, and the density of the fiber was read directly from the level it sought. The accuracy of this method is $\pm$ 0.005 g/cc.

The densities of ZrB_2, TiB_2, TiC, and W on B deposits which are greater than 2.50 g/cc were determined from the volume and mass of the deposit. The fiber specimen was weighed to an accuracy of $\pm$ 0.00002 gm and then the mass of the substrate or core was subtracted from the total mass of the specimen to obtain the net mass of the deposit. The mass of the core was computed from its length, diameter, and density, using the original substrate diameter, specimen length, and the density of the original substrate materials.

The volume of the deposit was computed from the overall diameter of the fiber, the original substrate diameter and specimen length. The overall diameter and specimen length were measured to $\pm$ 0.000635 cm and $\pm$ 0.01 cm, respectively.

This method of determining densities was satisfactory as long as the diameter of the specimens was reasonably uniform and the surface was smooth. All density specimens were examined with the microscope to verify the acceptability of its surface. The probable error in the density computed by this approach is about $\pm$ 3 percent of the value reported.

4. X-ray Diffraction Analysis

X-ray diffraction was used to identify the phases or materials present in the deposits of fibers produced in this program. All diffractions were run on a Norelco x-ray unit using the standard Debye-Scherrer method. Copper K α radiation was used with a nickel filter at 35 KW and 20 ma. Specimens were run on either a 57.3 or 114.6 mm diameter cameras. On many of the fibers, diffraction patterns were obtained on both the as-produced fiber and powdered samples of the fiber. Samples were carefully powdered with a mortar and pestle to minimize contamination and then placed in thin-walled glass tubes. Exposures were one hour for TiC, TiB_2 and graphite, about three hours for tungsten-coated boron, and about 2.5 hours for ZrB_2.

Identification of the diffraction spectra was made primarily from ASTM diffraction data cards.

5. Chemical Analyses for Titanium

Titanium diboride fibers were analyzed quantitively for titanium by the following procedure. First, the fibers were weighed on a Cahn Microbalance, and their lengths were measured. They were then placed in covered teflon beakers and dissolved in a hot solution composed of concentrated nitric acid and one milliliter of concentrated hydrofluoric acid. The solutions were cooled, five milliliters of concentrated sulphuric acid were added and the solutions were reheated without covers to remove the fluoride ion and water. When the volumes of liquid were reduced, the samples were transferred to Erlenmeyer flasks and covered with still heads for refluxing. They were heated until fumes of sulphur trioxide evolved for a few minutes. The samples were cooled and placed in volumetric flasks. Two milliliters of hydrogen peroxide, which forms a yellow colored complex ion with titanium, were added to each flask, and they were then filled with distilled water and mixed well. The absorbance of each sample was then measured on a Bausch and Lomb Colorimeter at 410 millimicrons against water as a blank. The absorbances of the samples were compared with a calibration curve which was prepared by plotting the concentrations of standard titanium solutions against their absorbances. In this way the number of milligrams of titanium in each fiber was obtained. This analysis was accurate to one-tenth of one percent.

Since the fibers consisted of TiB_2 and a substrate material, the weight of the substrate material had to be subtracted from the weights of the fibers to get an accurate weight of TiB_2. In this way, the proper ratio of Ti to TiB_2 could be determined. The weight of the substrate was computed from its original diameter and sample length and the density of the material. From the accuracies of the weights, measurements, and chemical analysis, the probable error in the ratio of Ti to TiB_2 for a typical fiber was calculated to be about $\pm$ 2 percent.

6. Determination of Elastic Modulus of Fibers

The elastic modulus of fibers was determined by a method based on the critical buckling load of a long slender column (the fiber). A short piece ($\sim$ 1/2 in.) of fiber was placed vertically in a small cone-shaped recess in a platen mounted on one of the heads of an Instron testing machine. The sample was held in place by a gel. A vertical compression force was then applied to the free end of the fiber by a matching platen with a cone-shaped recess. The cone-shaped recesses simply kept the sample aligned axially with the load. The cross-head speed was set at 0. 05 in. per minute and the chart speed at 2 in. per minute. The critical buckling load was noted as the maximum load at which the load deflection curve deviated from a straight line. The elastic modulus was then computed from the formula

$$E = \frac{64\ PL^2}{\pi^3 D^4\ 453.6}$$

where E is the elastic modulus in psi, P is the critical buckling in grams, L is the length of the fiber in inches, and D is the diameter of the fiber in inches. The diameter D was measured on an optical comparator and was averaged from several determinations.

VII. REFERENCES

1. N. Beecher and R. E. Rosensweig, "Ablation Mechanisms in Plastics with Inorganic Reinforcement", ARS Journal, 31, 1961, p. 532.

2. J. D. Bachelor, J. A. Simmons, and W. E. West, "Chemical Reactions Between Plastic Composite Materials and Propellant Exhaust Products", ASD-TDR-63-737, Vol. 1, Aug. 1963, Vol. 2, (classified).

3. E. P. Barlett, "Thermal Protection of Rocket-Motor Structures", Aerospace Engineering, Vol. 22, No. 1, Jan. 1963, p. 86.

4. I. E. Campbell, ed. in chief, "High-Temperature Technology", J. Wiley and Sons, N. Y., 1956.

5. Claude P. Talley, "Thermal Conductivity of Polycrystalline Boron", J. Phys. Chem., Vol. 63, 1959, p. 311.

6. W. G. Ramke and J. D. Latva, "Refractory Ceramics and Intermetallic Compounds", Aerospace Engineering, Vol. 22, No. 1, Jan 1963, p. 76.

7. Barry R. Emrich, "Literature Survey on the Synthesis, Properties and Applications of Selected Boride Compounds", ASD-TDR-62-873, Dec. 1962.

8. E. P. Bartlett, R. W. Baier, and E. L. Doughman, "Feasibility Investigation of Uncooled Thrust Chamber Designs", (U), Final Technical Report No. C-1898, Ford Motor Co., Aeronutronic Division, Nov. 1962, (Conf.).

9. E. P. Bartlett, "A Systematic Method for Determination of Ablation Rates in a Corrosive Environment", Sixth Symposium on Ballistic Missile and Aerospace Technology, Vol. 3, Academic Press Inc., New York, 1961, pp. 103-119.

10. Union Carbide Research Institute, "Research on Physical and Chemical Principles Affecting High-Temperature Materials for Rocket Nozzles", Contract No. DA-30-069-ORD-2787, Quarterly Progress Report, March 31, 1963 and earlier progress reports starting 1961.

11. R. A. Rindal, D. T. Flood, and R. M. Kendall, "Analytical and Experimental Study of Ablation Material for Rocket Engine Application", Vidya Division of Itek Corp., Interim Progress Report, March 18, 1963 to March 17, 1964, Contract No. NAS7-218.

12. R. A. Rindal, D. T. Flood, J. W. Schaefer, ibid, Fourth Quarterly Progress Report, May 19, 1964 to August 18, 1964.

13. JANAF Interim Thermochemical Tables, The Dow Chemical Company, Midland, Michigan.

14. R. C. Oliver and R. W. Baier, "Chemical Corrosion of Rocket Liner Materials and Propellant Performance Studies", Third Quarterly Report, March 15, 1963.

15. D. T. Flood, "Evaluation of Refractory Materials for Reinforcing Fiber Applications in a Simulated Oxygen Difluoride-Diborane Environment", Report No. 180, Vidya Division of Itek Corp., March 31, 1965.

16. J. J. Gebhardt and R. F. Cree, "Vapor Deposited Borides of Group IV-A Metals", AD 601861, June 1964.

17. J. J. Lander and L. H. Germer, Trans. AIME, Vol. 175, 1948, p. 648.

18. E. Mark Gold, ARS Journal, Vol. 32, 1962, p. 437.

19. C. P. Talley, "Combustion of Elemental Boron", Texaco Experiment Inc., TM-1211, May 1960.

20. V. A. Nieberlein, "Vapor Deposited Tungsten Coatings on Graphite", Ceramic Bulletin, Vol. 44, No. 1, 1965.

21. I. E. Campbell, et al, "The Vapor Phase Deposition of Refractory Materials", J. Electrochem. Soc., Vol. 96, 1949.

22. K. Knox, et.al., J. Chem. Soc., 1952, p. 1477.

23. G. I. Kozlor, Flame, Vol. 6, 1962, p. 253.

24. W. J. Hooker, Seventh Symposium (International) on Combustion, Butterworth, London, 1959, p. 949.

25. P. H. Higgs, et. al., Research and Development on Advanced Graphite Materials, WADD TR-62-72, Vol. 37, May 1964, p. 14.

26. J. Harvey, et. al., "The Structure of Pyrolytic Carbon", RAE-TN-MT-PHYS-361 (Great Britain Royal Aircraft Establishment, Farnborough, Hants, England), Oct. 1962.

27. R. J. Diefendorf and E. R. Stover, "Pyrolytic Graphite.... How Structure Effects Properties", Materials Progress, May 1962, p. 103-108.

28. Roger Bacon, "Growth Structure and Properties of Graphite Whiskers", J. Applied Physics, Vol. 31, No. 2, Feb. 1960.

29. P. H. Higgs, et. al., "Studies of Graphite Deposited by Pyrolytic Processes", WADD TR 61-72, Vol. 37, May 1964.

30. F. W. Glaser and B. Post, "System Zirconium-Boron", Journal of Metals, Vol. 5, 1953, p. 1118.

31. L. N. Hjelm, "Metal-Ceramic Composite Structural Materials", SAMPE Journal No. 1, June/July 1965, p. 8.

32. J. J. Gilman, National Bureau of Standard Monograph, No. 59, 1963.

33. S. S. Brenner, "Factors Influencing the Strength of Whiskers", ASM Seminar on Fiber Composite Materials, Philadelphia, Pa., Oct. 1964.

34. R. L. Hough, "Continuous Pyrolytic Graphite Composite Filaments", AIAA Journal, Vol. 3, 1965, p. 291.

35. L. R. McCreight, et. al., "A Survey of the State of the Art of Ceramic and Graphite Fibers", AFML-TR-65-105, May 1965, p. 159.

36. R. C. Oliver, et. al., "Chemical Corrosion of Rocket Liner Material and Propellant Performance Studies", 2nd Quarterly Report NOC-1960, Ford Motor Company, Jan. 1963.

DISTRIBUTION LIST FOR FINAL REPORT CR-54722

"Investigation of Fiber Systems of Ablative Materials"

CONTRACT NAS3-4196

Texaco Experiment Incorporated
Richmond, Virginia 23234

National Aeronautics and Space Administration (1)
Lewis Research Center
21000 Brookpark Road
Cleveland, Ohio 44135
Attention: Contracting Officer, MS 500-210

National Aeronautics and Space Administration (8)
Lewis Research Center
21000 Brookpark Road
Cleveland, Ohio 44135
Attention: Liquid Rocket Technology Branch, MS 500-209

National Aeronautics and Space Administration (1)
Lewis Research Center
21000 Brookpark Road
Cleveland, Ohio 44135
Attention: Technical Report Control Office, MS 5-5

National Aeronautics and Space Administration (1)
Lewis Research Center
21000 Brookpark Road
Cleveland, Ohio 44135
Attention: Technology Utilization Office, MS 3-16

National Aeronautics and Space Administration (3)
Lewis Research Center
21000 Brookpark Road
Cleveland, Ohio 44135
Attention: AFSC Liaison Office, MS 4-1

National Aeronautics and Space Administration (2)
Lewis Research Center
21000 Brookpark Road
Cleveland, Ohio 44135
Attention: Library

National Aeronautics and Space Administration (1)
Lewis Research Center
21000 Brookpark Road
Cleveland, Ohio 44135
Attention: Office of Reliability & Quality Assurance,
MS 500-203

National Aeronautics and Space Administration (1)
Lewis Research Center
21000 Brookpark Road
Cleveland, Ohio 44135
Attention: Mr. Robert Signorelli, MS 106-1

National Aeronautics and Space Administration (1)
Lewis Research Center
21000 Brookpark Road
Cleveland, Ohio 44135
Attention: Dr. Murray Pinns, MS 6-1

National Aeronautics and Space Administration (1)
Lewis Research Center
21000 Brookpark Road
Cleveland, Ohio 44135
Attention: Mr. Jerry Winter, MS 100-1

National Aeronautics and Space Administration (1)
Washington, D. C., 20546
Attention: Code RRM

National Aeronautics and Space Administration (2)
Washington, D. C., 20546
Attention: Code RPL

National Aeronautics and Space Administration (1)
Washington, D. C., 20546
Attention: Code SV

National Aeronautics and Space Administration (1)
Washington, D. C., 20546
Attention: Code MT

National Aeronautics and Space Administration (1)
Washington, D. C., 20546
Attention: Code RV1

National Aeronautics and Space Administration (1)
Washington, D. C., 20546
Attention: Code RV2

Scientific and Technical Information Facility (1)
P. O. Box 33
College Park, Maryland 20740
Attention: NASA Representative
Code CRT

National Aeronautics and Space Administration (1)
Ames Research Center
Moffett Field, California 94035
Attention: Library

National Aeronautics and Space Administration (1)
Ames Research Center
Moffett Field, California 94035
Attention: Dr. John Parker

National Aeronautics and Space Administration (1)
Ames Research Center
Moffett Field, California 94035
Attention: Bradford Wick

National Aeronautics and Space Administration (1)
Flight Research Center
P. O. Box 273
Edwards, California 93523
Attention: Library

National Aeronautics and Space Administration (1)
Goddard Space Flight Center
Greenbelt, Maryland 20771
Attention: Library

National Aeronautics and Space Administration (1)
Langley Research Center
Langley Station
Hampton, Virginia 23365
Attention: Library

National Aeronautics and Space Administration (1)
Langley Research Center
Langley Station
Hampton, Virginia 23365
Attention: William Brooks

National Aeronautics and Space Administration (1)
Langley Research Center
Langley Station
Hampton, Virginia 23365
Attention: Mr. E. E. Mathauser
Structures Research Division

National Aeronautics and Space Administration (1)
Langley Research Center
Langley Station
Hampton, Virginia 23365
Attention: Dr. George F. Pezdirtz
Spacecraft Materials Section

National Aeronautics and Space Administration (1)
Manned Spacecraft Center
Houston, Texas 77001
Attention: Library

National Aeronautics and Space Administration (1)
Manned Spacecraft Center
Houston, Texas 77001
Attention: J. G. Thibodaux, Code EP

National Aeronautics and Space Administration (1)
George C. Marshall Space Flight Center
Huntsville, Alabama 35812
Attention: Library

National Aeronautics and Space Administration (1)
Western Operations
150 Pico Boulevard
Santa Monica, California 90406
Attention: Library

National Aeronautics and Space Administration (1)
John F. Kennedy Space Center
Cocoa Beach, Florida 32931
Attention: Library

Jet Propulsion Laboratory (1)
4800 Oak Grove Drive
Pasadena, California 91103
Attention: Library

Jet Propulsion Laboratory (1)
4800 Oak Grove Drive
Pasadena, California 91103
Attention: Mr. Anthony Briglio, Propulsion Division

Office of the Director of Defense Research (1)
& Engineering
Washington, D. C., 20301
Attention: Dr. H. W. Schulz, Office of Assistant Director
(Chem. Technology)

Defense Documentation Center (1)
Cameron Station
Alexandria, Virginia 22314

RTD(RTNP) (1)
Bolling Air Force Base
Washington, D. C., 20332

Arnold Engineering Development Center (1)
Attention: AEOIM
Air Force Systems Command
Tullahoma, Tennessee 37389

AFSC(SCLT/Captain S. W. Bowen) (1)
Andrews Air Force Base
Washington, D. C., 20332

AFRPL(RPM) (1)
Edwards, California 93523

AFFTC(FTAT-2) (1)
Edwards AFB, California 93523

Office of Research Analyses (OAR) (1)
Attention: RRRT
Holloman Air Force Base, New Mexico 88330

Air Force Office of Scientific Research (1)
Washington, D. C., 20333
Attention: SREP, Dr. J. F. Masi

AFRPL(RPC) (1)
Edwards, California 93523

Wright-Patterson Air Force Base, Ohio 45433 (1)
Attention: AFML(MAAE)

Wright-Patterson Air Force Base, Ohio 45433 (1)
Attention: AFML(MAAM)

Commanding Officer (1)
Ballistic Research Laboratories
Aberdeen Proving Ground, Maryland
Attention: AMXBR-1
21005

Department of the Army (1)
U. S. Army Materiel Command
Washington, D. C., 20315
Attention: AMCRD-RC

Commanding Officer (1)
U. S. Army Research Office (Durham)
Box CM, Duke Station
Durham, North Carolina 27706

U. S. Army Missile Command (1)
Redstone Scientific Information Center
Redstone Arsenal, Alabama 35808
Attention: Chief, Document Section

Bureau of Naval Weapons (1)
Department of the Navy
Washington, D. C., 20360
Attention: DLI-3

Bureau of Naval Weapons (1)
Department of the Navy
Washington, D. C., 20360
Attention: RMMP-2

Bureau of Naval Weapons (1)
Department of the Navy
Washington, D. C., 20360
Attention: RMMP-4

Bureau of Naval Weapons (1)
Department of the Navy
Washington, D. C., 20360
Attention: RRRE-6

Commander (1)
U. S. Naval Missile Center
Point Mugu, California 93041
Attention: Technical Library

Commander (1)
U. S. Naval Ordnance Laboratory
White Oak
Silver Spring, Maryland 20910
Attention: Library

Commander (1)
U. S. Naval Ordnance Test Station
China Lake, California 93557
Attention: Code 45

Commander (Code 753) (1)
U. S. Naval Ordnance Test Station
China Lake, California 93557
Attention: Technical Library

Superintendent (1)
U. S. Naval Postgraduate School
Naval Academy
Monterey, California 93900

Commanding Officer (1)
Office of Naval Research
1030 E. Green Street
Pasadena, California 91101

Director (Code 6180) (1)
U. S. Naval Research Laboratory
Washington, D. C., 20390
Attention: H. W. Carhart

Director (1)
Special Projects Office
Department of the Navy
Washington, D. C., 20360

Commanding Officer (1)
U. S. Naval Underwater Ordnance Station
Newport, Rhode Island 02844
Attention: W. W. Bartlett

Commander (1)
U. S. Naval Weapons Laboratory
Dahlgren, Virginia 22448
Attention: Technical Library

Aerojet-General Corporation (1)
P. O. Box 296
Azusa, California 91703
Attention: Librarian

Aerojet-General Corporation (1)
11711 South Woodruff Avenue
Downey, California 90241
Attention: F. M. West, Chief Librarian

Aerojet-General Corporation (1)
Attention: Technical Library 2484-2015A
P. O. Box 1947
Sacramento, California 95809

Aeronutronic Division Philco Corporation (1)
Ford Road
Newport Beach, California 92600
Attention: Dr. L. H. Linder, Manager
Technical Information Department

Aeroprojects, Inc. (1)
310 East Rosedale Avenue
West Chester, Pennsylvania 19380
Attention: C. D. McKinney

Aerospace Corporation (1)
P. O. Box 95085
Los Angeles, California 90045
Attention: Library-Documents

Allied Chemical Corporation (1)
General Chemical Division
P. O. Box 405
Morristown, New Jersey 07960
Attention: Security Office

Celanese Corporation of America (1)
Box 3049
Asheville, North Carolina 28802

American Cyanamid Company (1)
1937 West Main Street
Stamford, Connecticut 06902
Attention: Security Officer

IIT Research Institute (1)
Technology Center
Chicago, Illinois 60616
Attention: C. K. Hersh, Chemistry Division

ARO, Inc. (1)
Arnold Engineering Development Center
Arnold AF Station, Tennessee 37389
Attention: Dr. B. H. Goethert
Chief Scientist

E. I. duPont deNemours and Company (1)
Eastern Laboratory
Gibbstown, New Jersey 08027
Attention: Mrs. Alice R. Steward

Esso Research and Engineering Company (1)
Special Projects Unit
P. O. Box 8
Linden, New Jersey 07036
Attention: Mr. D. L. Baeder

Ethyl Corporation (1)
Research Laboratories
1600 West Eight Mile Road
Ferndale, Michigan 48220
Attention: E. B. Rifkin, Assistant Director
Chemical Research

General Dynamics/Astonautics (1)
P. O. Box 1128
San Diego, California 92112
Attention: Library and Information Services (128-00)

Hercules Powder Company (1)
Allegany Ballistics Laboratory
P. O. Box 210
Cumberland, Maryland 21501
Attention: Library

Institute for Defense Analyses (1)
400 Army-Navy Drive
Arlington, Virginia 22202
Attention: Classified Library

Lockheed Propulsion Company (1)
P. O. Box 111
Redlands, California 92374
Attention: Miss Belle Berlad, Librarian

Lockheed Propulsion Company (1)
P. O. Box 111
Redlands, California 92374
Attention: Mr. Walter D. Hart

Marquardt Corporation (1)
16555 Saticoy Street
Box 2013 - South Annex
Van Nuys, California 91404

Minnesota Mining & Manufacturing Company (1)
900 Bush Avenue
St. Paul, Minnesota 55106
Attention: Code 0013 R&D
VIA: H. C. Zeman, Security Administrator

North American Aviation, Inc. (1)
Space & Information Systems Division
12214 Lakewood Boulevard
Downey, California 90242
Attention: Technical Information Center
D/096-722 (AJ01)

Rocket Research Corporation (1)
520 South Portland Street
Seattle, Washington 98108

Rocketdyne (1)
6633 Canoga Avenue
Canoga Park, California 91304
Attention: Library, Department 596-306

Rohm and Haas Company (1)
Redstone Arsenal Research Division
Huntsville, Alabama 35808
Attention: Librarian

Thiokol Chemical Corporation (1)
Alpha Division, Huntsville Plant
Huntsville, Alabama 35800
Attention: Technical Director

Thiokol Chemical Corporation (1)
Elkton Division
Elkton, Maryland 21921
Attention: Librarian

Thiokol Chemical Corporation (1)
Reaction Motors Division
Denville, New Jersey 07834
Attention: Librarian

Thiokol Chemical Corporation (1)
Rocket Operations Center
P. O. Box 1640
Ogden, Utah 84401
Attention: Librarian

Thiokol Chemical Corporation (1)
Wasatch Division
P. O. Box 524
Brigham City, Utah 84302
Attention: Library Section

United Aircraft Corporation (1)
Corporation Library
400 Main Street
East Hartford, Connecticut 06118
Attention: Dr. David Rix

United Aircraft Corporation (1)
Pratt & Whitney Fla. Res. & Dev. Ctr.
P. O. Box 2691
W. Palm Beach, Florida 33402

United Aircraft Corporation (1)
United Technology Center
P. O. Box 358
Sunnyvale, California 94088
Attention: Librarian

General Electric Company (1)
Apollo Support Department
P. O. Box 2500
Daytona Beach, Florida 32015
Attention: C. Day

Aerotherm Corporation (1)
460 California Avenue
Palo Alto, California 94304
Attention: Mr. Roald Rindal

The Boeing Company (1)
Missile & Information Systems Division
P. O. Box 3985
Seattle, Washington 98124
Attention: Robert H. Jewett for
Ruth E. Peerenboom (520)
Technical Library,
Processes Supervisor

General Electric Company (1)
Advanced Materials, Mall Zone M-78
Cincinnati 15, Ohio
Attention: D. S. Tomalin

The General Electric Company (1)
Valley Forge STC
P. O. Box 8555
Philadelphia, Pennsylvania 19101
Attention: Library

General Technologies Corporation (1)
708 North West Street
Alexandria, Virginia
Attention: D. F. Bazzarre

General Technologies Corporation (1)
708 North West Street
Alexandria, Virginia
Attention: J. C. Withers

Mr. J. S. Parkinson (1)
Johns-Manville Research & Engineering Center
P. O. Box 159
Manville, New Jersey

The Marquardt Corporation (1)
ASTRO Division
16555 Saticoy Street
Van Nuys, California
Attention: B. A. Webb

Monsanto Research Corporation (1)
Dayton Laboratory
Station B., Box 8
Dayton, Ohio 45407
Attention: Beverly A. Peters

TRW, Incorporated (1)
23555 Euclid Avenue
Cleveland, Ohio 44117
Attention: J. N. McCarthy

TRW Systems (1)
One Space Park
Redondo Beach, California 90278
Attention: Tech. Lib. Doc. Acquisitions

TRW Systems (1)
One Space Park
Redondo Beach, California 90278
Attention: Dr. Eugene Burns